Aus dem Institut für Anatomie und Zellbiologie
Abteilung Molekulare Neurowissenschaften
Geschäftsführender Direktor: Prof. Dr. E. Weihe
des Fachbereichs Medizin der Philipps-Universität Marburg

in Zusammenarbeit mit der

Section on Molecular Neuroscience
Group Leader: L. E. Eiden, Ph.D.
Laboratory of Cellular and Molecular Regulation
National Institute of Mental Health

The Neuropeptide PACAP Mediates Stimulus-Transcription Coupling in Hypothalamic-Pituitary-Adrenocortical Axis and Sympathetic Nervous System

Implications for Acute and Chronic Stress Responses

Inaugural-Dissertation
zur Erlangung des Doktorgrades der Naturwissenschaften (Dr. rer. nat.)
dem Fachbereich Medizin der Philipps-Universität Marburg
vorgelegt von

Nikolas Stroth aus Marburg
Marburg, 2010

Angenommen vom Fachbereich Medizin der Philipps-Universität Marburg
am: 11. Januar 2011

Gedruckt mit Genehmigung des Fachbereichs.

Dekan: Prof. Dr. M. Rothmund
Referenten: Prof. Dr. E. Weihe; L. E. Eiden, Ph.D.
1. Korreferent: Prof. Dr. T. D. Plant

1. Abstract (English)

Stress is a vital response of all organisms to the demands of life. By adjusting to stimuli from the outside world, and stimuli arising from its internal organs, the body is continually at work to ensure its proper function under a widely variable range of conditions. Thus, acute and adequate responses to such stimuli (stressors) are essential. However, when these responses are either insufficient or excessive, the well-being of the organism is at risk. Furthermore, if stress becomes chronic and the cost of continual adjustment rises, a plethora of illnesses can result. This phenomenon has grown into epidemic proportions, particularly in Western societies, with the physical and mental health of millions severely affected. Despite much research, the mechanisms underlying responses to stressors are still incompletely understood.

The biological substrate of stress responses in mammals, including humans, is known to comprise several compartments, which are connected in neuroendocrine circuits. Different neuroendocrine circuits mediate responses to different stressors, although important central and peripheral components of these circuits are shared. For example, the paraventricular nucleus of the hypothalamus (PVN), a central integrator of stressor-induced signaling, controls activity of the hypothalamic-pituitary-adrenocortical axis (HPA axis) as well as the autonomic nervous system (ANS). Through endocrine (pituitary hormones) and neural (sympathetic nerves) mechanisms, stressor-induced signaling converges on the adrenal glands, whose cortex and medulla produce the main effector molecules of the HPA axis and ANS, namely glucocorticoids and catecholamines, respectively.

Over the past decades, peptides have been established as crucial regulators of stress responses. The classical and most important examples include corticotropin-releasing hormone (CRH, hypothalamus) and adrenocorticotropic hormone (ACTH, pituitary) of the HPA axis. More recently, an exciting new candidate emerged, namely pituitary adenylate cyclase-activating polypeptide (PACAP). Proof for the concept that PACAP is a transmitter of the ANS during stress came with the description of PACAP-deficient mice, which are unable to adequately activate synthesis and release of catecholamines in response to insulin-induced hypoglycemia. Thus, under conditions of profound metabolic stress, PACAP-mediated signaling within the ANS is a matter of life and death. Early experiments with these PACAP-deficient mice indicated that their HPA axis is intact. However, recent data strongly suggested that PACAP plays an excitatory role during responses of the HPA axis to stressor exposure. The present work therefore focused on both the ANS and HPA axis, using PACAP-deficient compared to wild-type mice as models for stressor-induced responses in vivo.

Our experiments show that PACAP is required for normal responses to acute stressor exposure. Expanding previous results from our laboratory, evidence is provided for PACAP-dependent regulation of the catecholaminergic system in the adrenal medulla during responses of the ANS. By inducing the expression of enzymes required for epinephrine biosynthesis (tyrosine hydroxylase, phenylethanolamine N-methyltransferase), as well as neuropeptides involved in modulation of adrenal secretory activity (galanin, Tac1, VIP), PACAP appears to

provide a mechanism for plasticity during periods of high demand. Our data suggest that this PACAP-dependent stimulus-transcription coupling may proceed via stressor-specific mechanisms, as the induction of a number of transcription factors which are putatively responsible for the regulation of enzymes and neuropeptides (e.g. Egr1, Fos, Nur77) is PACAP-dependent in response to restraint, but not hypoglycemia. Furthermore, PACAP controls upregulation of transcripts encoding potential cytoprotectants (Ier3, Stc1) in the adrenal glands, in response to hypoglycemia and restraint.

Most importantly, our present work is the first to show that the endogenous PACAPergic system is required for activation of the HPA axis in response to stressor exposure. This appears to be mediated at the central level, via PACAP-dependent stimulation of hypophysiotropic neurons, as restraint-induced upregulation of CRH mRNA in the PVN is completely abolished in PACAP-deficient mice. Consequently, restraint-induced secretion of ACTH and corticosterone is blunted, particularly when stressor exposure is prolonged, while serum concentrations of both hormones in untreated mice are equivalent to those in wild-types. These PACAP-dependent effects seem to involve PACAP-dependent stimulus-transcription coupling throughout the HPA axis, and possibly rely on inducible transcription factors from the Nr4a family of orphan nuclear receptors. Thus, rapid regulation of Nur77 (Nr4a1), Nurr1 (Nr4a2) and Nor1 (Nr4a3) in the PVN, pituitary gland and adrenal cortex occurs in a PACAP-dependent pattern. The fact that stressor-induced upregulation of transcripts encoding steroidogenic acute regulatory protein (StAR) and steroidogenic factor 1 (SF-1) is significantly attenuated in adrenal glands from PACAP-deficient mice provides a link between PACAP-dependent central control of the HPA axis and peripheral corticosterone production.

Beyond the acute regulation of responses to stressor exposure, our results have implications for the understanding, and potentially the treatment, of disease states associated with chronic stress. In this regard, a crucial finding from the present work concerns stressor-induced corticosterone secretion. The initial phase is largely intact in PACAP-deficient animals, while more sustained secretion during prolonged stressor exposure becomes increasingly blunted. This suggests that chronic hypersecretion of glucocorticoids, such as during certain psychiatric illnesses, could be targeted by blockade of the PACAPergic system, without compromising acute HPA responses that are necessary for survival and health.

As mentioned, our experiments suggest that PACAP is a central regulator of the HPA axis, controlling activation in response to stressors at the level of the hypothalamic PVN. Future work will address the exact signaling mechanisms employed during PACAP-dependent stress responses, in order to reveal potential avenues for therapeutic intervention. To further clarify the involvement of this neuropeptide in chronic stress-related diseases, the PACAP-deficient mouse model will continue to be used as a valuable tool in experiments concerning the behavioral, physiological, cellular and molecular mechanisms of stress.

2. Abstract (German)

Stress ist eine notwendige Reaktion aller Organismen auf die Anforderungen des Lebens. Durch ständige Anpassung an Reize aus der Aussenwelt und seinen inneren Organen bewirkt der Körper, dass seine normale Funktion unter stark variierenden Bedingungen aufrecht erhalten werden kann. Akute und adäquate Reaktionen auf derartige Reize (Stressoren) sind daher lebenswichtig, während zu schwache oder exzessive Reaktionen ein Risiko für die Gesundheit darstellen. Wenn Stress zudem chronisch wird, die Kosten ständiger Anpassung also zu hoch werden, kann dies zu einer Vielzahl an Krankheiten führen. Dieses Phänomen hat mittlerweile epidemische Ausmaße erreicht, besonders in westlichen Ländern, in denen Millionen von Menschen chronisch an physischen und seelischen Krankheiten leiden. Trotz intensiver Forschungsanstrengungen sind die Mechanismen, die Stressreaktionen zugrunde liegen, noch nicht vollständig bekannt.

Die biologische Grundlage, auf der Stressreaktionen in Säugetieren (also auch dem Menschen) ablaufen, beinhaltet mehrere Bestandteile, die in neuroendokrinen Schaltkreisen organisiert sind. Unterschiedliche Schaltkreise bewirken Reaktionen auf unterschiedliche Stressoren, wobei wichtige zentrale und periphere Komponenten allen Schaltkreisen gemeinsam sind. Im Hypothalamus beispielsweise fungiert der Nucleus paraventricularis (PVN) als zentrale Schaltstelle zur Kontrolle der Hypothalamus-Hypophysen-Nebennierenrinden-Achse (HPA-Achse) sowie des autonomen Nervensystems (ANS). Mittels endokriner (Hormone der Hypophyse) und neuraler (sympathische Nerven) Mechanismen aktivieren Stressor-induzierte Signale die Nebennieren, deren Rinde und Mark die wichtigsten Wirkstoffe der HPA-Achse und des ANS herstellen, nämlich die Glucocorticoide und Catecholamine.

In den letzten Jahrzehnten konnte klar gezeigt werden, dass Peptide wichtige Regulatoren von Stressreaktionen sind. Als klassische und wichtigste Beispiele gelten hier CRH (corticotropin-releasing hormone, Hypothalamus) und ACTH (adrenocorticotropic hormone, Hypophyse) aus der HPA-Achse. Ein neuer, relativ kürzlich entdeckter Kandidat ist das Neuropeptid PACAP (pituitary adenylate cyclase-activating polypeptide). Mittels transgener Mäuse konnte bewiesen werden, dass PACAP ein bei Stress freigesetzter Botenstoff des ANS ist. PACAP-defiziente Mäuse sind nicht in der Lage, in Reaktion auf Insulin-induzierte Hypoglykämie die Synthese und Freisetzung von Catecholaminen adäquat zu aktivieren, so dass PACAP-abhängige Signale im Falle von metabolischem Stress zwischen Leben und Tod entscheiden. Erste Experimente mit diesen PACAP-defizienten Mäusen beschrieben ihre HPA-Achse als intakt. Neuere Daten jedoch liessen dringend vermuten, dass PACAP Stressreaktionen der HPA-Achse als exzitatorischer Botenstoff unterstützt. Die vorliegende Arbeit richtete sich daher sowohl auf das ANS als auch die HPA-Achse und nutzte das PACAP-defiziente Mausmodell, um Stressor-induzierte Reaktionen in vivo zu untersuchen.

Unsere Experimente zeigen, dass PACAP für den Ablauf akuter Stressreaktionen notwendig ist. Aufbauend auf vorherigen Befunden aus unserem Labor liefern wir Hinweise darauf, dass das catecholaminerge System des Nebennierenmarks während Stressreaktionen

des ANS PACAP-abhängig reguliert wird. Durch Induktion der Enzyme, welche die Biosynthese von Adrenalin steuern (Tyrosinhydroxylase, Phenylethanolamine N-methyltransferase), sowie von Neuropeptiden, welche die sekretorische Aktivität der Nebennieren modulieren (Galanin, Tac1, VIP), scheint PACAP funktionelle Plastizität im Zuge erhöhter Anforderungen zu gewährleisten. Diese Kopplung von Stimulus (Stressor) an Genexpression scheint Stressor-spezifischen Mustern zu folgen, denn Transkriptionsfaktoren, die für die Regulation der Enzyme und Neuropeptide in Frage kommen (z.B. Egr1, Fos, Nur77), werden zwar durch Immobilisierungsstress induziert, nicht aber durch Hypoglykämie. Desweiteren kontrolliert PACAP die Expression potentiell zytoprotektiver Faktoren (Ier3, Stc1) in den Nebennieren, sowohl in Reaktion auf Hypoglykämie als auch Immobilisierung.

Von besonderer Bedeutung ist die Tatsache, dass die vorliegende Arbeit erstmalig Beweise dafür liefert, dass endogenes PACAP für Stressor-induzierte Aktivierung der HPA-Achse notwendig ist. Dies scheint zentral gesteuert zu werden, mittels PACAP-abhängiger Stimulation hypophysiotroper Neurone des Hypothalamus, denn die Induktion von CRH mRNA im PVN nach Immobilisierungsstress fällt in PACAP-defizienten Mäusen vollständig aus. Infolgedessen ist auch die Sekretion von ACTH und Corticosteron vermindert, besonders bei länger anhaltendem Stress, wohingegen basale Konzentrationen beider Hormone im Blutkreislauf denen normaler Mäuse gleichwertig sind. Diese PACAP-abhängigen Effekte scheinen entlang der gesamten HPA-Achse mit PACAP-abhängigen Genexpressionsmustern einher zu gehen, wobei induzierbare Transkriptionsfaktoren der Nr4a-Familie (nukleäre Rezeptoren) eine Rolle spielen. Unmittelbar nach Stimulation werden Nur77 (Nr4a1), Nurr1 (Nr4a2) und Nor1 (Nr4a3) PACAP-abhängig im PVN, der Hypophyse und der Nebennierenrinde exprimiert. Die Stressor-induzierte Regulation von Transkripten, welche StAR (steroidogenic acute regulatory protein) und SF-1 (steroidogenic factor 1) kodieren, ist in den Nebennieren PACAP-defizienter Mäuse signifikant verringert. Dies stellt die Verbindung dar zwischen zentraler, PACAP-abhängiger Steuerung der HPA-Achse, sowie peripherer, PACAP-abhängiger Produktion von Corticosteron.

Über akute Stressreaktionen hinaus sind unsere Resultate potentiell bedeutsam für das Verständnis von Krankheiten, die mit chronischem Stress korrelieren. Diesbezüglich besonders wichtig sind unsere Ergebnisse zu PACAP-abhängiger Sekretion von Corticosteron. Während nämlich die initiale Phase in PACAP-defizienten Mäusen weitgehend intakt ist, ergibt sich im Verlauf anhaltender Stimulation eine deutliche Verminderung der Sekretion. Daher ist es denkbar, dass man die chronische Hypersekretion von Glucocorticoiden, die z.B. mit bestimmten psychiatrischen Erkrankungen einhergeht, durch Blockade von PACAP behandeln könnte, ohne dabei lebenswichtige akute Funktionen der HPA-Achse zu beeinträchtigen.

Weitere Experimente werden die Mechanismen PACAP-abhängiger Stressreaktionen genauer untersuchen, um potentielle neue Therapieansätze zu entdecken. Das PACAP-defiziente Mausmodell wird dabei auf allen Ebenen von Stress – Verhalten, Physiologie, sowie zelluläre und molekulare Mechanismen – weiterhin wertvolle Ergebnisse bezüglich der Rolle dieses Neuropeptides liefern.

3. Introduction

Experiences of “stress” or situations that are “stressful” are familiar to almost everyone in today’s fast-paced human world. Feelings of being “stressed” can arise from a variety of sources, including psychological pressure in the environments of the workplace, family and greater society. From a biological and physiological point of view, “stress” encompasses much more than those phenomena associated with contemporary use of the term, and the underlying scientific concepts have continuously evolved since the fundamental ideas were first formulated.

3.1. Historical definitions of stress

In his 1865 landmark publication “*Introduction à l'étude de la médecine expérimentale*” (Introduction to the study of experimental medicine), Claude Bernard postulated that all complex living organisms maintain a constant environment within themselves that he called “*le milieu intérieur ou intra-organique*” (internal environment). According to Bernard, this internal environment comprises the bodily fluids in which cells and organs are bathed while performing their normal function, and maintaining relative constancy of its composition is critical for life. He also held the belief that “*In experiments concerning bodies […] there are at least two milieus to consider: the external or extra-organismal and the internal or intra-organismal milieu*” (Bernard, 1865). Thus, he provided a framework for viewing physiological systems, which function under constant conditions maintained by the organisms themselves, in the context of the external world in which the organisms are embedded. This was further emphasized by Charles Richet, who stated that “*The living being is stable. It must be in order not to be destroyed, dissolved or disintegrated by the colossal forces, often adverse, which surround it*” (Richet, 1900). Building on and synthesizing these early ideas, Walter Cannon coined the term “homeostasis” in 1926, by which he meant “*the coordinated physiological reactions which maintain most of the steady states in the body*” (Cannon, 1929). According to Cannon, different threats to homeostasis, such as pain, hunger and strong emotions, could trigger these reactions in a common pattern, including increases in blood sugar, heart rate and epinephrine secretion. He interpreted them as “*biological adaptations to conditions in wild life which are likely to involve pain and emotional excitement, i. e., the necessities of fighting or flight*” (Cannon, 1927). In the following years, work initiated by Hans Selye provided evidence that, similar to Cannon’s “fight or flight” reaction, a “general alarm reaction” could be observed in animals after exposure to different noxious agents, leading him to suggest that it represents “*a response to damage as such*” rather than a specific response (Selye, 1936a). Selye was also responsible for introducing the term “stress” into the biological vocabulary, and has been credited with popularizing the general concept of a unitary stress response (Goldstein and Kopin, 2007).

The historical importance of the aforementioned researchers comprises three main aspects of their contributions. First, in new terms and more completely than their predecessors, they established that complex living organisms actively produce and maintain their

physiological state (internal environment) through the coordinated action of their organ systems. Second, they emphasized that complex organisms are open systems with diverse relations to their surroundings, such that maintenance of their physiological state is subject to disturbances arising in the outside world (external environment). Lastly, they made fundamental observations on the neuroendocrine systems that elaborate responses to these disturbances, providing a sound basis for future research into homeostasis and its regulation during stress.

3.2. Stressors and stressor-responsive pathways – current concepts

Since the groundbreaking contributions of scientists such as Bernard, Richet, Cannon and Selye, extensive research into all aspects of stress has been carried out. Using both tried and tested as well as novel and more sophisticated experimental techniques, much has been learned about the exact organization of the neuroendocrine pathways that underlie homeostatic reactions. While the fundamental facts discovered by the aforementioned scientists persist, their theories have been refined and expanded in recent years, leading to a more complete and systematic understanding of how stress occurs in the body.

3.2.1. Processive and systemic – two generalized pathways

Stimuli that trigger homeostatic reactions are called stressors and can arise from the internal or external environment of an organism. Stressors can be separated into a variety of categories, as exemplified by Cannon, who listed pain, hunger (starvation) and strong emotions as threats to homeostasis (Cannon, 1927). Other examples include injury, blood loss, hypoxia and exposure to a cold environment. It has become increasingly evident that the responses triggered by different stimuli proceed via different routes, reflecting the nature of the stressors and their potential impact on survival, and current concepts propose that two generalized pathways govern all stress responses. Psychological stressors, which do not acutely harm the organism, are relayed via multiple synaptic connections involving higher brain structures, and the corresponding pathway is termed “processive”. Processive stressors obtain physiological meaning only after signals from multiple sources have been assembled and interpreted, which requires parts of the limbic system (e.g. hippocampus, prefrontal cortex). On the other hand, physiological stressors that could immediately cause significant harm or death are more directly conveyed to the effector limbs of stress-reactive neuroendocrine circuitry, via the “systemic” pathway. Responses to systemic stressors involve simpler circuitry and fewer synaptic connections (Herman and Cullinan, 1997).The two pathways were proposed on the basis of experiments in which lesions of higher brain structures attenuated or abolished the responses to psychological stressors, while responses to physiological disturbances were unaffected [reviewed in (Herman and Cullinan, 1997; Herman et al., 2003)]. See Table 1 for common synonyms used in describing the processive and systemic pathways, together with the stressors that activate them, and Figure 1 for a schematic depiction.

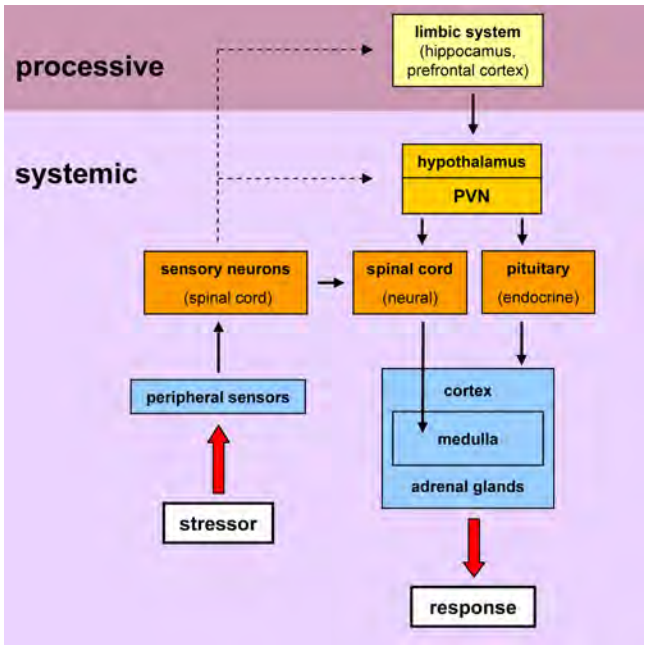

Figure 1. Simplified schematic of the two generalized pathways comprising stressor-responsive neuroendocrine circuitry. Both pathways share certain elements, such as the paraventricular nucleus of the hypothalamus (PVN) and the adrenal glands. However, the processive pathway involves a larger number of synapses and higher degree of connectivity, compared to the more direct connections underlying the systemic pathway. Note that the circuitry is depicted as a highly simplified schematic, with many structures omitted for clarity. Sympathetic and parasympathetic innervation of peripheral targets other than the adrenal glands is also not shown. Dotted lines indicate connections that proceed via multiple relays (not shown), e.g. in the brain stem. See the following sections for more detailed descriptions of the components and their role in governing responses to stressor exposure.

Pathway	Synonyms	Examples of stressors
processive	psychological, neurogenic, exteroceptive, anticipatory	restraint, fear, novelty, social challenges
systemic	physiological, metabolic, interoceptive, reactive	hypoglycemia, pain, hemorrhage, hypoxia

Table 1. The two generalized pathways that elaborate stress responses, common synonyms used to describe them, and examples of the stressors through which they are activated. See Herman et al. for excellent reviews concerning these pathways (Herman and Cullinan, 1997; Herman et al., 2003).

3.2.2. Systematic elements and principles of stressor-responsive pathways

According to current concepts of stress, the wiring schemes underlying stressor-responsive pathways contain several systematic elements (Goldstein and Kopin, 2007). *Sensors* are responsible for monitoring variables in the internal or external environment, such as blood pressure, blood sugar levels, ambient temperature, and sight or smell of a potential predator. Information about these variables is conveyed via afferent neural pathways to structures that compare this information with certain *setpoints*. If a sufficiently large discrepancy arises between information about the sensed variables and the corresponding setpoints, *effectors* are activated to counter the discrepancy and to reinstate homeostasis (Goldstein and Kopin, 2007). These elements operate in both the processive and systemic pathway. In fact, many of the cell groups and anatomical sites which carry out the aforementioned functions are shared by both pathways (see following sections). As mentioned earlier, the difference lies in the degree of connectivity and the extent to which higher brain centers are involved. In addition, there are several principles by which homeostatic systems operate. Among them, *negative feedback* ensures that responses to a stimulus are sufficient, yet not excessive, controlling the activity of effectors to provide adequate response magnitude and duration (Goldstein and Kopin, 2007).

3.3. Neuroendocrine circuitry underlying responses to stressor exposure

From an anatomical point of view, the aforementioned pathways can be defined as neuroendocrine circuits, based on the tissues, cells and mechanisms they employ. Some of these tissues and cells are specific to one pathway, while others are shared. Although they have been studied in great detail, revealing much of their functional characteristics, the neuroendocrine circuits summarized below and their detailed interactions during stress are still an area of active research. Note that, for the purpose of the present work, the collective term “stress axis” is used in reference to the sum of all ascending (afferent) and descending (efferent) pathways that contribute to stress responses in vivo.

3.3.1. Hypothalamic-pituitary-adrenocortical axis (HPA axis)

Signals from peripheral sensors indicating the presence of a stressor are propagated via neuronal processes to spinal cord and medulla oblongata. By means of “short circuit” communication, immediate reflexes are initiated, or signals are relayed to the brain via “long circuit” connections [(Pacak and Palkovits, 2001); see Figure 1 for a simplified schematic]. In the paraventricular nucleus of the hypothalamus (PVN), excitatory signals from the brain stem and other sources are integrated with inhibitory signals, including those from limbic structures such as the hippocampus and prefrontal cortex (Herman et al., 2003). This involves a myriad of complex and multidirectional connections, with the “microenvironment” of the PVN (regions immediately adjacent to the nucleus) playing a critical role (Herman et al., 2002).

The PVN of the rat can be divided into several subregions, based on the size, packing density, chemical characteristics and projection targets of its neuronal constituents (Armstrong et al., 1980; Kiss et al., 1991; Swanson and Kuypers, 1980). A subpopulation of cells in the dorsolateral aspect of the medial parvocellular region, which in total comprises roughly 3000 small-sized neurons in the rat (Kiss et al., 1991), expresses the neuropeptide corticotropin-releasing hormone (CRH). Most of these CRH-containing neurons send projections to the external zone of the median eminence (Swanson et al., 1983), where CRH is released into the hypothalamic-hypophyseal portal system. Upon reaching corticotrope cells of the anterior pituitary gland, CRH causes secretion of adrenocorticotropic hormone (ACTH), which in turn is distributed via the general circulation as an endocrine messenger (Whitnall, 1993). ACTH finally stimulates the cortex of the adrenal glands to synthesize and release steroid hormones, among which the glucocorticoids (corticosterone in rodents, cortisol in humans) produced in the adrenocortical zona fasciculata (Keegan and Hammer, 2002) are the most important factors during stress (Herman and Seroogy, 2006).

Within this neuroendocrine chain of events, CRH-containing hypophysiotropic neurons in the PVN are the principal starting point for what is known as the *hypothalamic-pituitary-adrenocortical axis* (HPA axis; see hypothalamus, pituitary and adrenal cortex in Figure 1). They have been recognized as the central locus at which glucocorticoid secretion is regulated, integrating excitatory and inhibitory inputs from a multitude of sources (Herman et al., 2002;

Herman et al., 2003). These specialized cells have also been termed “CRH motoneurons” (Swanson et al., 1987), reflecting the fact that they drive responses of the HPA axis to homeostatic challenge via CRH-stimulated ACTH release, followed by ACTH-dependent glucocorticoid secretion. Importantly, in addition to cells in the hippocampus and anterior pituitary, these neurons are also crucial targets for glucocorticoid-mediated negative feedback within the HPA axis. Thus, via both rapid (independent of transcription, non-genomic) and delayed (transcription-dependent, genomic) mechanisms, involving effects at the cell membrane and in the nucleus, glucocorticoid action in the nervous system results in a net suppression of HPA axis output (Keller-Wood and Dallman, 1984; Prager and Johnson, 2009; Tasker et al., 2006), presumably to prevent the system from reacting excessively to stressor exposure.

3.3.2. Autonomic nervous system (ANS)

The *autonomic nervous system* (ANS) comprises sympathetic and parasympathetic components, with the former being further divided into sympathoadrenal and sympathoneural parts (Kvetnansky et al., 2009; Pacak and Palkovits, 2001). In the PVN, a subpopulation of parvocellular neurons, distinct from the population of hypophysiotropic neurons (see above), projects to targets in the brain stem and spinal cord (Swanson and Kuypers, 1980). These so-called preautonomic neurons of the ventromedial and dorsal parvocellular PVN are the most important cells for integration of excitatory and inhibitory signals impinging on the ANS (Herman et al., 2002; Ulrich-Lai and Herman, 2009). Their efferent targets are preganglionic neurons of the sympathetic and parasympathetic ANS, residing in the intermediolateral column (IML) of the thoracolumbar and craniosacral spinal cord, respectively. Processes of these preganglionic neurons extend to form synaptic contacts with second-order neurons in autonomic ganglia, from which efferent signals are propagated via postganglionic fibers to finally reach their target organs, e.g. in the cardiovascular and digestive system (Ulrich-Lai and Herman, 2009). The characteristic feature of the sympathetic ANS is an immediate and fast response to stressors, e.g. a drop in blood pressure, allowing regulation of heart rate and blood vessel tone within seconds. Such rapid responses, elaborated via the aforementioned synaptic connections, set it apart from the relatively sluggish HPA axis, whose more protracted responses take minutes to manifest due to the successive action of multiple hormones. Reflex activation of the parasympathetic ANS balances sympathetic activity, causing the responses to be short-lived (Ulrich-Lai and Herman, 2009).

The sympathoadrenal system was defined in early experiments by Walter Cannon and others, based on the fact that sympathetic innervation of the adrenal medulla, occurring via the splanchnic nerve, is required for the recovery of normal blood sugar levels after insulin-induced hypoglycemia (Cannon et al., 1924). According to the architecture of the ANS outlined above, the medulla of the adrenal gland can be regarded as a modified sympathetic ganglion. It should be noted, however, that activation of the adrenal medulla and other parts of the sympathetic ANS do not always occur in parallel or to the same extent. This has prompted leading

researchers in the field to propose using a different description, namely “adrenomedullary hormonal system” instead of “sympathoadrenal system”, as the latter term implies coordinated activity of epinephrine-releasing (adrenal medulla, endocrine response) and norepinephrine-releasing (sympathetic nerves, neural response) components of the ANS (Goldstein and Kopin, 2008). With this caveat in mind, we will use the term “*sympathoadrenal*” when referring to functional connections between the sympathetic splanchnic nerve and chromaffin cells of the adrenal medulla, the source from which epinephrine is released in response to a variety of stressors (Goldstein and Kopin, 2008).

3.3.3. Interactions between HPA axis and ANS – special role of the adrenal glands

A wealth of evidence accumulated over many decades supports differentiation of stressor-responsive pathways into an HPA and ANS component, as outlined above. However, it is important to recognize that the whole story is more complex. First of all, most stressors activate HPA axis and ANS, and both systems share the PVN (central regulator) and adrenal glands (peripheral effectors) as crucial components of their functional anatomy. Between both systems, there are anatomical and functional interactions at multiple levels (Kvetnansky et al., 1995). Many of these interactions occur at the level of the adrenal glands, whose activity is controlled chiefly via endocrine and neural mechanisms. Given the importance of the main adrenal secretory products (cortisol and epinephrine) for a wide variety of stress-related human diseases (Chrousos, 2009; Cohen et al., 2007), it is warranted to briefly address some details concerning functional anatomy of the glands, especially as it relates to stressor-induced activation and cross-talk between HPA axis and ANS.

The adrenal glands consist of two main compartments, namely an outer cortex and inner medulla. In response to stressor exposure, activation of the HPA axis culminates in secretion of glucocorticoids from the cortex, and activation of the ANS leads to release of epinephrine from the medulla. Glucocorticoid-dependent control of the enzyme that catalyzes the final step in epinephrine synthesis constitutes a fundamental mechanism by which the HPA axis interacts with the ANS. Thus, classical experiments established that the activity of phenylethanolamine N-methyltransferase (PNMT) requires glucocorticoids (Wurtman, 1966), and more recent studies using transgenic mice showed adrenomedullary PNMT expression to be completely abolished in glucocorticoid receptor-deficient animals (Finotto et al., 1999). Although no bona fide portal system exists in the adrenal glands, which had been the subject of much controversy, the centripetal blood flow from the cortex to the medulla and the ultrastructural features of the adrenal vasculature provide the basis for glucocorticoid-dependent control of adrenomedullary PNMT (Bassett and West, 1997; Breslow, 1992; Coupland and Selby, 1976; Kikuta and Murakami, 1984; Murakami et al., 1989; Sparrow and Coupland, 1987; Tokunaga, 1996; Vinson et al., 1985). Based on measurements in the adrenal vein and the general circulation, it can be estimated that cells of the adrenal medulla are exposed to glucocorticoid concentrations approximately 10-100 times above those encountered

by other cells (Mannelli et al., 1982; Padayatty et al., 2007; Stowasser et al., 2001; Sweat, 1955; Wurtman, 1966). Conversely, autonomic nerves supplying the adrenal glands have been demonstrated to affect cortical glucocorticoid secretion (Engeland, 1998; Ulrich-Lai and Engeland, 2002), which appears to be at least partly mediated by neuropeptides such as PACAP, galanin and VIP (Ehrhart-Bornstein et al., 1998; Holgert et al., 1998; Whitworth et al., 2003). Furthermore, it is now clear that the zonal distinction of cortex versus medulla is not as strict as originally thought, since islands of chromaffin cells can be found in the cortex, and markers of cortical cells are expressed in cells of the medulla. Thus, although the centripetal organization of blood flow through the adrenals does not allow for endocrine effects, paracrine mechanisms are recruited for intraadrenal signaling from medullary cells to the cortex (Bornstein et al., 1997; Bornstein et al., 1994; Ehrhart-Bornstein et al., 1998; Whitworth et al., 2003).

Taken together, the adrenal glands are not only important peripheral effectors of the HPA axis and ANS, but also a locus of interaction between these two stressor-responsive systems. Their activity during health and disease is therefore tightly controlled by complex mechanisms, involving hormonal and neural pathways.

3.3.4. Stressor-specific responses of the HPA axis and ANS

During at least the first half of the twentieth century, responses of the body to stressor exposure were thought to follow a stereotypic pattern. Walter Cannon and Hans Selye, two towering figures of early stress research, posited that there is a unitary response to a wide variety of stimuli, and they respectively emphasized secretory activity of the adrenal medulla and cortex as its hallmark (Cannon, 1927; Selye, 1936a). Although their groundbreaking work has lost none of its historic impact, we now know that both Cannon's and Selye's stories are incomplete, and their theories have been refined in recent decades. With respect to what has been called Selye's "doctrine of nonspecificity", experimental results obtained with different stressors and stressor intensities were incompatible with a nonspecific response (Pacak et al., 1995), and a direct test of the doctrine failed to support it (Pacak et al., 1998). It has become quite clear that different stressors induce relatively specific patterns of sympathoadrenal, sympathoneural and HPA axis activity, reflected in stressor-specific elevations of circulating epinephrine, norepinephrine and ACTH, respectively (Goldstein and Kopin, 2008; Pacak and Palkovits, 2001). These patterns are the consequence of stressor-specific activation of neuroendocrine circuitry (Pacak and Palkovits, 2001), which corresponds to the generalized pathways of processive and systemic stress responses mentioned above (Herman and Cullinan, 1997; Herman et al., 2003).

3.4. Dysfunction of stressor-responsive systems – chronic stress and disease

The molecules secreted by the HPA axis and ANS affect virtually all bodily functions. Basal activity and responsiveness of these systems must therefore be tightly controlled to ensure proper conditions at rest and following stressor exposure. According to Chrousos and others, homeostatic reactions follow an inverted U-shape dose-response pattern (dose = activity of the system; response = homeostatic effect), with “optimal” homeostasis occurring in the middle of the curve (Chrousos and Gold, 1992). Such optimal homeostasis is in contrast to insufficient or excessive homeostatic reactions (left and right part of the curve), both of which can have harmful consequences for the organism (Chrousos, 2009). Chronic disturbances of the HPA axis and ANS are now well known to correlate with a myriad of disease states, affecting (among others) the immune, gastrointestinal and cardiovascular systems, as well as neurological function and mental health (Chrousos, 2009; Cohen et al., 2007; de Kloet et al., 2005; Herman and Seroogy, 2006). According to one theory, homeostatic responses that were originally beneficial have “at this time in evolutionary history […] become maladaptive”, causing increased prevalence of complex disorders, especially in Western societies (Chrousos, 2004). With respect to the central nervous system, chronic stress and elevated HPA axis activity have been implicated as risk factors for the development and progression of anxiety and depression, as well as Alzheimer’s and Parkinson’s diseases (Chrousos, 2009; de Kloet et al., 2005; Herman and Seroogy, 2006). Thus, the etiology and management of stress have become the focus of much preclinical and clinical research.

3.5. Animal models of stress

To elucidate the biological underpinnings of stress, it is necessary to study the molecular, cellular, physiological, psychological and social mechanisms affecting an organism’s function in health and disease. Immense progress has been made in this area thanks to the use of animal models. For example, the neuroendocrine pathways mediating the response to low blood glucose concentrations (systemic stressor) have been unraveled, such that the brain regions, efferent neural routes and peripheral targets are now known. With respect to the contribution of the sympathoadrenal system, this was achieved largely by means of physiological experiments, using insulin-induced hypoglycemia in mammals as an experimental stressor (Cannon et al., 1924; Cantu et al., 1968; Cantu et al., 1963; de Vries et al., 2005). In recent decades, transgenic mouse models have expanded the scope and refined the methods of stress research in vivo, allowing dissection of molecular pathways by targeting specific genes. For example, mouse strains under- or overexpressing the glucocorticoid receptor, or harboring conditional and region-specific deletions, have greatly contributed to the understanding of glucocorticoid signaling pathways in the brain, and how they contribute to the impact of HPA axis activity on mental health (Chourbaji et al., 2008; Kolber and Muglia, 2009).

Several important aspects of stress-induced effects on brain function are most likely unique to the human condition, and thus nearly impossible to reproduce in other species. For example, situations of social-evaluative threat, where task performance is under the scrutiny of observers, represent powerful stressors in humans (Kudielka and Wust, 2010). Social evaluation (processive stressor) increases salivary cortisol concentrations, while task performance without evaluation does not, and has been shown to induce feelings of shame or lower social self-esteem (Gruenewald et al., 2004). These latter phenomena of human experience are beyond the scope of laboratory animal models. Nevertheless, responses of the HPA axis and ANS to stressor exposure can be triggered in relatively specific ways, allowing us to ask specific questions about the underlying biological mechanisms.

3.5.1. Insulin-induced hypoglycemia – a systemic stressor

Injection of insulin causes a rapid drop in blood glucose concentrations. Since glucose is the main energy source for the body, and indispensable particularly for the brain, insulin-induced hypoglycemia poses an immediate threat to well-being and survival. As such, it elicits a so-called counterregulatory response that does not require higher brain centers, based on which hypoglycemia is classified as a “systemic” stressor (see above). The sympathoadrenal component of this counterregulatory response was first described by Cannon and others, who showed that epinephrine secretion from the adrenal medulla, mediated via sympathetic outflow through the splanchnic nerves, was strongly increased after induction of hypoglycemia (Cannon et al., 1924). The source of the splanchnic nerve fibers that stimulate adrenomedullary secretion was later determined to be the upper thoracic spinal cord (Cantu et al., 1963). Further upstream, the counterregulatory response originates in the central nervous system, specifically the ventromedial hypothalamus, where neuronal sensors detect low blood glucose concentrations and trigger sympathoadrenal activation (Borg et al., 1995; de Vries et al., 2005).

In addition to the aforementioned, a number of other neuroendocrine structures are activated during hypoglycemia, and the HPA axis is stimulated (Pacak and Palkovits, 2001). In a recent study, Goldstein and Kopin performed a meta-analysis of experiments in which activity of the HPA axis, sympathoadrenal and sympathoneural systems had been measured concurrently, using plasma concentrations of ACTH, epinephrine and norepinephrine as indices, respectively. They showed that hypoglycemia induces very pronounced activation of the HPA axis, and massive activation of the sympathoadrenal system, while sympathoneural activity was only mildly affected (Goldstein and Kopin, 2008). These results are in line with the crucial importance of adrenocortical glucocorticoids and adrenomedullary epinephrine for the restoration of normal blood sugar concentrations.

In summary, for the purpose of the experiments described in the present work, insulin-induced hypoglycemia provides a convenient model to study regulation of ANS and HPA axis activity in response to acute stressor exposure.

3.5.2. Restraint – a processive stressor

The inability to move freely or at will can be an extremely threatening experience, for example because it increases the likelihood of being preyed on by a predator. Although health and well-being might not be acutely at risk, physical restraint is therefore a powerful psychological stressor. In biomedical research, this was recognized many decades ago and subsequently exploited as an experimental approach to the effects of psychological stress on health. For example, more than ten years before Walter Cannon formulated his theories concerning the sympathoadrenal "fight or flight" reaction, Hirsch and Reinbach found that rabbits responded with an increase in blood glucose when tied to a laboratory bench. They termed this phenomenon "Fesselungshyperglykämie" (hyperglycemia due to restraint), which we now know is caused by sympathoadrenal activation, and pointed out that it was a significant potential confounding factor in laboratory studies on sugar metabolism (Hirsch and Reinbach, 1913). Hans Selye subsequently introduced restraint as an actual experimental stressor in his studies on injury- and toxin-induced physiological reactions. He found that "*the mere excitement of an animal the free motion of which is interfered with (by tying the legs together or wrapping the animal tightly in a towel)*" had significant consequences, such as enlargement of the adrenal glands (Selye, 1936b). Since then, a number of restraint procedures have been developed and adjusted to the specific needs of a wide range of research settings (Buynitsky and Mostofsky, 2009; Glavin et al., 1994; Pare and Glavin, 1986). Early applications focused on the production of gastrointestinal ulcers caused by severe restraint, to screen for pharmacological compounds with protective effects (Pare and Glavin, 1986). From there, the focus shifted towards the involvement of the central nervous system in peripheral diseases (Glavin et al., 1994), with current applications of restraint including a large number of studies on stress-induced behavioral changes (Buynitsky and Mostofsky, 2009). Most frequently, rats and mice are used as experimental animals.

It is important to note that the terms "restraint" and "immobilization" are sometimes used interchangeably. Both can represent a number of methods, such as wrapping of the animal in cloth, wire mesh or plastic, or restricting the size of the home cage (most commonly termed restraint). Alternatively, the animal is tied to a laboratory bench, in a prone or supine position, with all four limbs extended (most commonly termed immobilization). In the latter case, the animals often struggle quite significantly, trying to wrestle their limbs free, while in the former case movement is mostly prevented. For these reasons, stress resulting from pain, rather than the inability to move per se, has to be considered as a factor influencing experimental outcome. It is therefore important to pay close attention to the exact procedure used in a particular study.

Variables used in restraint experiments include duration, repetition (single or repeated exposure) and combination with other stressors, such as restraint plus foot shock or water immersion (Pare and Glavin, 1986). In contrast to foot shock (lower or higher current) and water immersion (lower or higher temperature), as well as pharmacological agents (lower or higher doses), it has been argued that restraint / immobilization intensity can not be varied

quantitatively within a given procedure (Pacak et al., 1998). However, as outlined above, it is quite clear that some procedures entail more or less severe physical impact on the animal. Restraint is therefore most appropriately viewed as a mixed psychological / physical stressor.

The responses triggered by repeated stressor exposure have been the subject of a large number of experiments, aimed at elucidating the mechanisms that underlie chronic stress in humans. Intriguingly, a single exposure to a severe stressor was found to cause a change in reactivity of the HPA axis, such that subsequent exposures to the same (homotypic) stressor elicit a reduced response, a phenomenon that is called desensitization or habituation (Armario et al., 2004; Girotti et al., 2006). In contrast, exposure to a different (heterotypic) stressor yields a more pronounced response, indicating sensitization of the HPA axis. Importantly, habituation appears to be specific to the nature of the stressor, occurring after restraint but not hypoglycemia (Armario et al., 2004), supporting the notion that processive and systemic stressor-responsive pathways (see above) function via partially distinct mechanisms. With respect to expression of catecholamine-synthesizing enzymes in the sympathoadrenal system, the effects of repeated stressor exposure depend on the tissue (e.g. adrenal medulla versus locus coeruleus), the gene (TH, DBH or PNMT) and the stressor (e.g. cold versus immobilization). Some effects require repeated exposures while others are maximal after only one, some effects habituate while others do not (McMahon et al., 1992; Sabban and Serova, 2007).

A single acute exposure to predominantly psychological stressors (such as restraint) can have pronounced long-term neuroendocrine, neurochemical, neuroelectrical, neuroanatomical and behavioral consequences, some of which take days or weeks to fully manifest. Based on this observation, animal models for human posttraumatic stress disorder (PTSD) have been developed, aimed at understanding how a single traumatic event can cause strong and long-lasting anxiety, fear and emotional disturbance (Armario et al., 2008; Armario et al., 2004; Miller and McEwen, 2006; Siegmund and Wotjak, 2006).

A recent meta-analysis showed that restraint causes very strong activation of the ANS and massive activation of the HPA axis (Goldstein and Kopin, 2008). Therefore, taken together with the above considerations, restraint is a useful and convenient model to study both acute and chronic effects of stress on the function of the peripheral and central nervous system. In the present work, experiments were focused on acute aspects of restraint-induced responses.

3.6. Pituitary adenylate cyclase-activating polypeptide (PACAP)

Pituitary adenylate cyclase-activating polypeptide (PACAP) was discovered more than 20 years ago, during a search for hypothalamic factors that stimulate hormone release from the pituitary gland (Miyata et al., 1989). Via functional screening of ovine hypothalamic extracts, Miyata and others purified a polypeptide of 38 amino acids that strongly stimulated accumulation of cyclic adenosine monophosphate (cAMP) in rat pituitary cells, which they termed PACAP38 (Miyata et al., 1989). Subsequently, an additional hypothalamic fraction corresponding to the N-terminal

27 amino acids of PACAP38 was isolated, which is now known as PACAP27, the second biologically active form of the peptide (Miyata et al., 1990). Furthermore, it was found that prepro-PACAP, the precursor from which PACAP38 and PACAP27 are derived, contains an additional peptide, termed PACAP-related peptide or PRP (Vaudry et al., 2000). The gene encoding PACAP (ADCYAP1 in human, Adcyap1 in mouse) has been cloned, localizing to human chromosome 18 and mouse chromosome 17 (Cummings et al., 2002; Hosoya et al., 1992; Miyata et al., 2000; Yamamoto et al., 1998). Several alternative transcripts exist, which have been proposed to be important for specific expression of PACAP in different tissues and during development (Cummings et al., 2002), but detailed evidence regarding these suggestions is still scarce. Based on sequence homology, PACAP is now recognized as a member of the PACAP-VIP-glucagon-GHRH-secretin superfamily of peptides, displaying a remarkably high degree of conservation across species, suggesting that it is evolutionarily ancient and functionally important (Vaudry et al., 2009; Vaudry et al., 2000).

In vivo, PACAP38 is far more abundant than PACAP27 (Arimura et al., 1991), and throughout the present work, the term PACAP will be used to indicate functions carried out by both peptides (unless otherwise indicated). PACAP binds to three G protein-coupled receptors (GPCR), namely VPAC1, VPAC2 and PAC1 (Vaudry et al., 2009), of which VPAC1 and VPAC2 are shared with vasoactive intestinal peptide (VIP) (Laburthe et al., 2002). Just a few years after the discovery of PACAP, it was found that PAC1, the PACAP-specific of the three receptors, is expressed as a variety of alternatively spliced forms, which allow fine-tuning of responses to ligand binding (Spengler et al., 1993). For example, in the third intracellular loop of the PAC1 receptor, absence (null) or presence of short cassettes (hip, hop) determines coupling of the receptor to downstream intracellular signaling proteins, and it has been shown that the PAC1hop variant mediates secretion of catecholamines from adrenomedullary cells (Mustafa et al., 2007). Overall, the diversity of coupling and signaling mechanisms available to PACAP via its three receptors, which activate effectors such as adenylate cyclase (AC), phospholipase C (PLC) and phospholipase D (PLD) (McCulloch et al., 2000), appears to underlie the pleiotropic role played by this neuropeptide in a variety of tissues and organ systems (Vaudry et al., 2009). With respect to the nervous system, PACAP is known to affect development, functional maturation, protection from insult, and regeneration (Somogyvari-Vigh and Reglodi, 2004; Waschek, 2002). Among a plethora of other functions, PACAP has therefore emerged as an attractive candidate for neuroprotective intervention in conditions such as Alzheimer's disease and stroke (Chen et al., 2006; Dogrukol-Ak et al., 2009).

3.6.1. Expression of PACAP in stressor-responsive neuroendocrine circuits

Neuroanatomical studies have shown that PACAP is expressed throughout the rodent nervous system, being particularly abundant in the hypothalamus (Hannibal, 2002). In the hypothalamic PVN, PACAP has central access to the ANS and HPA axis via preautonomic and hypophysiotropic neurons, respectively, indicated by tracing of synaptic connections (Das et al., 2007; Yi et al., 2010) and the demonstration of PACAPergic nerve terminals innervating CRH-

containing neurons (Legradi et al., 1998). Furthermore, PACAP is expressed in neurons of the hypothalamus and brain stem that project to the intermediolateral column (IML) of the spinal cord (Das et al., 2007; Farnham et al., 2008). PACAP is also expressed in the IML itself (Hamelink et al., 2002) and in nerve terminals supplying the adrenal glands (Frodin et al., 1995; Hamelink et al., 2002; Holgert et al., 1996; Moller and Sundler, 1996). Thus, potential loci of PACAPergic effects are found throughout neuroendocrine circuitry of the stress axis, both in ascending (afferent) and descending (efferent) pathways. Note that the above examples are of PACAPergic structures whose involvement in activation of the ANS and HPA axis has been quite clearly demonstrated (see below). Additional potential sites have been omitted from the present report in the interest of clarity.

3.6.2. Expression of PACAP in adrenal glands – some controversial findings

A number of studies have addressed whether PACAP is expressed in the adrenal glands. Early experiments using radioimmunoassay detected PACAP-like material, without asserting whether the source would be afferent nerve endings or parenchymal cells (Arimura et al., 1991; Ghatei et al., 1993). Subsequently, several groups published immunohistochemical evidence for PACAP peptide being contained in adrenal nerve terminals, but not in adrenomedullary chromaffin or ganglion cells (Frodin et al., 1995; Hamelink et al., 2002; Holgert et al., 1996; Moller and Sundler, 1996), a finding that is contrasted by two papers that report the opposite pattern (Shiotani et al., 1995; Tabarin et al., 1994). The transcript encoding PACAP has been detected by RT-PCR and Northern blot in independent experiments (Ghatei et al., 1993; Mazzocchi et al., 2002; Miyata et al., 2000), with one of the studies indicating that expression is restricted to the adrenal medulla (Mazzocchi et al., 2002). Given that PACAP expression in the adrenal medulla could provide a paracrine mechanism for modulation of adrenal secretory function (Conconi et al., 2006), final proof regarding its presence or absence from parenchymal cells is desirable.

3.6.3. Functional role of PACAP during acute stress responses

Intracerebroventricular or intrathecal injections of PACAP into the central nervous system (CNS) elicit increased sympathetic and decreased parasympathetic nerve activity (Farnham et al., 2008; Tanida et al., 2010; Yi et al., 2010), as well as increased corticosterone secretion (Agarwal et al., 2005; Yi et al., 2010), clearly indicating the functional relevance of the neuroanatomical arrangements mentioned above. Furthermore, behavioral manifestations of stress are acutely elicited in rodents when PACAP is injected into the CNS (Agarwal et al., 2005; Legradi et al., 2007; Norrholm et al., 2005). Our group has provided compelling evidence for the involvement of the endogenous PACAPergic system in responses of the ANS and HPA axis to stressor exposure, using mice in which the gene encoding PACAP is disrupted. First, we showed that PACAP-deficient mice display an insufficient counterregulatory response to insulin-induced hypoglycemia, with diminished catecholamine biosynthesis and secretion from the adrenal medulla. These results suggested that PACAP release from the sympathoadrenal

synapse is required for survival during metabolic stress (Hamelink et al., 2002). Second, we recently found that sustained corticosterone secretion from the adrenal cortex, elicited by restraint, is impaired in PACAP-deficient mice, which appears to be due to insufficient biosynthesis of CRH in the hypothalamus (Stroth and Eiden, 2010). Thus, after exposure to acute systemic and processive stressors, an intact PACAPergic system is required for fully functional responses of the ANS and HPA axis.

3.6.4. Effects of PACAP on global gene expression patterns

As mentioned above, PACAP displays remarkable biological pleiotropy, suggesting that PACAP-induced signaling can exert a variety of effects on a given cell type, depending on its developmental and functional status. Towards this end, several studies have investigated the transcriptome of different cells and tissues in response to PACAP. Studies from our group defined two basic categories of genes (including only those whose expression increases) that would emerge from experiments in cell culture and in vivo, respectively. First, *PACAP-responsive* genes are those whose transcript abundance increases after exposure of cells to PACAP. Second, *PACAP-dependent* genes are those whose transcript abundance increases after experimental treatment or insult in wild-type, but not in PACAP-deficient mice (Eiden et al., 2008; Samal et al., 2007). Using suppression subtractive hybridization and microarray analysis, several studies provided evidence that PACAP controls genomic programs underlying cellular survival, growth arrest, differentiation and neurite outgrowth, using the PC12 pheochromocytoma cell line and sympathetic neurons as a model (Braas et al., 2007; Eiden et al., 2008; Grumolato et al., 2003; Ishido and Masuo, 2004; Ravni et al., 2006; Vaudry et al., 2002). Furthermore, transcriptomic responses of the cerebral cortex to ischemia (Chen et al., 2006), as well as the basal transcriptome of the adrenal glands (Samal et al., 2007), have been determined by our laboratory in wild-type versus PACAP-deficient mice. However, no data are available to date regarding PACAP-dependent effects of stressor exposure on gene expression profiles in stressor-responsive neuroendocrine tissues.

4. Specific aims of the present work

As outlined above, PACAP has recently been identified as a mediator of stress responses in vivo. Although its function in the counterregulatory response of the ANS to insulin-induced hypoglycemia is established at the physiological level (Hamelink et al., 2002), there are still open questions regarding PACAP-dependent mechanisms of cellular plasticity in the adrenal glands, specifically with respect to gene expression programs recruited during stress. Also, the mouse strain developed in our laboratory has been fully backcrossed since the first experiments were conducted, making a careful reassessment of its phenotype necessary. Most importantly, although initial data suggested otherwise, there is a wealth of evidence clearly indicating that HPA axis activity will be blunted during stress in PACAP-deficient mice, pointing towards PACAP as a central regulator of the hypothalamus. In this context, the main questions underlying the present work were as follows:

1. Are PACAP-deficient mice normal in the absence of stress, i.e. do their serum hormone concentrations and gene expression profiles resemble those of wild-type mice?
2. What are the hormone secretion patterns and gene expression profiles elicited by stressor exposure in neuroendocrine circuits, most importantly the hypothalamus, pituitary and adrenal glands (HPA axis), in PACAP-deficient compared to wild-type mice?
3. Overall, are PACAP-deficient mice a useful model for the study of acute and chronic stress responses in vivo?

To address these questions, gene expression profiles were measured on the transcriptome scale, to discover candidate genes implicated in PACAP-dependent stress responses. Time courses of gene expression changes, as well as their precise cellular localization, were determined in subsequent experiments. Measurements of circulating hormones were carried out to determine the extent of endocrine responses in wild-type compared to PACAP-deficient mice. All methods and experimental procedures are detailed in the following sections.

5. Materials and Methods

5.1. Experiments in vivo

5.1.1. Mouse strains

The PACAP-deficient mouse strain used in the present work was first described by Hamelink and others (Hamelink et al., 2002). Mice carrying the null allele of the gene encoding PACAP (Adcyap1) were mated with wild-type C57BL/6 mice (National Cancer Institute's Animal Production Program) over twelve generations, such that a complete backcross was achieved. This provides a homogenous genetic background for all experiments, minimizing potential phenotypic contributions of the strain in which the initial gene targeting was performed (129SvJ). It also allows commercially available C57BL/6 mice to be used as paired controls for PACAP-/- animals generated in-house. For our experiments, mice were generated either via heterozygous breeding pairs, in which case littermate controls were used, or by mating homozygous males and females. In some cases, C57BL/6 mice (see above) were ordered as controls. For a description of the genotyping method, see the corresponding section below.

All mice were housed in a temperature- (24˚C on average) and humidity-controlled breeding facility, with 12h/12h light/dark cycle. Regular rodent chow (Rodent NIH-31, Zeigler Bros) and tap water were provided ad libitum. Upon weaning (typically at three weeks of age), mice from a given litter were separated into males and females, and they received serially numbered ear tags to allow unambiguous identification. Corresponding to each unique ear tag number, a small tail biopsy for genomic DNA extraction and genotyping (see below) was obtained. Pups from heterozygous breeding pairs were routinely genotyped, and pups from homozygous breeders were intermittently tested to verify correct genotype assignment. Tail biopsies or genomic DNA preparations were archived to allow future verification if necessary.

Note that several synonyms for the two PACAP genotypes are used interchangeably throughout the present work. These synonyms are WT and PACAP+/+ for wild-type mice, versus knock-out, KO and PACAP-/- for PACAP-deficient mice.

5.1.2. Experiments involving exposure to stressors

In the animal facility, mice were separated by sex and housed 2-5 per cage. About 18 hours before an experiment, mice were transported to the laboratory and placed into individual home cages. In addition to the time frame (between 09:00 AM and 12:00 noon) during which experiments were conducted, parameters that could affect reactivity to stressors were carefully controlled, i.e. noise levels and traffic in the laboratory were kept to a minimum. Thus, although the mice were not individually accustomed to handling prior to the experiments (other than the handling associated with regular activities of caretakers in the animal facility), a stable baseline condition was established to minimize variability in the results, especially with regards to measurement of stress hormone secretion.

All procedures were approved by the National Institute of Mental Health Animal Care and Use Committee (NIMH ACUC). We made every effort to minimize the number of mice used in each experiment.

5.1.2.1. Transient versus prolonged stressor exposure

Hypoglycemia and restraint (see below) were applied either in a transient or prolonged fashion, for two main reasons. The first was to assess whether a brief stimulus is sufficient for hormone release and gene induction, or whether it has to be present for an extended period of time in order to elicit the full response. The second was to assess whether responses are transient, i.e. whether hormone concentrations and mRNA abundance return to baseline after an initial rapid change. In other words, the two variations address the onset and recovery of responses to stressor exposure. The following schematic depicts the setup:

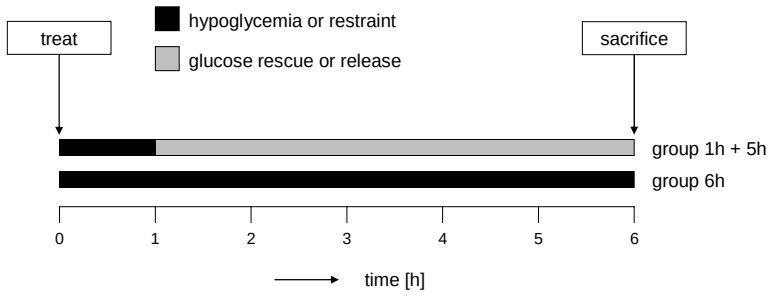

In this example, “group 1h + 5h” represents transient stressor exposure, whereas “group 6h” represents prolonged exposure. The control group consists of untreated animals (sacrificed without prior treatment).

5.1.2.2. Insulin-induced hypoglycemia (systemic stress)

For all experiments involving hypoglycemia, mice were fasted overnight (approximately 18 hours) by removing all chow from the cages, while water remained available ad libitum. Human recombinant insulin (Humulin R, Eli Lilly & Co) was diluted in sterile saline solution (0.9% NaCl) to a working concentration of 0.5 U/ml. For each mouse, intraperitoneal (i.p.) injection of 4 µl per gram body weight thus equaled a dose of 2 U/kg body weight. This setup was chosen to avoid injection of excessive volumes. Mice were returned to their home cage after injection.

In the first set of experiments, mice were killed after different intervals following injection of insulin. These experiments thus represent “prolonged stressor exposure”, and the corresponding groups of mice are labeled 1h, 2h, 4h etc. In subsequent experiments, mice were injected with glucose (2 g/kg, i.p.) 1h after injection of insulin in order to terminate the hypoglycemic stimulus. These experiments thus represent 1h of systemic stress followed by several hours of recovery (“transient stressor exposure”), and the corresponding groups are labeled 1h + 2h, 1h + 5h, 1h + 11h etc. Control mice were either injected with saline or

untreated (see description of results and figure legends for details). All experiments were started between 09:00 AM and 12:00 noon.

5.1.2.3. Cholinergic ganglionic blockade

To determine the effect of cholinergic neurotransmission on adrenal gene expression during stress, antagonists for nicotinic (chlorisondamine) and muscarinic (atropine) acetylcholine receptors were employed. Chlorisondamine and atropine (Sigma-Aldrich) were diluted in sterile saline solution (0.9% NaCl) to concentrations of 2 mg/ml and 0.4 mg/ml, respectively. For each mouse, 2.5 µl of the resulting solution per gram body weight (injected i.p.) thus equaled co-administered doses of 5 mg/kg chlorisondamine and 1 mg/kg atropine.

Experiments with ganglionic blockade involved two injections per mouse, namely pre-treatment (injection 1) with either the two antagonists or saline, followed by treatment (injection 2) with either insulin or saline. Thus, these experiments included four groups: saline + saline ("control"), saline + insulin ("hypoglycemia"), antagonists + saline ("antagonist control") and antagonists + insulin ("ganglionic blockade"). Note that injections 1 and 2 were administered i.p. into the left and right lower abdominal region, respectively.

5.1.2.4. Restraint (processive stress)

Mice were restrained in tapered plastic film envelopes (DecapiCones, Braintree Scientific), such that they were held immobile, with all four limbs underneath them, unable to turn around or perform significant movement. DecapiCones feature a hole in the front where the animal's head is located, and to assure unobstructed breathing, this hole was widened. After being restrained, mice were placed into their home cage. The total time needed for pickup, restraint and return to the home cage was less than one minute. Similar to the systemic stress paradigm, stressor exposure was either prolonged or transient, such that mice were restrained and killed at different time points thereafter, or restrained for 1h, released into their home cage, and killed 5h after release. The corresponding groups were labeled 1h, 3h and 6h (prolonged stressor exposure) or 1h + 5h (transient stressor exposure). Untreated mice (non-stressed controls) were picked up from their home cage by the tail, placed in DecapiCones and decapitated immediately (time from pickup to decapitation <20 seconds). Mice from the prolonged restraint groups were decapitated while still restrained. Restraint-released mice (group 1h + 5h) were picked up and decapitated the same way as untreated animals.

5.1.3. Dissection of tissue samples

Tissue samples were collected either for RNA extraction or preparation of frozen sections. All samples were stored at -80˚C until use.

5.1.3.1. Tissue samples for RNA extraction

Immediately after mice were killed, a cut through the skin of the abdomen was made along the midline, and the abdominal cavity was revealed. Adrenal glands were dissected, excess

adipose tissue was carefully removed, and both glands per mouse were pooled into a regular 1.5 ml polypropylene tube on dry ice (solid carbon dioxide).

For dissection of frontal cerebral cortex, hippocampus and hypothalamus, the whole brain was removed from the skull and placed in an ice-chilled rodent brain matrix (RBM-2000C, ASI Instruments). Four razorblades were then used to make four coronal cuts, with the following coordinates based on an atlas of the mouse brain (Paxinos and Franklin, 2001):

Cut 1: through the optic chiasm, approx. at Bregma 0.02.

Cut 2: 3 mm caudal of cut 1, through the mammillary bodies, approx. Bregma -3.08; from the slice obtained between cuts 1 and 2, the hypothalamus (Hy) was excised as a block of 2x2 mm (width x height) by cutting dorsal of the third ventricle and 1 mm each left and right of the ventral midline. From the same tissue slice, samples of hippocampus (Hc; both hemispheres separate) were obtained. Hc was carefully dissected starting from the caudal aspect of the tissue slice, since the most rostral part (about 1 mm of the slice) contains no hippocampal tissue. It must also be noted that Hc does not include the entire hippocampus, as tissue more caudal to cut 2 was discarded. Thus, Hc represents mostly the dorsal hippocampus, while some ventral parts were excluded.

Cut 3: 1 mm rostral of cut 1, approx. Bregma 0.98.

Cut 4: 1 mm rostral of cut 3, approx. Bregma 1.98; from the slices obtained between cuts 1+3 and 3+4, frontal cortex (FrCx; both hemispheres separate) was dissected by removing and discarding the most ventrolateral aspects of the slices, while retaining cerebrocortical tissue. The aforementioned Bregma coordinates from the mouse brain atlas (Paxinos and Franklin, 2001) and other landmarks were used for orientation.

Pituitary glands (Pit) were carefully collected from the cranial cavity after removal of the brain and frozen in polypropylene tubes on dry ice.

5.1.3.2. Tissue samples for frozen sections

To prepare samples for frozen sections, individual adrenal glands were embedded in O.C.T. compound (Tissue-Tek, Sakura Finetek) in disposable vinyl specimen molds (Cryomold Intermediate, Sakura Finetek) and quickly dropped into liquid nitrogen. Whole brain samples were dropped into isopentane (2-methylbutane), which had been placed in a container on dry ice and cooled to about -50˚C, for rapid freezing without cracking of the tissue. All samples were stored at -80˚C until use.

5.1.4. Measurement of circulating stress hormones

Secretion of ACTH and corticosterone is a classical readout for activation of stress responses in mammals. In our experiments, both hormones were measured in serum, using immunoassays either based on radioactive or chromogenic detection methods.

5.1.4.1. Collection of serum from trunk blood

Immediately after mice were decapitated, their trunk blood was collected into 1.5 ml polypropylene tubes and allowed to coagulate at room temperature for approximately one hour. Samples were subsequently centrifuged (10 minutes at 10,000 x g), the resulting blood clot was removed, and the serum was transferred to fresh tubes. Residual debris was removed via a second centrifugation step (5 minutes at 10,000 x g), after which serum samples were immediately frozen and stored at -80˚C until assayed.

5.1.4.2. ACTH ELISA and corticosterone EIA or RIA

Circulating levels of ACTH were measured using an enzyme-linked immunosorbent assay (ELISA, MD Bioproducts). Corticosterone was measured using either an enzyme-based test (EIA, Assay Designs) or radioimmunoassay (RIA, Coat-A-Count, Siemens Medical Solutions Diagnostics). In each case, samples from individual mice were measured in duplicate. All three kits are commercially available and were used according to the manufacturer's instructions. Serum samples were diluted 1:2 in calibrator A (for ACTH ELISA), 1:10 in assay buffer (corticosterone EIA) or used undiluted (corticosterone RIA).

5.2. Molecular biological techniques

5.2.1. RNA extraction

Before reverse transcription and quantitative PCR can be carried out to quantify gene expression (i.e. mRNA abundance), it is necessary to isolate RNA from the tissues of interest. In our experiments, total RNA was extracted from mouse adrenal glands, hypothalamus, pituitary, frontal cortex and hippocampus using a commercially available kit (RNeasy Mini, Qiagen). For this purpose, frozen tissue samples were transferred to polypropylene tubes containing 600 µl of lysis buffer RLT (RNeasy Mini) and immediately homogenized using an ultrasonic processor (GE 130PB, Hielscher). All subsequent steps were carried out according to the manufacturer's instructions. After removal of tissue debris via centrifugation, homogenates were applied to spin columns, in which RNA is bound to a silica-based membrane. RNA was washed using buffers from the kit and several centrifugation steps, and eluted in RNase-free water.

5.2.2. Determination of nucleic acid concentration

To determine the concentration of total RNA after extraction and purification, a fraction of each sample (2 µl) was measured on a NanoVue spectrophotometer (GE Healthcare). For each batch of samples, RNA yields (calculated as concentration x elution volume) were recorded and compared to previous batches as a means of “quality control” of the extraction procedure. For all tissues studied, it was found that yields were very consistent.

Preparations of DNA (e.g. after isolation of plasmids from transformed cells) or cDNA (e.g. after gel extraction of PCR-derived fragments) were also measured using the NanoVue spectrophotometer. It is worth noting that spectrophotometry does not differentiate between nucleic acids, i.e. measures RNA and DNA using the same wavelengths, such that each preparation has to be as pure as possible in order to give reliable and meaningful results.

5.2.3. DNase treatment of extracted RNA

After extraction, RNA from all mouse tissues was treated with RNase-free DNase I (Roche Diagnostics) in order to remove genomic DNA. The protocol was standardized, such that downstream applications (reverse transcription, PCR etc.) could be conducted in a uniform fashion. All steps were carried out on ice unless otherwise indicated. Per sample, 2.5 µg of total RNA were added to a 0.5 ml polypropylene tube and mixed with 5 µl 10x Incubation Buffer (Roche). After addition of 10 units DNase I (Roche), DEPC-treated water was added to a final volume of 50 µl and tubes were incubated at 37˚C for 30 minutes. Finally, 2 µl of 0.2 M EDTA were added and tubes were heated to 75˚C for 10 minutes. Samples were subsequently stored at -80˚C or used directly for reverse transcription (see below).

For smaller tissue samples, i.e. tissues where RNA yield was significantly lower, the above protocol was slightly adjusted. Thus, 1 µg total RNA was mixed with 2 µl 10x Incubation Buffer and 5 units DNase I, and DEPC-treated water was added to a final volume of 20 µl. In the case of the original (see above) and the adjusted protocol, 10 µl of the final reaction volume were used in reverse transcription (see below).

5.2.4. Reverse transcription (cDNA synthesis)

To synthesize cDNA, reverse transcription was carried out using DNase-treated total RNA. For this purpose, 10 µl aliquots of each DNase-treated sample were added to 0.5 ml polypropylene tubes. Given a starting amount of 2.5 µg RNA (original protocol) or 1 µg RNA (adjusted protocol) during DNase treatment (see above), 10 µl represent about 0.5 µg RNA per reverse transcription reaction. All enzymes, buffers and other reagents used in reverse transcription were from a commercial kit (SuperScript First-Strand Synthesis System, Invitrogen). All steps were carried out on ice unless otherwise indicated.

To the DNase-treated RNA aliquots (10 µl each), 1 µl random hexamers and 1 µl 10 mM dNTP mix were added. Samples were incubated at 65˚C for 5 minutes and then on ice for 2 minutes. The remaining components were premixed (per sample: 2 µl 10x RT buffer, 4 µl 25 mM $MgCl_2$, 2 µl 0.1 M DTT, 0.5 µl RNase OUT, 1 µl SuperScript Reverse Transcriptase [50

U/µl] and 0.5 µl RNase-free water) and 10 µl mix were added per sample. Subsequently, samples were incubated at 25˚C for 10 minutes, 42˚C for 50 minutes, 70˚C for 15 minutes and then quickly chilled on ice. The final reaction volume (22 µl per sample) was diluted 1:2 by addition of 22 µl RNase-free water, and cDNA was stored at -20˚C until use.

As a negative control, aliquots of RNA were processed as above, but in the absence of the reverse transcriptase enzyme. These so-called -RT (or "minus RT") controls allow identification of contamination from genomic DNA or exogenous sources, preventing false-positive results. Thus, whenever -RT reactions yielded a band in subsequent PCR, the samples were excluded and cDNA synthesis was repeated using different RNA aliquots.

5.2.5. Extraction of genomic DNA from mouse tail biopsies

Mouse tail biopsies were suspended in 500 µl tail lysis buffer (see "Self-made reagents", section 5.6.1.1) and incubated overnight on a thermomixer (Eppendorf) at 50˚C and 600 rpm. On the next day, samples were vortexed and then centrifuged (12,000 x g for 5 minutes) to remove residual fur and tissue debris. DNA was precipitated by transferring the supernatants to fresh tubes containing 500 µl isopropanol, mixing well, and centrifuging at 12,000 x g for 1 minute. The isopropanol was then carefully discarded and the DNA pellet washed by adding 300 µl of ice cold 70% ethanol and vortexing. After centrifugation (12,000 x g for 1 minute) the ethanol was discarded, the DNA pellet was allowed to air-dry and subsequently resuspended in 300 µl TE buffer. A final incubation on the thermomixer (10 minutes, 50˚C, 1000 rpm) was performed to ensure complete dissolution of the DNA.

5.2.6. Polymerase chain reaction (PCR)

The polymerase chain reaction (PCR) is an extremely versatile technique widely used in practically every molecular biology laboratory. It allows the specific isolation and amplification of DNA fragments for a variety of purposes, and numerous applications have been derived from the original method. In our experiments, conventional PCR was used to generate DNA fragments complementary to cellular mRNA transcripts, and to detect the presence of wild-type or knock-out gene alleles in DNA samples from individual mice.

5.2.6.1. Amplification of transcripts of interest

After synthesis of cDNA, primers (short DNA oligonucleotides; see section 5.6.2 for all sequences) specific for a given gene of interest were used in PCR to amplify a fragment corresponding to the gene's expressed mRNA. Thus, in tissues such as hypothalamus, pituitary and adrenal glands, expression of the target gene could be detected, and a specific fragment could be amplified for use in downstream applications. In cases where fragments were intended to serve as standards for quantitative PCR (qPCR), primers were chosen that amplify relatively short fragments, as these are necessary for qPCR. Fragment length was typically between 100-200 base pairs (bp; minimum 84, maximum 247). Most of these primers were retrieved from a validated database in which all primers are designed according to uniform

criteria (Wang and Seed, 2003). If no primers were available in the database, they were designed using Primer3 (available online, e.g. at http://frodo.wi.mit.edu) based on the current mRNA Reference Sequence (RefSeq) for the genes of interest. Primers to be used in the generation of templates for cRNA production were designed to yield sizes between 400-500 bp, and were based on the same RefSeqs that were used to design primers for qPCR (where applicable, i.e. where primers for qPCR had been designed before).

Reagents used for PCR were from one commercial source (AmpliTaq Gold reagents and GeneAmp dNTP mix, Applied Biosystems). Primers were ordered from IDT (Integrated DNA Technologies). In a typical PCR, a master mix was prepared by mixing (per sample) 2.5 µl 10x PCR buffer, 1 µl $MgCl_2$ (25 mM), 2 µl dNTP mix (2.5 mM of each dNTP), 0.1 µl AmpliTaq Gold DNA polymerase, and 17.4 µl DEPC-treated water. To the resulting 23 µl per sample, 1 µl of a pre-made mix of forward and reverse primers (5 µM each; final concentration 200 nM) and 1 µl cDNA template were added, for a final reaction volume of 25 µl. Samples were pipetted into 0.2 ml PCR tubes (MicroAmp, Applied Biosystems). PCR was performed on a PTC-200 thermocycler (MJ Research), and a typical program looked as follows:

Step	temperature	time
1	95°	5 minutes
2	95°	30 seconds
3	60°	45 seconds
4	72°	45 seconds
5	return to step 2	34 times
6	72°	7 minutes
7	4°	forever

Since the DNA sequences and thermodynamic characteristics of the oligonucleotide primers define the exact conditions for a given PCR program, the above parameters were adjusted when needed. For example, the temperature used for annealing of the primers to the cDNA template (step 3) was raised when unspecific amplification occurred, or lowered in case of no amplification. For transcripts whose abundance was very low, additional cycles were inserted (step 5) to further prolong the chain reaction. When PCR remained unsuccessful, alternative primers were designed and tested.

In some cases, e.g. when target transcript abundance was low (larger volumes needed for visualization on agarose gels), or the amplified fragment was to be extracted from the agarose gel or purified from the PCR mixture, the volume of all reagents was linearly scaled up (e.g. doubled) according to the specific need.

5.2.6.2. Genotyping PCR

Genotypes were determined by gel electrophoresis of PCR products generated using primers for the wild-type and knock-out alleles of the gene encoding PACAP (see section 5.6.2 for primer sequences). Wild-type mice (homozygous, alleles +/+) display one band around 510 bp,

while knock-out mice (homozygous, alleles -/-) display a single band around 310 bp (Hamelink et al., 2002). Samples from heterozygous mice (genotype +/-) result in two PCR products, apparent as two bands around 510 bp and 310 bp. DNA samples from mice of known genotypes were frequently included as controls to ensure generation of correctly sized PCR products. PCR reagents were from one commercial source (Invitrogen). Samples were pipetted into 0.2 ml PCR tubes (MicroAmp, Applied Biosystems) as follows:

Reagent	volume [µl]	final concentration
10x PCR buffer	5	1x
$MgCl_2$ (50 mM)	1.5	1.5 mM
dNTP mix (10 mM each)	1	200 nM
primer Neo-OF (10 µM)	1	500 nM
primer PACAP-2-R (10 µM)	1	500 nM
primer PNT1-R (10 µM)	1	500 nM
Platinum Taq Polymerase	0.5	0.05 U/µl
genomic DNA from tail biopsies	1	not applicable
DEPC-treated water	38	not applicable

The following program was run on a PTC-200 thermocycler (MJ Research):

Step	temperature	time
1	94˚C	3 minutes
2	94˚C	30 seconds
3	63˚C	45 seconds
4	72˚C	1 minute
5	return to step 2	34 times
6	72˚C	10 minutes
7	4˚C	forever

5.2.7. Agarose gel electrophoresis

After completion of PCR, an aliquot of each sample was used for agarose gel electrophoresis. This method allows visualization of specific cDNA fragments as bands, separated according to their size, indicating successful PCR and expression of the target gene in the tissue of interest. In addition, specific bands (i.e. the fragments they represent) can be excised from the gel, purified and used in downstream applications. Gels were prepared as 1-2% agarose (UltraPure Agarose, Invitrogen) in 1x TAE buffer (Quality Biologicals), and ethidium bromide (Invitrogen) was added to the gel for a final concentration of 0.5 µg/ml. Ethidium bromide intercalates into DNA and fluoresces when exposed to ultraviolet light, allowing visualization of bands.

Typically, for simple visualization of bands, 15-20 µl PCR product were mixed with 2-4 µl 6X Orange DNA Loading Dye (Fermentas), carefully dispensed into the gel pockets, and subjected to electrophoresis at 5 V/cm for about 45-60 minutes (depending on the expected

fragment sizes). In cases where the bands were to be extracted from the gel, larger volumes (up to 40 µl) of the PCR product were loaded. To identify bands based on their electrophoretic migration pattern, size markers were run in parallel with the samples (GeneRuler 100 bp Plus DNA Ladder, Fermentas). Bands were visualized, and corresponding images saved as digital files, using a dedicated imaging system (KODAK Image Station 440 CF).

5.2.8. Gel extraction of PCR-derived cDNA fragments

After exposure to ultraviolet light, specific bands were identified and excised using a scalpel. Slices of agarose gel containing cDNA fragments of interest were processed using a commercially available kit, based on DNA binding to silica membranes and subsequent column purification, according to the manufacturer's instructions (NucleoSpin Extract II, Macherey-Nagel). After elution, cDNA concentrations were measured (see "Determination of nucleic acid concentration") and samples were stored at -20˚C until use.

5.2.9. Purification of cDNA fragments from PCR mixtures

In cases where cDNA fragments had previously been properly identified, e.g. by means of gel electrophoresis and/or sequencing, they were purified directly from the PCR reaction mixture. This method circumvents electrophoresis, excision from the gel and removal of agarose, resulting in a simpler workflow and potentially cleaner samples. Purification of cDNA fragments was carried out using the same kit employed for gel extraction (NucleoSpin Extract II, Macherey-Nagel).

5.2.10. Serial dilution of cDNA fragments for standard curves

To generate standard curves for quantitative PCR, i.e. a range of known cDNA concentrations against which transcript abundance in a sample can be measured, serial dilutions of gel-extracted or purified cDNA fragments were generated. The first standard concentration was prepared to represent 1 pg/µl of the cDNA of interest. Via serial 1:5 dilutions in DEPC-treated water, the following standards were made: 0.2, 0.04, 0.008, 0.0016, 0.00032, $6.4*10^{-5}$ pg/µl. Occasionally, when transcript abundances in experimental samples were found to be outside of this range, more or less concentrated standards were added as needed. All standards were stored at -20˚C and used repeatedly, unless their performance deteriorated, in which case fresh serial dilutions were prepared.

5.2.11. Quantitative PCR (qPCR)

Quantitative PCR represents one of the many technological developments based on the conventional PCR method. In contrast to conventional PCR, where amplified fragments are visualized at the end of the procedure (endpoint PCR), quantitative PCR allows for detection of amplification products as they appear in the reaction (real-time PCR). In our experiments, detection was accomplished through the use of a fluorescent dye (SYBR Green I) that binds to double-stranded DNA, thus producing increasing levels of fluorescence as amplification

products accumulate. We used a master mix containing SYBR Green I, dNTPs, DNA polymerase, $MgCl_2$, and several additional components (iQ SYBR Green Supermix, Bio-Rad). Reactions were assembled in 96-well optical PCR plates (Bio-Rad) as follows: per sample, 10 µl master mix, 1 µl primer mix (5 µM each; see 5.6.2 for sequences) and 9 µl DEPC-treated water were combined, and 20 µl of this mixture were dispensed into each well. Duplicates of cDNA samples (2 µl per well) prepared from tissues of interest were then added for a final volume of 22 µl per well. Plates were loaded into an iCycler iQ Real Time PCR System (Bio-Rad) and run using the following PCR conditions:

Step	temperature	time
1	95˚C	3 minutes
2	95˚C	10 seconds
3	55˚C	45 seconds
4	return to step 2	39 times
5	95˚C	1 minute
6	55˚C	1 minute

Finally, to verify generation of a unique amplicon, a melting curve was performed (80 steps of +0.5˚C increments, 10 seconds each, from 55˚C to 95˚C).

Fluorescence data were continuously monitored and recorded by the iCycler's software (Optical System Software, Version 3.1, Bio-Rad). Based on the cDNA standard curves included in each run, the software calculated transcript abundance in unknown samples. Values for standards and samples were transferred to a Microsoft Excel spreadsheet in which further calculations were carried out (see "Calculation of experimental results", section 5.4.1).

Note that the combination of reverse transcription (RT) and quantitative PCR (qPCR) is sometimes referred to as qRT-PCR in the present work.

5.2.12. Microarray expression analysis

To determine the expression levels of thousands of transcripts in parallel, DNA oligonucleotide microarrays were used. These microarrays consist of small chips on which thousands of oligonucleotides are printed in a regular grid, each representing a particular mRNA. Our experiments were carried out by the NINDS/NIMH/NHGRI Microarray Core facility, using in-house printed chips equipped with the Array-Ready Oligo Set for the Mouse Genome, Version 3.0 (originally provided by Qiagen). This set of DNA oligonucleotides covers about 70% of the mouse genome (Verdugo and Medrano, 2006), as known at the time the experiments were carried out (2007-2008). To compare gene expression levels between two cohorts of samples or conditions, e.g. between wild-type and PACAP-deficient mice, or between untreated and stressed animals, RNA was extracted and processed according to a typical two-color hybridization workflow. In this method, samples are labeled with the fluorescent dyes Cy3 (condition 1) or Cy5 (condition 2), mixed, and subsequently applied to the microarray chips using specialized chambers. Over time, samples from the two conditions hybridize with the

oligonucleotides on the chips. After laser-induced excitation, a given spot (nucleic acid sequence) on the microarray will thus emit more or less Cy3 and Cy5 fluorescence, reflecting the abundance of the corresponding complementary nucleic acid sequence in the samples. Gene expression levels (mRNA abundances) are thus ultimately measured as ratios of fluorescent light at two wavelengths, and comparisons of mRNA abundance between conditions 1 and 2 (e.g. untreated and stressed) are made based on these ratios.

5.2.12.1. Amplification and labeling of RNA

RNA was extracted from tissues as usual. For amplification (Amino Allyl MessageAmp II aRNA Amplification Kit, Applied Biosystems/Ambion) and fluorescent labeling (CyDye Post-Labeling Reactive Dye Pack, GE Healthcare), commercial kits were used by the Microarray Core facility, according to modified manufacturer's instructions. Briefly, the procedure entails amplification of input RNA through cDNA synthesis followed by in vitro transcription. By coupling to reactive moieties incorporated into the amplified RNA (aRNA), Cy3 and Cy5 labels are introduced, after which the labeled aRNA is purified and fragmented.

5.2.12.2. Microarray hybridization

Cy3- and Cy5-labeled aRNA preparations were mixed, applied to the DNA microarrays in specialized 12-chamber hybridization mixers (MAUI Mixers FL, BioMicro Systems, now Roche NimbleGen), and incubated about 18-24 hours at 45°C. After hybridization, microarrays were washed and dried.

5.2.12.3. Self-self hybridization controls

To control for dye-specific effects occurring during microarray hybridization, which potentially influence the measured gene expression ratios, different controls are commonly used. During our experiments, so-called self-self hybridizations were most often included to control for potential dye bias (Fang et al., 2007). Self-self hybridizations were carried out by pooling samples from different experimental groups (e.g. aliquots of every sample from the study), splitting this pool in half and labeling one half each with Cy3 or Cy5. Thus, after hybridization on microarrays, theoretically all gene expression ratios should be 1. In experiments where self-self controls were present, genes with spurious self-self ratios (greater than 1.5 or smaller than 0.66, respectively) were excluded from further analysis. Alternatively, a dye swap was performed, i.e. the labeling of the two sample cohorts with Cy3/Cy5 was reversed in a second hybridization, and results from the two hybridizations were checked for congruence.

5.2.12.4. Scanning, data acquisition and analysis

Microarrays were scanned using a DNA Microarray Scanner (Agilent Technologies). Primary image processing was carried out using the DeArray suite for IPLab software (Scanalytics Inc.) and data were obtained from the Microarray Core facility as image and result files. These were uploaded into the mAdb microarrary analysis environment (http://madb.nci.nih.gov) and

analyzed. Analysis entailed normalization (LOWESS correction), quality-filtering (Ratio Quality Measure >= 0.8) and statistical evaluation (SAM, significance analysis of microarrays), where false discovery rate was typically set to ~1%. Data were subsequently exported to Microsoft Excel, and only those transcripts with 2-fold or greater difference in abundance between conditions 1 and 2 (untreated and stressed, or wild-type and PACAP-deficient) were retained. Multiple oligonucleotide targets representing a single Entrez GeneID were collapsed by calculating the average of the respective mean expression ratios.

5.2.13. Cloning of PCR-derived fragments

Cloning provides a means to modify (recombine) and propagate DNA fragments by inserting them into vectors, introducing these vectors into cells, growing the cells (thereby replicating the inserted recombinant DNA) and finally isolating DNA from them. Different vectors, in conjunction with an array of restriction enzymes, provide a variety of options for modification of DNA, and recombinant DNA technology has provided powerful tools for molecular biology. Also, once cells harboring recombinant DNA have been produced, they can be frozen and stocked for future propagation and use.

For our experiments, a relatively simple plasmid vector was employed whose features of interest consist of two promoters, in opposite orientation, to which the bacteriophage-derived SP6 and T7 RNA polymerases bind. The pGEM-T vector (Promega) can therefore be used to produce RNA species of defined orientation, i.e. sense or antisense relative to a cellular mRNA, after a cDNA fragment ("insert") specific to this mRNA is inserted between the SP6 and T7 promoters and in vitro transcription is performed (see below).

5.2.13.1. Ligation of inserts into a plasmid vector

After extraction from agarose gels or direct purification from PCR mixtures, cDNA fragments were used for ligation. During this process, the ends of the cDNA fragment are joined with the open ends of the vector via the enzymatic activity of a DNA ligase. Reactions were assembled in 0.5 ml polypropylene tubes by mixing 5 µl 2x Rapid Ligation Buffer, 1 µl pGEM-T Vector (50 ng), 3 µl PCR product, and 1 µl T4 DNA Ligase. Based on the concentrations of cDNA fragments obtained during purification, and given that the inserts were all about 0.5 kb in size, the molar ratio of vector to insert typically was about 3:1 (see pGEM-T manual for details). After incubation at room temperature and 4°C for 1h each, ligated samples were either stored at 4°C or used for transformation of bacterial cells.

5.2.13.2. Transformation and plating of competent cells

In order to produce relatively large quantities of very pure DNA sequences of interest, cDNA fragments were introduced into bacterial cells after ligation into the pGEM-T vector. These cells take up exogenous DNA quite readily (they are "competent" for transformation) and grow fast, thereby effectively amplifying the cDNA fragments that were introduced. The cells used in our experiments were from a strain of Escherichia coli that does not require electroporation

(OneShot MAX Efficiency DH10B-T1R Competent Cells, Invitrogen), making it very easy to handle. Reactions were assembled according to the manufacturer's instructions, briefly as follows: one vial of competent cells (50 µl) per ligated fragment was thawed on ice, 5 µl of each fragment were dispensed directly into the competent cells, both were mixed by tapping the vial gently and then incubated on ice for 30 minutes. Vials were subsequently incubated for exactly 30 seconds in a water bath at 42°C (without mixing or shaking!) and quickly placed on ice afterwards. After addition of 250 µl pre-warmed (42°C) SOC medium (Invitrogen) per vial, all samples were incubated in a shaker/incubator at 37°C for exactly 1 hour at 225 rpm. In the meantime, using ready-made powdered mixes (E. coli FastMedia, Fermentas), two agar plates were prepared per sample, containing ampicillin (50 µg/ml), IPTG (100 µg/ml) and X-gal (100 µg/ml). After incubation, 20 µl (plate 1) and 50-200 µl (plate 2) of bacterial cell suspension were spread on these plates. Plates were inverted and incubated at 37°C overnight. Remaining bacterial cell suspension was stored at 4°C and plated out the next day, if necessary.

5.2.13.3. Selection and culture of bacterial cells harboring recombinant DNA

On the day after plating, bacterial cultures were inspected for clones harboring the pGEM-T vector and carrying the successfully inserted cDNA fragment of interest. Clones that did not take up the vector or an insert-negative vector (i.e. empty vector DNA without fragment of interest) appeared blue, while clones that successfully incorporated the vector plus insert appeared white. Single white clones were picked using sterile inoculating loops and transferred to 15 ml conical polypropylene tubes (Sarstedt) containing 4 ml LB broth (Quality Biological) supplemented with 100 µg/ml ampicillin. Tubes were incubated in a shaker overnight at 37˚C and 225 rpm. On the next morning, cell suspensions were checked for sufficient bacterial growth and absence of obvious contamination, and either stored at 4˚C or directly used for preparation of frozen stocks or DNA extraction (see below).

5.2.13.4. Frozen stocks of bacterial cell cultures

Frozen stocks of bacterial cell suspension cultures are a convenient means of archiving the recombinant DNA contained in the cells. For this purpose, glycerol was added as a cryoprotectant as follows: the 15 ml tubes containing bacterial cultures were agitated so that the cells were evenly suspended. 200 µl glycerol (UltraPure Glycerol, Invitrogen) were dispensed into tubes suitable for freezing at very low temperatures (NUNC CryoTubes, Thermo Fisher Scientific). 800 µl bacterial culture were added, and thorough mixing was achieved by pipetting up and down several times. Tubes were placed on dry ice for immediate freezing and transferred to -80˚C for long-term storage.

5.2.14. Isolation of plasmid DNA from transformed cells

For extraction of plasmid DNA from bacterial cells, a commercial column-based kit was used (QIAprep Spin Miniprep Kit, Qiagen). As starting material, an aliquot of 1.7 ml bacterial cell suspension per culture was transferred to a 2 ml polypropylene tube, and the cells were

condensed into a pellet by centrifugation (3 minutes at 12,000 x g). Subsequent steps were carried out according to the manufacturer's instructions, and DNA was eluted with 50 µl DEPC-treated water. Quality and quantity of DNA in all batches of preparations were monitored as described above (see "Determination of nucleic acid concentration") and found to be very consistent.

5.2.15. Identity verification of cloned DNA via sequencing and BLAST

To confirm that fragments of interest were cloned correctly, and to avoid spurious results in downstream applications, aliquots of every plasmid DNA were sequenced by the NINDS DNA Sequencing Facility. Reactions were carried out on ABI PRISM 3100 Genetic Analyzers (Applied Biosystems). Using standard SP6 and T7 oligonucleotides for priming, both strands of the plasmid DNA were read, and resulting sequences were saved as digital files. These files were opened using freely available software (Chromas Lite Version 2.01) and exported in FASTA format. Finally, sequences were analyzed using a nucleotide BLAST algorithm (http://blast.ncbi.nlm.nih.gov) by querying the "Mouse genomic plus transcript" database. All sequences were found to exactly match the transcript sequences they were designed for, and sense versus antisense strand orientation of the cloned fragments was determined.

5.2.16. Preparation of radioactively labeled complementary RNA (cRNA) probes

RNA probes complementary to expressed mRNA (cRNA probes) can be used to detect transcripts of interest in cells or tissues. While other methods (such as real-time PCR) allow more precise quantification of transcript abundance in extracts of cells or tissues, cRNA probes hybridize with their corresponding mRNA at the very location of its expression, and this location can be revealed using specific labeling and detection strategies. Thus, in situ hybridization histochemistry (see below) using cRNA probes provides important information about gene expression in complex tissues such as the brain.

5.2.16.1. Production of DNA templates for in vitro transcription (Insert-PCR)

After confirming the identity and orientation of every cloned fragment (insert) by sequencing, corresponding plasmid DNA was used in a PCR primed with oligonucleotides corresponding to the SP6 and T7 promoter sequences. Since these promoters flank the multiple cloning site of the pGEM-T vector, PCR using SP6 and T7 primers resulted in amplification of the entire insert adjacent to the promoters. After purification from the PCR mixture, amplicons could thus be used for in vitro transcription (see below). For insert-PCR, reactions were scaled up to a final volume of 100 µl per fragment, containing 10 ng of plasmid DNA and 200 nM of each primer. The insert-PCR program was adjusted relative to typical programs, based on relatively large amounts of template DNA and larger amplicon sizes:

Step	temperature	time
1	95˚C	3 minutes
2	94˚C	45 seconds
3	60˚C	1 minute
4	72˚C	1 minute
5	return to step 2	29 times
6	72˚C	6 minutes
7	4˚C	forever

In addition to sequencing, insert-PCR provided information on the orientation of cDNA fragments inserted into the pGEM-T vector. By priming the reaction with either an SP6 or T7 promoter-bearing oligonucleotide and a fragment-specific forward primer, the RNA polymerase (SP6 or T7) that produces sense or antisense transcripts during in vitro transcription (see below) could be deduced. In our experiments, sequencing and insert-PCR were used as a means of cross-validation, and they agreed in all cases.

5.2.16.2. In vitro transcription, DNase treatment and purification of cRNA

In our experiments, cRNA probes were initially prepared using non-radioactive methods, in which UTP labeled with digoxigenin (DIG) is incorporated and later revealed using chromogenic or fluorescent techniques (DIG RNA Labeling Kit, DIG Nucleic Acid Detection Kit and HNPP Fluorescent Detection Set; Roche Diagnostics). However, the adrenal cortex was found to display an unacceptably large degree of unspecific staining, both with sense and antisense probes, such that subsequent experiments were carried out using only radioactively labeled cRNA.

Per reaction, an aliquot of ^{35}S-labeled UTP [uridine 5'-(alpha-thio)triphosphate, 1250 Ci/mmol, 12.5 mCi/ml; Perkin Elmer] was dispensed into a 0.5 ml polypropylene tube and dried in a refrigerated centrifugal evaporator (SpeedVac Concentrator, Savant). The desired volume of sense probes was only half of the volume needed for antisense probes. Thus, for the preparation of antisense and sense cRNA, 4 µl and 2 µl ^{35}S-UTP were typically used, respectively, and volumes of all other reagents were scaled accordingly. All steps during the procedure were carried out on ice unless otherwise indicated, and volumes in the subsequent paragraphs correspond to the protocol followed for production of an antisense probe.

A master mix was prepared by combining (per antisense probe) 1 µl NTP-U (mixture of ATP, CTP and GTP; 5 mM each; Bioline), 1 µl DTT (100 mM; Roche), 1 µl 10x Transcription Buffer (Roche), 0.5 µl RNase inhibitor (40 U/µl; Bioline) and 0.5 µl DEPC-treated water (Quality Biologicals). Dried radioactive aliquots were resuspended in 5 µl plasmid DNA, which equaled 90-180 ng DNA. After addition of 4 µl master mix and 1 µl SP6 or T7 RNA polymerase (Roche), tubes were incubated for 90 minutes at 37°C in a water bath. To remove template DNA, 1 µl RNase-free DNase I was added (Roche) and tubes were incubated for another 15 minutes at 37°C in the water bath. The reaction volume was brought to 40 µl ($volume_{pre}$) by addition of 29 µl DEPC-treated water, and an aliquot of 1 µl was added to 5 ml of scintillation cocktail (Ultima

Gold, Perkin Elmer) to determine radioactivity (dpm_{pre}) on a scintillation counter (LS6500, Beckman Coulter). Unincorporated nucleotides were removed by column purification according to the manufacturer's instructions (RNase-free Micro Bio-Spin P-30 Tris Chromatography Columns, Bio-Rad). After elution from the column, the reaction volume was determined ($volume_{post}$) and another aliquot of 1 µl was prepared for scintillation counting (dpm_{post}). The efficiency with which ^{35}S-UTP was incorporated into the cRNA probes was calculated using the following formula:

$$\% \text{ incorporation} = (dpm_{post} * volume_{post} * 100) / dpm_{pre} * volume_{pre})$$

Efficiency of incorporation was monitored as a quality index for the in vitro transcription reaction, and was usually found to be between 60-80%.

5.2.16.3. Dilution of radioactive cRNA in hybridization buffer

Hybridization buffer was prepared in 10 ml aliquots and stored at -20°C until use. It was made up of 10% dextran sulfate (EMD Chemicals), 600 mM NaCl, 10 mM Tris-HCl (both Quality Biological), 1 mM EDTA disodium salt (Promega), 0.05% yeast tRNA (Invitrogen), 1x Denhardt's solution (USB Corporation), 100 µg/ml sonicated salmon sperm DNA (SABiosciences, now Qiagen) and 50% formamide. To achieve a specific activity of 50,000 dpm/µl ($activity_{final}$), hybridization buffer, 1 M DTT (Roche) and DEPC-treated water were added to the purified cRNA probes according to the following formula:

$$\text{total final probe volume} = dpm_{post} * (volume_{post} / activity_{final})$$

Hybridization buffer was added to make up 90% of the total final probe volume, DTT was added to make up 2%, and DEPC-treated water to fill up the remainder. Probes were stored at -20°C and used within days after preparation.

5.3. In situ hybridization histochemistry

In situ hybridization histochemistry (ISH) allows visualization of gene expression in tissues, providing important information concerning the function of complex organs such as the brain. The molecular biological aspects of the method rely on the pairing of bases in nucleic acids (hybridization), and gene transcripts (mRNA) can in principle be detected via complementary DNA or RNA probes. An advantage of DNA probes is their rapid availability, as oligonucleotide synthesis has become very cheap in recent years. In our experiments, complementary RNA probes were used, primarily for two reasons:

1. RNA:RNA hybrids are more stable than DNA:RNA once they have formed in situ.
2. Relatively long cRNA (400-500 bases) provides very good specificity of hybridization.

In addition to these molecular biological considerations, ISH involves histochemical techniques that have been developed and refined over many years. Together, they provide an essential tool for the understanding of gene expression and function in the context of tissues and organisms.

5.3.1. Preparation of frozen sections

Frozen sections were prepared using a cryostat (Thermo Microm HM 525, Thermo Fisher Scientific), which consists of a microtome housed in a temperature-controlled chamber. Tissue samples were removed from storage at -80°C and transferred to the cryostat, where they were allowed to equilibrate to chamber temperature (around -18°C) for at least 20 minutes. Brains and adrenal glands (left gland per mouse) were then embedded in O.C.T. compound (Tissue-Tek, Sakura Finetek) and thoroughly frozen using the cryostat's heat extractor. After cutting at 14 µm thickness, sections (one brain per slide, or two adrenals per slide) were carefully thaw-mounted onto microscope slides (Fisherbrand Superfrost Plus, Thermo Fisher Scientific), air-dried at room temperature, and either processed directly or stored at -80˚C.

5.3.2. Prehybridization

All prehybridization steps were carried out at room temperature, with solutions agitated in beakers using magnetic stir bars. For fixation, the glass slides with air-dried sections were immersed in 4% formaldehyde in PBS (freshly prepared from paraformaldehyde) for 60 minutes. After three washes in PBS (10 minutes each), sections were permeabilized using 0.4% Triton X-100 in PBS for 10 minutes, washed again in PBS for 5 minutes, and then rinsed in distilled water. Acetylation was carried out in TEA buffer (1.3% triethanolamine in PBS, pH 8.0) by adding 1.25 ml acetic anhydride while stirring vigorously, and then incubating for 10 minutes. This was followed by washing in PBS for 10 minutes and rinsing in distilled water. Finally, sections were dehydrated by rinsing in 50% and 70% isopropanol for one minute each, allowed to air-dry, and either used directly or stored frozen at -20˚C until hybridization.

5.3.3. Hybridization

To create a humidified incubation chamber, the bottom of a plastic dish (NUNC BioAssay Dish, Thermo Fisher Scientific; dimensions: 245 x 245 x 30 mm, length x width x height) was covered with blotting paper (3MM Chr, Whatman, part of GE Healthcare) soaked in 50% formamide. For sections of mouse brain, 20 µl of radioactive probe were dispensed onto an 18 x 18 mm glass cover slip. For sections of mouse adrenal glands, 25 µl of probe were dispensed onto a 22 x 22 mm glass cover slip. By lowering the slide with the tissue sections facing the drop of probe solution, the cover slips were carefully picked up, such that they adhered closely to the glass slide, covering the section completely. Care was taken to exclude air bubbles. Slides were then placed in the humidified chamber and incubated in an oven at 65˚C for 16-18 hours.

5.3.4. Posthybridization

One by one, slides were picked up from the humidified chamber, briefly dipped into a beaker containing 2x SSC, and the glass cover slips were carefully lifted off using a forceps. Slides were placed into a slide holder in a second beaker with 2x SCC until all cover slips had been removed. All subsequent washing steps in SSC and distilled water were carried out in beakers where solutions were agitated using a magnetic stir bar.

Slides were washed in 2x SCC and 1x SCC (20 minutes each), before removal of non-specifically bound probes was accomplished by incubation in RNase buffer (see "Self-made reagents") for 1 hour at 37˚C. Subsequently, washes were carried out in 1x, 0.5x and 0.2x SSC (20 minutes each), followed by a "hot wash" in 0.2x SCC at 60˚C for 1 hour. After additional washes in 0.2x SSC and distilled water (15 minutes each), slides were dehydrated by rinsing in 50% and 70% isopropanol for one minute each, and allowed to air-dry.

5.3.5. Autoradiography using film (regional analysis)

After posthybridization, slides were aligned in an 8 x 10 inch autoradiography cassette (Research Products International). In a darkroom, a sheet of autoradiography film (Kodak Biomax MR, Carestream Health) was then apposed to the sections on the slides, and the cassette was closed tightly and stored for various exposure times. Films were developed using an automatic processor (Kodak X-OMAT 2000A, Carestream Health) and visually inspected. For transcripts with very high abundance in a given tissue, signals were evident after as little as 4 hours of exposure, whereas others took around 20 hours to appear. In our experiments, film autoradiography was used to estimate the exposure time of sections after coating with emulsion (see below), and to analyze gene expression at the regional level. For the latter purpose, the films were scanned at high resolution (2400 or 4800 dpi) on a conventional flatbed scanner (Scanjet 4890, Hewlett-Packard).

5.3.6. Autoradiography using emulsion (cellular analysis)

In order to identify individual cells expressing transcripts of interest, radioactive cRNA probes can be visualized in tissue sections after coating with autoradiographic emulsion. The energy emitted during radioactive decay generates microscopic silver grains while passing through the emulsion, and these silver grains can be visualized under a microscope, together with the underlying cells. In our experiments, autoradiography emulsion Type NTB (Carestream Molecular Imaging) was diluted 1:2 in double distilled water and stored as aliquots at 4˚C, tightly shielded from light to avoid even the slightest unintentional exposure. All work involving emulsion was carried out in a darkroom. An aliquot of emulsion was placed in a water bath at 42°C, together with a special glass dipping cuvette (Dip Miser, Electron Microscopy Sciences), and equilibrated for about 45 minutes. Subsequently, the emulsion was carefully poured into the cuvette, allowed to sit for a few minutes, after which a glass slide was dipped into the emulsion to check for air bubbles.

Slides with tissue sections, sorted according to estimated exposure times, were dipped into the emulsion, excess emulsion was drained on the rim of the cuvette, and slides were tapped carefully on a paper towel. Slides were then placed in a gridded paper box, in an upright fashion, with the frosted end facing the experimenter. Several open plastic tubes containing desiccant (Drierite, W.A. Hammond Drierite) were also placed in the box to ensure a dry atmosphere, and the box was left in the darkroom overnight. On the next day, dried slides were sorted into boxes, which were wrapped in two layers of aluminum foil, and placed at 4°C. After varying exposure times (40-90 hours), development was carried out as follows: slides were placed into a metal slide holder and submerged in a glass jar containing Developer D-19 (Kodak; obtained through Ted Pella Inc.) for 4 minutes, followed by tap water for 30 seconds, and Fixer (Kodak) for 10 minutes. Lastly, slides were rinsed in running demineralized water overnight.

5.3.7. Counterstaining of tissue sections

After rinsing overnight, glass slides carrying the tissue sections were cleaned by carefully removing residual emulsion from the back of the slides, using a razor blade and tissue wipes. All following steps were carried out in glass staining jars, each holding about 400 ml of solution. Sections were briefly stained in cresyl violet solution (see section 5.6.1.3) for about 1 minute to visualize cells without masking hybridization signals (silver grains). After washing in demineralized water (twice for 2 minutes), slides were passed through a graded series of isopropanol (70%, 80%, 96%, 100%, 100%; 2 minutes each) and fully dehydrated via three steps of xylene (5 minutes each). One by one, slides were removed from the last xylene jar, covered with DPX mounting medium (Sigma) and a cover slip, and allowed to cure in a fume hood overnight.

5.3.8. Microscopic analysis of tissue sections

Images of tissue sections were obtained through a microscope (Eclipse 50i, Nikon Instruments) connected to a CCD camera (Retiga 1300i Fast 1394, QImaging) and captured using iVision software (version 4.0.14, BioVision Technologies) running on an Apple Macintosh computer. To visualize silver grains as bright white speckles over cells, a Darklite illuminator was used (Micro Video Instruments). Most images were obtained using 4x or 20x microscope objectives.

5.4. Calculation of experimental results

5.4.1. Calculation of gene expression levels based on qPCR data

Based on the cDNA standard curves included in each qPCR run, the thermocycler's software determined transcript abundance (pg/µl) in unknown samples (result). We then calculated transcript abundance per tissue, e.g. per pair of adrenal glands or pituitary, based on the elution volume of total RNA after extraction (30 µl), RNA aliquots used for DNase treatment (x) and cDNA synthesis (1:5), dilution of cDNA after synthesis (1:2), and the cDNA aliquot used for

qPCR (1:22). The following formula is based on the standard workflow for a pair of adrenal glands:

$$\text{expression per tissue} = \text{result} * 22 * 2 * 5 * [1/(x / 30\ \mu l)] * 2$$

The final multiplier (2) is added to achieve the correct expression level in pg/µl, because 2 µl of each standard were dispensed per well.

5.4.2. Calculation of circulating hormone levels

Corticosterone levels were determined via radioimmunoassay (RIA) or enzyme immunoassay (EIA). RIA samples were measured on a gamma counter (Wizard 1470, Wallac) and results were calculated by the counter's internal software (RiaCalc WIZ program 3.4), based on a weighted parabolic regression. EIA samples were measured on a microplate spectrophotometer (SpectraMax 340, Molecular Devices) and results were calculated using dedicated software (SoftMax Pro 5.3, Molecular Devices) based on four parameter logistic curve fitting. Circulating levels of ACTH were measured via ELISA, using the same microplate spectrophotometer and software as for the corticosterone EIA. However, data were exported to Prism 4 (GraphPad Software) and results calculated using a cubic spline interpolation algorithm. Since results from these assays can in principle be analyzed using different mathematical procedures, we compared these procedures and found the results to be practically identical, showing that our data were reliable and robust.

5.5. Statistical analyses

For all statistical analyses, Prism 4 (GraphPad Software) was used. Results from experiments in vivo were usually calculated using two methods. First, the effects of treatment (stressor exposure) within genotype were assessed, separately for wild-type and PACAP-deficient mice, using one-way analysis of variance (ANOVA). Dunnett's post-test was used to compare untreated mice and mice at various treatment time points. Second, the effects of genotype, i.e. differences between wild-type and PACAP-deficient mice at each of these time points, were analyzed by two-way ANOVA with Bonferroni post-test. In cases where experiments included only one treatment period, effects and differences were assessed by one-way ANOVA with Newman-Keuls post-test (comparison of all four groups). Whenever only two groups were compared, a two-tailed unpaired t-test was used. P values of <0.05 were considered significant. Details concerning statistics are listed in the figure legends.

5.6. Chemicals, buffers and other reagents

Common chemicals (salts, alcohols, solvents etc.) were obtained through Sigma-Aldrich or Thermo Fisher Scientific, unless otherwise indicated. Common buffers (TAE, PBS, SSC), DEPC-treated water and miscellaneous solutions (Tris-HCl, NaCl, 10% and 20% SDS etc.) were from Quality Biological. Sources of special materials, such as enzymes, kits and apparatuses are listed directly in the sections describing the experiments to which they pertain. Oligonucleotides were purchased from Integrated DNA Technologies.

5.6.1. Self-made reagents

Some reagents were prepared as needed, e.g. when they could not be obtained from commercial sources. Their recipes are listed here.

5.6.1.1. Tail lysis buffer

100 mM Tris-HCl, pH 8.0
200 mM NaCl
5 mM EDTA
0.2% SDS
0.2 mg/ml Proteinase K (Roche)
Store at 4°C. Use no longer than one month.

5.6.1.2. RNase buffer

10 mM Tris-HCl, pH 8.0
500 mM NaCl
1 mM EDTA
40 µg/ml RNase A (Roche)
2000 U RNase T1 (Roche)
Store at 4°C. Can be used 10-15 times.

5.6.1.3. Cresyl violet staining solution

5 g cresyl violet acetate (Sigma-Aldrich)
600 ml demineralized water
60 ml 1 M sodium acetate (from acetic acid, sodium salt)
340 ml 1 M acetic acid
Stir in the dark for several days.
Filter before use!

5.6.2. Oligonucleotide primers

Table 2A: Primers for qRT-PCR

primer	sequence (5'-3')	amplicon [bp]	Primer Bank ID
3ßHSD-F	TGGACAAAGTATTCCGACCAGA	250	6680289a1
3ßHSD-R	GGCACACTTGCTTGAACACAG		
AVP-F	GCCAGGATGCTCAACACTACG	123	6753150a1
AVP-R	TCTCAGCTCCATGTCAGAGATG		
CRH-F	CTCAGCAAGCTCACAGCAAC	141	N.A.
CRH-R	GGAGCTGCGATATGGTACAGA		
DBH-F	CGGCTACTGCACAGACAAGTG	91	N.A.
DBH-R	GCCCGTCAGGTGTGTATGAA		
Dusp1-F	ATGCAGCTCCTGTAGTACCC	102	7305423a3
Dusp1-R	ATATCCTTCCGAGAAGCGTGA		
Egr1-F	AGCGAACAACCCTATGAGCAC	100	6681285a2
Egr1-R	TCGTTTGGCTGGGATAACTCG		
Fos-F	CGGGTTTCAACGCCGACTA	166	6753894a1
Fos-R	TTGGCACTAGAGACGGACAGA		
Fosl1-F	ATGTACCGAGACTACGGGGAA	140	6753896a1
Fosl1-R	CTGCTGCTGTCGATGCTTG		
GAL-F	GGCAGCGTTATCCTGCTAGG	104	6753940a1
GAL-R	CTGTTCAGGGTCCAACCTCT		
Ier3-F	GCTCTGGTCCCGAGATTTTCA	195	19526808a1
Ier3-R	AGATGATGGCGAACAGGAGAA		
Nor1-F	AGGATTCACTGATCTCCCCAA	140	7657397a1
Nor1-R	GATGCAGGACAAGTCCATTGC		
Nur77-F	TTGAGTTCGGCAAGCCTACC	100	6754216a1
Nur77-R	GTGTACCCGTCCATGAAGGTG		
Nurr1-F	AACACTGAAATTACTGCCACCA	138	7305325a2
Nurr1-R	TTCTACCTTAATGGAGGACTGCT		
P45011ß-F	AGACACAAGAGAAAGAGGAT	183	N.A.
P45011ß-R	TAGCACTCTAAGGAAGAGAA		
P450c17-F	GCGGATAGTAGTAGCTCCTGG	117	6681097a3
P450c17-R	ACACAGTGAGTTGGCTTCCTG		
P450c21-F	TACAGACCCTTCACGACTGTG	102	6753570a2
P450c21-R	GGTTGGGGAGGAACCTGAG		
P450scc-F	AAAGACCGAATCGTCCTAAACC	117	9789921a3
P450scc-R	CTTGATGCGTCTGTGTAAGACT		
PNMT-F	GACTGGAGTGTGTATAGTCAGCA	109	6679405a3
PNMT-R	CGATAGGCAGGACTCGCTTC		
POMC-F	ATGCCGAGATTCTGCTACAGT	170	6679415a1
POMC-R	TCCAGCGAGAGGTCGAGTTT		
SF-1-F	GCCCTGTTGGATTACACCTTG	135	20522231a2
SF-1-R	GTTGCCCAAATGCTTGTGGTA		

StAR-F	ATGTTCCTCGCTACGTTCAAG	122	31543776a1
StAR-R	CCCAGTGCTCTCCAGTTGAG		
Stc1-F	CTACTTTCCAGAGGATGATCGC *	100	N.A.
Stc1-R	ACTTCAGTGATGGCTTCCGG		
TH-F	CTGTCTCGGGCTTTGAAAGTG	163	6678337a2
TH-R	GACGCACAGAACTGAGGAGG		
VGluT1-F	GAGCGCAAATACATTGAGGATGC	131	33859827a3
VGluT1-R	CAAAAGTTCGCAACGATGATGG		
VGluT2-F	TGGAAAATCCCTCGGACAGAT	120	31543717a1
VGluT2-R	CATAGCGGAGCCTTCTTCTCA		
VIP-F	AGTGTGCTGTTCTCTCAGTCG	162	30794516a1
VIP-R	GCCATTTTCTGCTAAGGGATTCT		
VMAT2-F	ATGCTGCTCACCGTCGTAG	247	27369732a1
VMAT2-R	GGACAGTCGTGTTGGTCACAG		
PAC1-F	GGCCCTGTAGTTGGCTCTATAATGG	**	N.A.
null-R	GAGAGAAGGCAAATACTGTG	187/271	N.A.
hop-R	AGAGTAATGGTGGATAGTTCTGACA	200	N.A.
hip-R	TGGGGACTCTCAGTCTTAAA	142	N.A.

Table 2B: Primers for generation of cRNA probe templates

primer	sequence (5'-3')	amplicon [bp]	target RefSeq
CRH-F2	ATCCGCATGGGTGAAGAATA	408	NM_205769.1
CRH-R2	AAGCGCAACATTTCATTTCC		
Egr1-F2	CCACAACAACAGGGAGACCT	466	NM_007913.5
Egr1-R2	TCTTGCGTTCATCACTCCTG		
GAL-F2	GTGACCCTGTCAGCCACTCT	422	NM_010253.3
GAL-R2	ACGATTGGCTTGAGGAGTTG		
Nor1-F2	GTGTCGGGATGGTTAAGGAA	455	NM_015743.2
Nor1-R2	CTGAAGTCGATGCAGGACAA		
Nur77-F2	CAATGCTTCGTGTCAGCACT	450	NM_010444.1
Nur77-R2	TCTGCCCACTTTCGGATAAC		
Nurr1-F2	AGTCTGATCAGTGCCCTCGT	432	NM_013613.1
Nurr1-R2	AATGCAGGAGAAGGCAGAAA		
SP6	CGATTTAGGTGACACTATAG	***	N.A.
T7	TAATACGACTCACTATAGGG	***	N.A.

Table 2C: Primers for PACAP genotyping

primer	sequence (5'-3')	amplicon [bp]
Neo-OF	CACCGGCCTTTAGGGACCCTTGTA	wild-type allele yields 510 bp,
PACAP-2-R	GCTATTCGGCGTCCTTTGTTTTTAACCC	knock-out allele yields 310 bp;
PNT1-R	TAGGGGAGGAGTAGAAGGTGGCGC	heterozygotes display both sizes

Table 2: Primers used for qRT-PCR, generation of cRNA probe templates and genotyping. (A) Mouse primers were retrieved from Primer bank (http://pga.mgh.harvard.edu/primerbank/index.html) (Wang and Seed, 2003) or designed using Primer3 (available online, e.g. at http://frodo.wi.mit.edu). (B) Primers were designed using Primer3 and the indicated official reference sequences (RefSeq). (C) Primers for PACAP genotyping are based on Hamelink and others (Hamelink et al., 2002). * Stc1-F was originally designed for rat, therefore there is one mismatch with mouse Stc1 mRNA (second base is a T instead of G). ** Detection of all three PAC1 splice variants is carried out with a universal forward primer and variant-specific reverse primers. Primer combination PAC1/null yields two fragments, which indicate the expression of null (187 bp) and hop (271 bp), respectively. *** PCR amplification of subcloned fragments using SP6 and T7 primers yields different amplicon sizes for each fragment. Thus, no amplicon size is indicated for these two primers. F denotes forward primer, R denotes reverse primer. N.A., not applicable. Note that primer names were chosen based on the most commonly used name for the corresponding gene product in mouse. For example, neuropeptides and catecholaminergic enzymes are labeled in capital letters, whereas most other factors are labeled according to their gene symbol or most common synonym. See http://www.ihop-net.org/UniPub/iHOP for a comprehensive database of synonyms for any given factor. In the text, measurements of mRNA abundance are described as such, and references to peptide or protein levels are clearly distinguished to avoid confusion.

5.7. Index of commercial sources of materials and reagents

The following is a list of companies and institutions from which materials and reagents were obtained. In the description of materials and methods used in our experiments, companies are listed only by their name, whereas additional information can be found here.

Company	Location
Agilent Technologies	Santa Clara, CA, USA
Applied Biosystems	Foster City, CA, USA
Applied Biosystems/Ambion	Austin, TX, USA
ASI Instruments	Warren, MI, USA
Assay Designs	Ann Arbor, MI, USA
Beckman Coulter	Brea, CA, USA
Bioline	Taunton, MA, USA
Bio-Rad	Hercules, CA, USA
BioVision Technologies	Exton, PA, USA
Braintree Scientific	Braintree, MA, USA
Carestream Health	Rochester, NY, USA
Carestream Molecular Imaging	New Haven, CT, USA
CEDARLANE Laboratories	Burlington, NC, USA
Electron Microscopy Sciences	Hatfield, PA, USA
Eli Lilly & Co.	Indianapolis, IN, USA
EMD Chemicals	Gibbstown, NJ, USA
Eppendorf	Hamburg, Germany
Fermentas	Glen Burnie, MD, USA
GE Healthcare	Piscataway, NJ, USA
GraphPad Software	La Jolla, CA, USA
Hewlett-Packard	Palo Alto, CA, USA
Hielscher	Ringwood, NJ, USA
Integrated DNA Technologies	Coralville, IA, USA
Invitrogen	Carlsbad, CA, USA
Macherey-Nagel	Düren, Germany
MD Bioproducts	St Paul, USA
Micro Video Instruments	Avon, MA, USA
MJ Research	Waltham, MA, USA
Molecular Devices	Sunnyvale, CA, USA
National Cancer Institute's Animal Production Program	Frederick, MD, USA
Nikon Instruments	Melville, NY, USA
NUNC	Roskilde, Denmark
Perkin Elmer	Boston, MA, USA
Promega	Madison, WI, USA
Qiagen	Valencia, CA, USA

QImaging	Surrey, BC, Canada
Quality Biological	Gaithersburg, MD, USA
Research Products International	Mt. Prospect, IL, USA
Roche Diagnostics	Mannheim, Germany
Roche NimbleGen	Madison, WI, USA
Sakura Finetek	Torrance, CA, USA
Sarstedt	Newton, NC, USA
Scanalytics Inc.	Fairfax, VA, USA
Siemens Medical Solutions Diagnostics	Los Angeles, CA, USA
Sigma-Aldrich	St. Louis, MO, USA
Ted Pella Inc.	Redding, CA, USA
Thermo Fisher Scientific	Waltham, MA, USA
USB Corporation	Cleveland, OH, USA
W.A. Hammond Drierite	Xenia, OH, USA
Zeigler Bros.	Gardners, PA, USA

Some companies have been merged with or acquired by others, such that they no longer operate under their original name. Companies that no longer exist are not listed here.

Note that ™, ©, ® and other symbols representing intellectual property rights or proprietary technologies have been omitted from the text for clarity. All rights to names and methods lie with the respective companies.

6. Results

6.1. Observations concerning the phenotype of PACAP-deficient mice

Several laboratories have reported the generation of mouse strains in which the gene encoding PACAP is disrupted (Colwell et al., 2004; Gray et al., 2001; Hamelink et al., 2002; Hashimoto et al., 2001). The mice used in our laboratory harbor the PACAP knock-out allele first described by Hamelink and others, which in the meantime has been fully backcrossed into the C57BL/6 strain. To determine how these mice compare with reported phenotypes, we assessed several basic parameters over the course of our studies.

6.1.1. Fertility is impaired in PACAP-deficient mice

It has previously been shown that disruption of the gene encoding PACAP causes deficits in female fertility, defined as the ratio of productive matings (where the female delivers pups) to the total number of matings. In a study where the PACAP knock-out allele had been backcrossed over 10 generations into the C57BL/6 strain, fertility of PACAP-deficient mice was only 21% compared to 100% measured for wild-types (Isaac and Sherwood, 2008). Results from another group showed higher values, which depended on the background strain, such that PACAP-deficient compared to wild-type fertility was 33% versus 85%, or 50% versus 80%, respectively, in two different mouse lines (Shintani et al., 2002). In our hands, where PACAP+/+ and PACAP-/- mice were maintained on the C57BL/6 background via breeding of homozygous pairs, the aforementioned results were largely confirmed. Thus, fertility of PACAP-deficient compared to wild-type mice was 52% versus 84%, the latter number agreeing exactly with the value for C57BL/6 in standard mouse breeding literature (Green and Witham, 1991).

6.1.2. Postnatal survival of PACAP-deficient mice appears to be normal

Whereas previous studies have reported increased rates of postnatal death in PACAP-deficient mice (Gray et al., 2001) due to inadequate heat production (Gray et al., 2002), we found no direct evidence for this phenotype in our strain. However, it should be noted that the average temperature in our animal facility (24˚C) is above the temperature at which the aforementioned effects were described (21˚C). Also, we did not monitor every single breeding pair at all times, such that exact calculations of litter size and pup survival rate were not possible. This caveat also pertains to the calculation of fertility, although the results clearly appear robust (see above).

6.1.3. PACAP deficiency causes a lean phenotype

Measuring body weights before and after fasting (approx. 18 hours overnight), we found that PACAP-deficient mice are significantly lighter than their corresponding wild-type controls (before fasting: PACAP+/+ 31.95+/-0.74 g, PACAP-/- 27.3+/-0.44 g; N = 49; see Figure 2A). This is in agreement with recent reports using two different PACAP-deficient strains, even

though these reports provide different explanations for the leaner phenotype (Adams et al., 2008; Tomimoto et al., 2008). Our finding of lower body weight was replicated in several cohorts, also occurred in female mice (see Figure 2B), and correlated with lower amounts of fat tissue observed during organ dissection (not quantified). In addition to being leaner, PACAP-deficient mice in our study lost more body weight as a consequence of food deprivation (PACAP +/+ 9.0+/-0.32%, PACAP -/- 11.83+/-0.43% of initial body weight; N = 49). Statistically significant differences in weight loss were found in most but not all cohorts. Representative results are shown in Figure 2A.

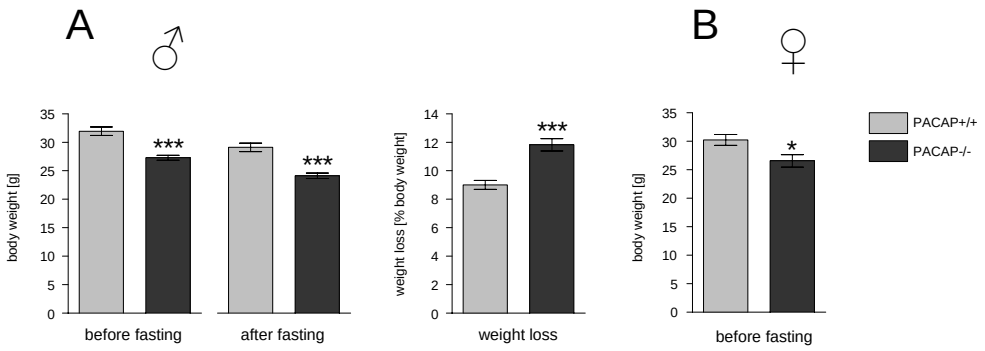

Figure 2. PACAP deficiency causes a lean phenotype. (A) Male mice. Average weight before and after fasting (approx. 18h without food; water continuously available ad libitum), as well as weight loss, were compared between wild-type and PACAP knock-out mice (N = 49 per genotype; average age: 4.2 months). (B) Female mice. Average weight before fasting was recorded and compared between genotypes (N = 16-17 per genotype; average age: 8.8 months). Data are displayed as means +/- SEM. Asterisks indicate significant difference from wild-types. Unpaired t-test (*p<0.05, ***p<0.0001).

6.1.4. Hypoglycemia-induced mortality is higher than previously reported

Initial experiments with the PACAP-deficient mice generated in our laboratory revealed a significant deficiency in the response to sustained systemic stress, such that 10-15% died from hypoglycemia within a few hours after i.p. injection of 2 U/kg insulin (Hamelink et al., 2002). In the present series of studies conducted with fully backcrossed PACAP-/- mice, this number was substantially higher when the same dose was administered, resulting in mortality rates of up to 40% per cohort. Therefore, we adjusted the hypoglycemia paradigm as follows: 1h after insulin injection as usual (2 U/kg, i.p.), mice were injected with glucose (2 g/kg, i.p.) and returned to their home cage. Glucose injections were highly effective, preventing mortality in 100% of the mice. The adjusted experimental paradigm thus represents transient systemic stress, as rescue with glucose eliminates the initial stressor. This is in contrast to prolonged systemic stress, where insulin injection is followed by sustained hypoglycemia without rescue. Results in the following sections are specifically labeled to reflect these two different paradigms.

It should be noted that wild-type mice never showed obvious symptoms of hypoglycemic shock after i.p. administration of insulin at a dose of 2 U/kg, while PACAP-deficient mice invariably did. Within less than one hour after injection, they displayed lower breathing rates, hyporesponsiveness to touch, significant hypothermia, and mild to massive convulsions.

6.2. Microarray analysis of brain and adrenal glands in untreated mice

6.2.1. Basal transcriptome of the adrenal glands

In a first survey, microarray analysis of the adrenal gland transcriptome had yielded no dramatic differences between wild-type and PACAP-deficient mice (Samal et al., 2007). However, the cDNA microarray platform used in this early study did not provide the same level of gene annotation and genome coverage available with current platforms. Therefore, we analyzed the basal transcriptome of the adrenal glands in wild-type (WT) and PACAP-deficient (knock-out, KO) mice using high density DNA oligonucleotide microarrays. Using both adrenal glands per mouse, total RNA was extracted from six individual KO mice. After amplification and labeling, these samples were hybridized with fractions of a pool generated from six WT samples, which had been amplified and labeled in parallel. Data derived from microarray hybridizations were extracted, normalized, quality-filtered and statistically evaluated in mAdb (http://nciarray.nci.nih.gov) and subsequently exported to Microsoft Excel. Here, only those transcripts with 2-fold or greater difference in abundance between the two genotypes were retained. Genes with spurious self-self ratios (greater than 1.5 or smaller than 0.66, respectively) were removed. Multiple oligonucleotide targets representing a single Entrez GeneID were collapsed by calculating the average of the respective mean expression ratios. Tables 3a and 3b (see appendix) show the results derived from this global expression analysis.

It was found that, as measured by microarray, there was a larger number of genes expressed more abundantly in adrenal glands from PACAP KO mice (40 transcripts, 39 of which have GeneIDs; see Table 3b, appendix) than there were genes expressed less abundantly (16 transcripts, 15 of which have GeneIDs; see Table 3a, appendix). The overall number of differentially expressed genes was small, supporting the notion that lack of PACAP does not grossly perturb basal function of the adrenal glands. This is further corroborated by the fact that none of the genes were expressed at a greater than ~3.7-fold difference (see Elovl3, Alb, Nefl).

6.2.2. Basal transcriptome of the cerebral cortex

For analysis of the cerebrocortical transcriptome, samples obtained from 3-4 month old male mice were used. As in the case of the adrenal glands, the cutoff for differential expression was defined as a 2-fold difference in abundance per transcript. Only eight PACAP-dependent genes were found in the cerebral cortex based on this definition (see Table 4, appendix). As noted for the adrenal glands, the absence of large differences in the cerebrocortical transcriptome between wild-type and PACAP-deficient mice suggests that there are no gross abnormalities in this tissue under basal resting conditions.

6.3. Microarray analysis of gene expression patterns in mouse adrenal glands after sustained systemic stress

Having established that the transcriptome of the adrenal glands is not very different between wild-type and PACAP-deficient mice under basal conditions, i.e. in untreated animals, we set out to determine changes in gene expression in response to stress. Although the adrenal glands are composed of two main functional zones, namely the cortex and medulla, whose structural integrity is lost during total RNA extraction, we reasoned that microarray analysis should provide important initial clues regarding the functional state of the glands. There are a number of genes whose expression is known to be restricted to either the cortex or the medulla, allowing preliminary assignment to the zones after generation of global gene expression patterns. Ultimately however, after validation by qRT-PCR, important novel candidate transcripts must be followed up by in situ hybridization histochemistry to provide unequivocal information regarding their localization.

6.3.1. Differential gene expression during hypoglycemia

To screen for genes differentially expressed in the adrenal glands during sustained systemic stress, we conducted a first microarray experiment (Experiment 1) using insulin-induced hypoglycemia as the stressor. Female mice (average age 15 months, age range 12-17 months) were treated with insulin (2 U/kg, i.p.) and killed 3h thereafter. Adrenal glands were excised, total RNA was extracted, and microarray hybridization was carried out as described. The experimental design was as follows: samples from six insulin-treated wild-type (WT) mice were pooled, and fractions of this pool were hybridized with samples from six individual insulin-treated PACAP-deficient (KO) mice. Duplicates of these six hybridizations were carried out as a dye-swap control (labeling of WT/KO with Cy3/Cy5 reversed), such that a total of 12 microarray slides were used, each slide representing hybridization of insulin-treated WT versus insulin-treated KO.

Analysis after 3h of hypoglycemia revealed 62 unique transcripts whose abundance in wild-types was at least 2-fold higher, i.e. appeared *PACAP-dependent* (Table 5a, appendix). Of those, 58 represent known genes with official symbol and GeneID, while four transcripts were identified as Ensembl clones or UniGene clusters. Interestingly, two neuropeptides were differentially expressed, both of which have previously been shown to be upregulated by hypoglycemia-induced stress in rat adrenal glands (Anouar and Eiden, 1995; Fischer-Colbrie et al., 1992). Thus, GAL (encoding galanin; 2.28-fold) and Tac1 (encoding tachykinins, including substance P; 4.45-fold) were more abundantly expressed in wild-types. On the other hand, 66 unique transcripts (representing 64 known genes and two uncharacterized clones) were 2-fold more abundant in adrenal glands from PACAP-deficient mice compared to wild-types, i.e. appeared *PACAP-repressed* (Table 5b, appendix). Somewhat surprisingly, the latter group included a number of genes whose expression is induced by PACAP in PC12 cells in culture, such as Dusp1 (dual specificity phosphatase 1), Egr1 (early growth response 1), Fosl1 (fos-like

antigen 1), Ier3 (immediate early response 3), Nr4a1 (Nur77) and Nr4a2 (Nurr1) (Eiden et al., 2008; Samal et al., 2007), all of which are rapid response genes.

6.3.2. Upregulation of gene expression induced by hypoglycemia

In microarray Experiment 2, male WT and KO mice (average age six months, age range 4.8-6.4 months) were injected with insulin (2 U/kg, i.p.) or 0.9% saline. Three hours after the injection, both adrenals were excised per animal and processed for microarray hybridization as described. This time, however, the experimental setup was as follows: for each genotype, samples from six saline-treated mice were pooled, and fractions of this pool were hybridized with samples from six individual insulin-treated mice. Expression levels (signal ratios) as measured by microarray thus represent insulin-treated WT versus saline-treated WT, and insulin-treated KO versus saline-treated KO. In other words, the effect of insulin-induced systemic stress was assessed within genotype, separately for WT and KO. No dye-swap was performed.

The experiment revealed induction of a large number of transcripts in adrenal glands from PACAP-deficient mice after 3h of stress, whereas wild-type mice displayed relatively few changes. Thus, 222 transcripts showed two-fold or higher induction in KO compared to only 41 transcripts in WT adrenals (Table 6a, appendix). The genes upregulated after hypoglycemia in WT mostly represented a subset of those induced in KO mice, with only nine transcripts being PACAP-dependent (Table 6b, appendix; Figure 3a). Five of these PACAP-dependent genes are Ensembl clones for which no functional annotation was available at the time of analysis.

6.3.3. Overlap between differentially expressed and stress-regulated genes

The two microarray experiments above served to address two basic questions. First, which are the genes differentially expressed in WT and KO adrenal glands during systemic stress? Second, which are the genes upregulated by systemic stress in WT and KO? While answers to each warrant further investigation, we were especially interested in the overlapping set, i.e. the list of genes that are both differentially expressed in the first and upregulated in only one genotype in the second experiment, respectively. For example, a transcript that is more abundant in WT adrenal glands, and upregulated only in WT after insulin-induced hypoglycemia, would appear very likely to be truly PACAP-dependent. Only one transcript (Hhip, hedgehog-interacting protein) appeared to be PACAP-dependent according to this “overlap criterion”. Its expression level was found to be 2-fold greater in WT compared to KO adrenal glands after 3h of hypoglycemia (Experiment 1) and upregulated 2.17-fold in WT (Experiment 2), with no significant change seen in KO mice. On the other hand, 36 transcripts displayed the opposite profile, i.e. were expressed at higher levels in KO versus WT adrenals, and upregulated only or more strongly in KO mice (see Table 7, appendix; see also Venn diagram Figure 3b), thus appearing to be PACAP-repressed in vivo. Notably, 39% (14/36) of these transcripts have recently been shown to be rapidly upregulated by PACAP in PC12 cells, including Dusp1, Egr1, Fosl1, Ier3, Nur77 and Nurr1 (Eiden et al., 2008).

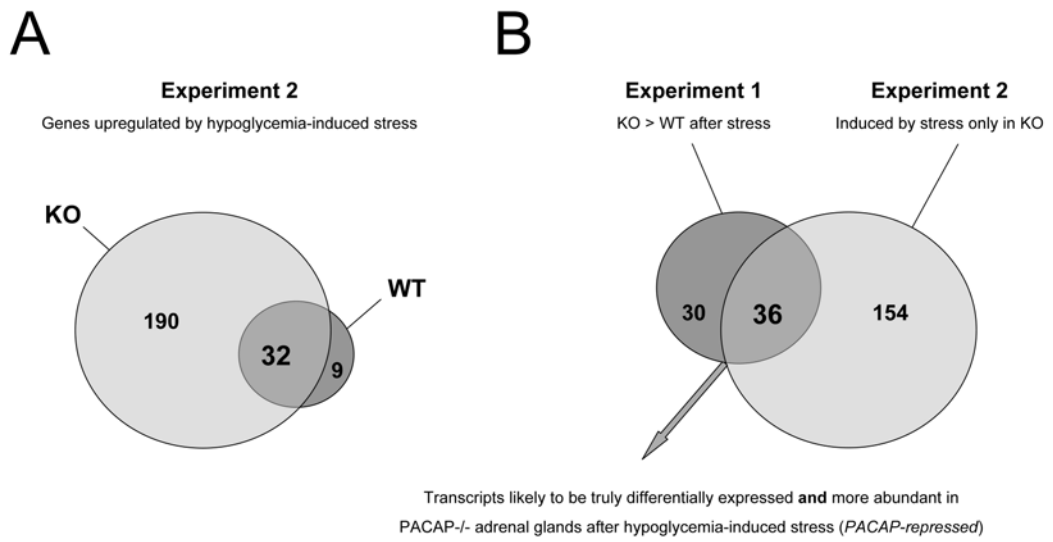

Figure 3. Venn diagrams illustrating results from microarray Experiments 1 and 2. (A) Of all the genes upregulated in mouse adrenal glands during 3h of sustained systemic stress (Experiment 2), only 9 are upregulated exclusively in wild-type (WT) mice. The remainder is either upregulated in both genotypes (32 genes) or only in PACAP knock-out (KO) mice (190 genes). (B) Overlap of Experiment 1 (comparison of stressed KO with stressed WT) and Experiment 2 (comparison of stressed versus control, each for KO and WT). We found 36 candidates in common between the 190 genes upregulated only in KO (Experiment 2) and the 66 genes expressed at higher levels in KO versus WT (Experiment 1); see Table 7 in the appendix. These 36 candidates are very likely to be truly *PACAP-repressed*. Only one transcript (Hhip) displayed the opposite profile, such that the overlap of our two microarray experiments revealed only one *PACAP-dependent* candidate.

6.4. Validation of microarray results by qRT-PCR

Microarray experiments 1 and 2 had both been carried out with samples obtained after 3h of prolonged systemic stress. To confirm the regulation of some of the target genes thus identified, aliquots of the same RNA samples used for microarray analysis in Experiment 2 were reverse transcribed and subjected to quantitative PCR. We found that, as indicated by microarray, transcripts encoding Ier3 and Nurr1 were upregulated in PACAP-deficient adrenal glands after 3h of hypoglycemia, reaching significantly higher levels than those observed in wild-type mice at the same time point. On the other hand, Egr1 was induced to the same extent in both genotypes, even though microarray had indicated higher expression levels in PACAP-deficient adrenal glands. Thus, two out of three transcripts we tested confirmed the microarray results (Figure 4), both with respect to differential expression (more abundant in KO, Experiment 1) and induction (upregulated 2-fold only in KO, Experiment 2). It is worth noting that the relatively small (and statistically non-significant) increases in Ier3 and Nurr1 expression observed after insulin injection in wild-type mice were only 2.3-fold and 2.9-fold compared to saline, respectively. Since qRT-PCR provides a more sensitive and quantitative measurement of mRNA levels, it is perhaps not surprising that both Ier3 and Nurr1 failed to meet the cutoff (2-fold induction) during analysis of data from wild-types in Experiment 2, as microarrays tend to underestimate the magnitude of differences in transcript abundance.

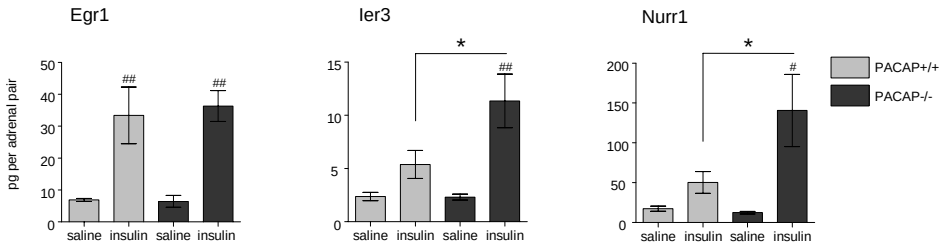

Figure 4. Confirmation of microarray results by qRT-PCR. Male mice (N = 4 per time point; average age: 6 months) were injected with 0.9% saline or 2 U/kg insulin (both i.p.) and killed 3h thereafter. Data from qRT-PCR of both adrenal glands per mouse are displayed as means +/- SEM. Pound signs indicate significant difference between saline and insulin within each genotype. Asterisk indicates significant difference between genotypes. One-way ANOVA with Newman-Keuls multiple comparison test; $^{\#}p<0.05$, $^{\#\#}p<0.01$, $*p<0.05$.

As mentioned, transcripts encoding Egr1, Ier3 and Nurr1 are rapidly induced in PC12 cells after treatment with PACAP (Eiden et al., 2008). Since our microarray experiments and corresponding qRT-PCR validation were carried out after 3h of sustained hypoglycemia, we questioned whether earlier time points after insulin injection might reveal a *PACAP-dependent* gene expression pattern, rather than a *PACAP-repressed* pattern as observed so far. We therefore performed a time course study in which mice were left untreated (controls) or injected i.p. with 2 U/kg insulin and killed 1h, 2h, 4h or 6h thereafter. As shown in Figure 5, all three transcripts were already upregulated 1h after insulin injection, with Egr1 and Nurr1 reaching identical maximal levels in both genotypes. Only Ier3 appeared PACAP-dependent at this time point. Beyond this earliest regulation, the expression patterns differed markedly between wild-type and PACAP-deficient adrenal glands. Thus, supporting the microarray study and corresponding validation by qRT-PCR, all three transcripts remained elevated in knock-out mice, an effect that reached statistical significance for Egr1 and Ier3. Taken together, these experiments indicate that after an initial peak occurring rapidly after stressor exposure, expression is sustained in PACAP-deficient adrenal glands during prolonged hypoglycemia, while levels in wild-types return to baseline.

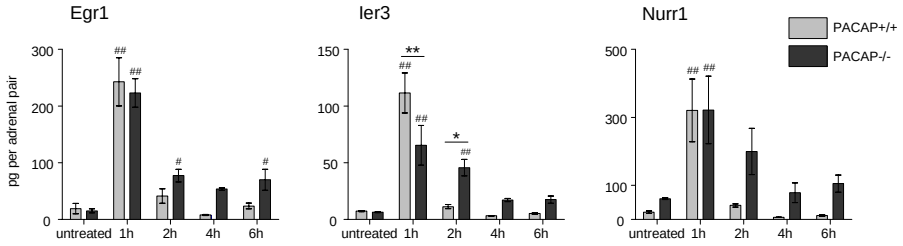

Figure 5. Prolonged hypoglycemia induces sustained expression of rapid response genes in adrenal glands from PACAP-deficient mice. Data from qRT-PCR of both adrenal glands per mouse are displayed as means +/- SEM (N = 3-4 male mice per time point; average age: 11.5 months). Pound signs indicate significant difference between untreated and post-injection time points within each genotype (one-way ANOVA with Dunnett's multiple comparison test; $^{\#}p<0.05$, $^{\#\#}p<0.01$). Asterisks indicate significant difference between genotypes (two-way ANOVA with Bonferroni post-test; $*p<0.05$, $**p<0.01$).

Overall, the qRT-PCR results confirm our microarray data, in that induction of gene expression was correctly indicated for 3/3 (100%) of the transcripts tested, while differential expression was correctly called in 2/3 cases (66%; Ier3 and Nurr1), using intra-sample validation (i.e. aliquots of the same RNA for microarray and qRT-PCR). Therefore, having successfully used global expression analysis as a means of capturing genes potentially involved in stress signaling, several transcripts identified in microarray Experiments 1 or 2 were chosen as candidates for further experiments.

As noted earlier, we found that insulin-induced prolonged systemic stress caused mortality in PACAP-deficient mice, at rates far exceeding those previously reported (Hamelink et al., 2002). Therefore, in most of the subsequent experiments, transient stress was provoked via insulin-induced hypoglycemia, followed 1h later by glucose injection.

6.5. Regulation of rapid response genes and inducible transcription factors during transient systemic stress is largely unaffected by PACAP knock-out and occurs even in the presence of cholinergic antagonists

When applied to PC12 cells in culture, PACAP increases expression of rapid response genes, including regulators of transcription and cellular signaling (Eiden et al., 2008). In the first set of our present experiments (prolonged systemic stress; see above), two examples of these *PACAP-responsive* genes (Egr1 and Nurr1) were found not to be PACAP-dependent in the adrenal glands in vivo. In a second part of the study (transient systemic stress), we extended our analysis to include more of these candidate genes and determine their expression patterns.

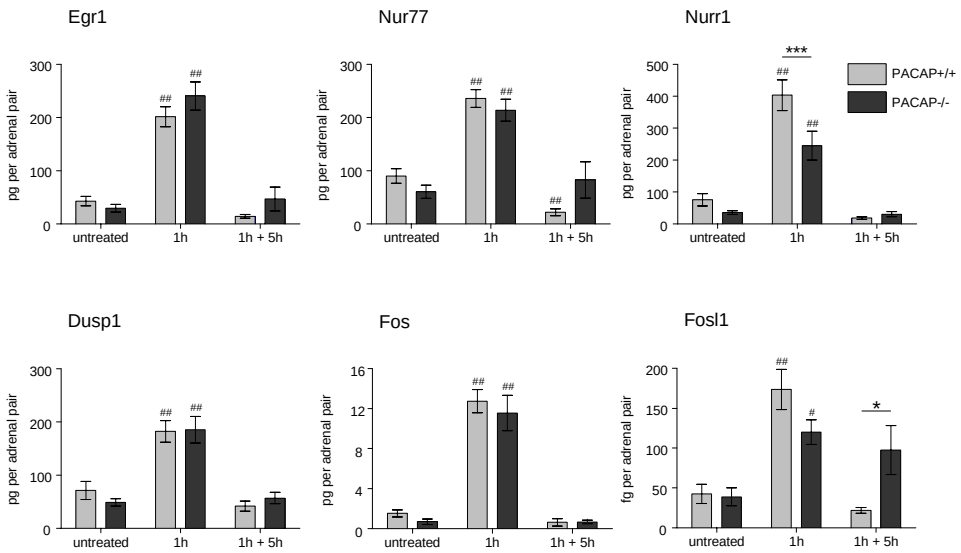

Figure 6. Rapid upregulation of genes encoding inducible transcription factors and signaling proteins in response to transient hypoglycemia is largely unaffected by PACAP knock-out. Data from qRT-PCR of both adrenal glands per mouse are displayed as means +/- SEM (N = 6-13 male mice per time point; average age: four months). Pound signs indicate significant difference between untreated and post-treatment time points within each genotype (one-way ANOVA with Dunnett's multiple comparison test; $^{\#}p<0.05$, $^{\#\#}p<0.01$). Asterisks indicate significant difference between genotypes (two-way ANOVA with Bonferroni post-test; $*p<0.05$, $***p<0.001$).

Consistent with the results obtained after prolonged systemic stress, initial induction of most rapid response genes we tested was equivalent in both genotypes. Thus, 1h after injection of insulin, robust upregulation was observed for Egr1 and Nur77, two transcription factors known to be regulated by diverse stimuli in a variety of tissues (see Figure 6). Likewise, Dusp1 and Fos (FBJ osteosarcoma oncogene) expression displayed an identical pattern in adrenal glands from wild-type and PACAP-deficient mice. In contrast to prolonged hypoglycemia, where microarray and qRT-PCR had indicated sustained induction of rapid response genes in PACAP-deficient adrenal glands, transient hypoglycemia provoked transient induction, with expression levels returning to baseline after the initial peak at 1h. An exception to this pattern was Fosl1. Diverging from the first set of results, Nurr1 mRNA upregulation was blunted by about 40% in PACAP-deficient relative to wild-type mice (see Figure 6).

The main neurotransmitter at the sympathoadrenal synapse, i.e. the interface between the sympathetic splanchnic innervation and adrenal chromaffin cells, is acetylcholine (ACh), and PACAP is known to be a co-transmitter for ACh in splanchnic nerve terminals. Since the rapid induction of transcripts like Egr1 and Nur77 appeared unaffected by PACAP knock-out, we therefore reasoned that their expression in response to systemic stress could be inhibited by pretreatment with cholinergic antagonists. To pharmacologically block nicotinic and muscarinic ACh receptors, respectively, chlorisondamine (5 mg/kg, i.p.) and atropine (1 mg/kg, i.p.) were co-administered 15 minutes prior to injection of insulin. These doses have previously been shown to block hypoglycemia-induced gene expression in the adrenal glands (Kanamatsu et al., 1986). Mice were either pretreated with saline or antagonists, treated 15 minutes later with saline or insulin, and killed 1h after treatment. Thus, there were one control and three experimental groups per genotype, according to pretreatment + treatment, respectively: control (saline + saline), hypoglycemia (saline + insulin), antagonist control (antagonists + saline) and ganglionic blockade (antagonists + insulin).

In wild-type mice (Figure 7, left panels), insulin-induced stress significantly upregulated expression of Egr1 and Nur77, to the same extent as seen in previous experiments. Pretreatment with antagonists alone (antagonist control) provoked the same magnitude of upregulation, and values from mice in the ganglionic blockade group were indistinguishable from the two other experimental groups. Thus, all three experimental groups showed significantly higher expression levels of Egr1 and Nur77 compared to the control. There were no statistically significant differences between the three experimental groups. Essentially the same pattern was found in adrenal glands from PACAP-deficient mice, with all three experimental groups displaying higher Egr1 and Nur77 mRNA abundance compared to controls (Figure 7, right panels). The only statistically significant exception was that Egr1 was more abundant in the two insulin-treated groups than in the antagonist control group.

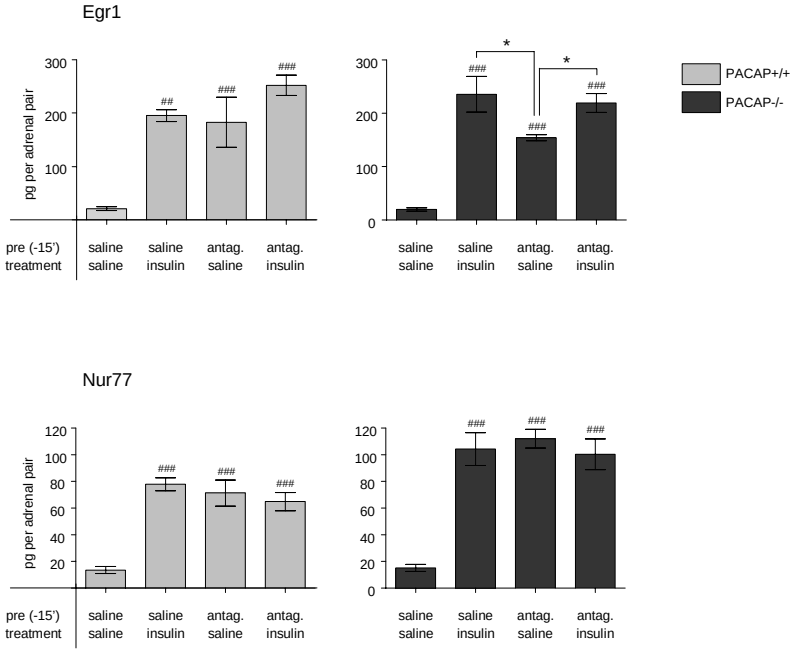

Figure 7. Pharmacological blockade of cholinergic signaling does not prevent hypoglycemia-induced expression of rapid response genes in the adrenal glands, even in PACAP-deficient mice. Mice were pretreated with saline or cholinergic antagonists (antag.; 5 mg/kg chlorisondamine plus 1 mg/kg atropine, co-administered i.p.) 15 minutes before treatment with saline or insulin, and adrenal glands were dissected 1h after treatment. Data from qRT-PCR of both adrenal glands per mouse are displayed as means +/- SEM (N = 4 male mice per time point; average age: 5.4 months). Values are means +/- SEM. Pound signs indicate significant difference from the saline control group ($^{\#\#}p<0.01$, $^{\#\#\#}p<0.001$). Asterisk indicates differences between other groups ($*p<0.05$). One-way ANOVA with Newman-Keuls Multiple comparison test.

In PACAP-deficient mice, pretreatment with cholinergic antagonists followed by saline elicited mild symptoms reminiscent of insulin-induced hypoglycemia. Although somewhat less obvious, the same was true for wild-types, which also became noticeably hyporesponsive. Pretreatment with antagonists followed by treatment with insulin provoked clear signs of stress in wild-type mice. This was in stark contrast to previous experiments, where wild-type mice had never been visibly affected by insulin treatment alone. Animals were hyporesponsive, had reduced breathing rates, and rested on the floor of their cages in a sprawled, immobile position. Thus, although cholinergic blockade did not inhibit stress-induced gene expression as expected, it was clearly physiologically effective.

6.6. Systemic stress-induced expression of the “promiscuous” rapid response gene Egr1 occurs in the adrenal cortex and medulla

Several rapid response genes, most prominently Egr1 and Fos, have been described as “promiscuous” because their expression is induced by a variety of factors in many cells and tissues. This discriminates them from genes whose inducible expression appears in a more

specific fashion, e.g. in response to cellular depolarization (Machado et al., 2008). Rapid induction of Egr1 mRNA occurred equally pronounced in both PACAP genotypes, with some of our evidence suggesting that expression is transient in wild-type but sustained in PACAP-deficient adrenal glands, at least under conditions of prolonged systemic stressor exposure. Since the latter phenomenon could potentially be explained by zonal differences in expression, e.g. genotype-independent induction in adrenal medulla but PACAP knock-out-specific maintenance in cortex, we determined the cellular localization of Egr1 mRNA using in situ hybridization histochemistry. Mice were subjected to insulin-induced hypoglycemia, killed 1h after treatment, and adrenal glands were analyzed after autoradiographic processing of frozen sections.

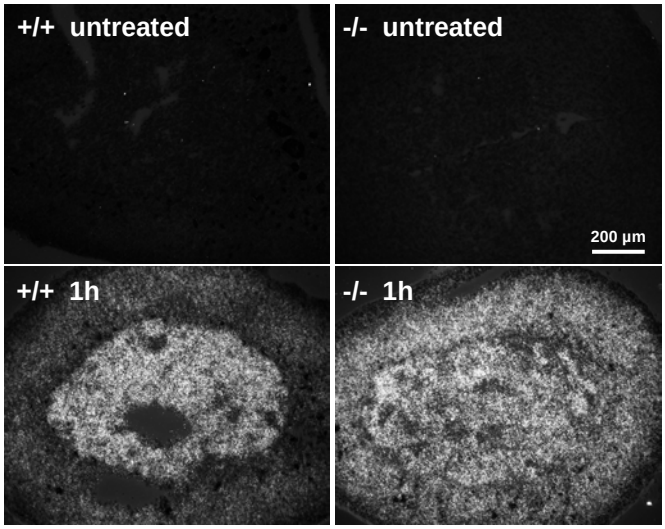

Figure 8. In situ hybridization of Egr1 mRNA in mouse adrenal glands after hypoglycemia-induced stress. Frozen sections of adrenal glands from wild-type (+/+) and PACAP-deficient mice (-/-) were incubated with a ^{35}S-labeled cRNA probe for Egr1. After coating with autoradiographic emulsion and exposure for 40 hours, slides were developed and silver grains (representing specific hybridization signals) were visualized using darkfield microscopy. Scale bar = 200 µm. Note strong increase of signals in cortex and medulla.

Evaluation of tissue sections after relatively short exposure times (40 h) revealed very low Egr1 expression levels in untreated mice. Within 1h after insulin injection, substantial induction occurred in both genotypes, with intense hybridization signals throughout both adrenal cortex and medulla (Figure 8). While we did not analyze large series of sections and did not quantify in situ expression levels (e.g. via densitometry on autoradiographic film or silver grain counting on sections), Egr1 mRNA abundance in the adrenal cortex appeared to be somewhat higher in PACAP-deficient compared to wild-type mice. Induction throughout the gland suggests that both hormonal (HPA axis) and neural signals (via the splanchnic nerve) participate in regulation of Egr1 expression in response to systemic stress.

6.7. PACAP controls expression of critical adrenomedullary factors

6.7.1. Expression of adrenomedullary neuropeptides implicated in adrenal secretory activity is PACAP-dependently induced during stress

Microarray Experiment 1 revealed differential expression of GAL (encoding galanin) after 3h of systemic stress, with higher levels found in wild-type compared to PACAP-deficient adrenal glands (Table 5a, appendix). However, no upregulation was found in microarray Experiment 2, even though GAL mRNA is known to be induced by hypoglycemia in the rat (Anouar and Eiden, 1995). To determine whether GAL mRNA is indeed induced in mouse adrenal glands during stress, we conducted several additional experiments with wild-type mice and measured expression by qRT-PCR. Prolonged hypoglycemia (insulin, 2 U/kg i.p.) was found to increase GAL abundance within 6h. Absolute expression levels and magnitude of stress-induced upregulation were very similar in male and female mice (Figure 9A). Transient hypoglycemia in male mice elicited a pattern that was virtually identical (Figure 9B).

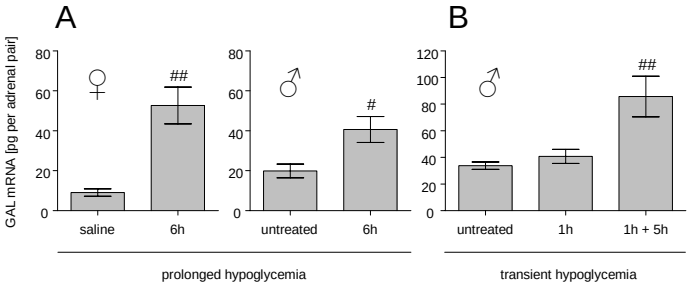

Figure 9. Upregulation of GAL mRNA in mouse adrenal glands after systemic stress. Wild-type mice were injected with insulin (2 U/kg, i.p.) and killed 1h or 6h later. (A) Prolonged hypoglycemia in female (N = 3 per group; average age: 8 months) and male mice (N = 4 per group; average age: 11.5 months). Controls were injected with saline or untreated. (B) Transient hypoglycemia in male mice (N = 7-8 per group; average age: 4.5 months). Mice in the 1h + 5h group received insulin, followed 1h later by glucose (2 g/kg, i.p.), and were killed 5h after the glucose injection. Controls were untreated. Data from qRT-PCR of both adrenal glands per mouse are displayed as means +/- SEM. (A) Pound signs indicate significant difference from controls (unpaired t-test; $^{\#}p<0.05$, $^{\#\#}p<0.01$). (B) Pound signs indicate significant difference from untreated (one-way ANOVA with Dunnett's Multiple comparison test; $^{\#\#}p<0.01$).

Having established upregulation after 6h in adrenal glands from wild-type mice, we determined whether control of GAL mRNA expression is PACAP-dependent, as expected based on microarray Experiment 1. Thus, a time course after transient stressor exposure was performed, where wild-type and PACAP-deficient mice were killed at various times (2h, 5h, 11h) after a 1h period of hypoglycemia. GAL mRNA was significantly induced as early as 3h after insulin injection, and abundance was significantly higher in wild-types at all time points tested. A very modest but statistically significant upregulation also occurred in PACAP-deficient mice (Figure 10A). Similarly, expression of VIP (vasoactive intestinal peptide) was found to be PACAP-dependent, in that abundance was significantly higher in wild-type adrenal glands at most time points. Hypoglycemia induced VIP mRNA 2.5-fold and 1.8-fold in wild-type and PACAP-deficient mice, respectively, although the increase in wild-types did not reach statistical significance (Figure 10A, following page).

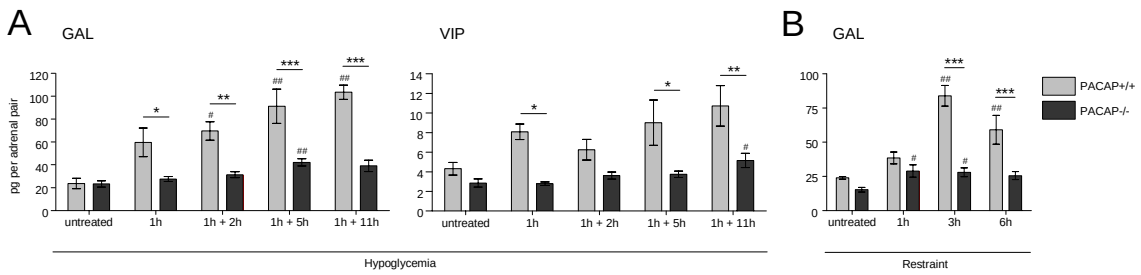

Figure 10. Upregulation of GAL and VIP mRNA in mouse adrenal glands after hypoglycemia- and restraint-induced stress. (A) Male mice (average age: 3.8 months; N = 4 per group) were injected with insulin (2 U/kg, i.p.), followed 1h later by glucose (2 g/kg, i.p.), and killed at various times after glucose injection. Controls were untreated. (B) Male mice (average age: 5.5 months; N = 5 per group) were continuously restrained for different durations and compared to untreated controls. Data from qRT-PCR of both adrenal glands per mouse are displayed as means +/- SEM. Statistical analysis is identical for A and B. Pound signs indicate significant difference from controls (one-way ANOVA with Dunnett's Multiple comparison test; $^{\#}p<0.05$, $^{\#\#}p<0.01$). Asterisks indicate significant difference between genotypes (two-way ANOVA with Bonferroni post-test; $*p<0.05$, $**p<0.01$, $***p<0.001$).

Expression of GAL mRNA in response to restraint displayed the same magnitude and PACAP-dependent pattern seen after hypoglycemia, suggesting that induction of this neuropeptide is a common element of the adrenal reaction to stress. Upregulation was much more pronounced in wild-type mice, leading to significantly higher expression levels compared to PACAP-deficient animals (Figure 10B). It is worth noting that GAL mRNA abundance was very consistent across all experiments, with basal and maximal levels in male and female mice being very similar.

In situ hybridization was carried out to assess the localization of stress-induced GAL mRNA expression. Adrenal gland sections from mice subjected to transient hypoglycemia were used for this purpose. In control animals (untreated), weak hybridization signals were observed in the adrenal medulla, and only few cells displayed sizeable GAL expression. In contrast, a marked increase in GAL-specific signal was observed after treatment (group 1h + 5h), which was restricted to the medulla and clearly more pronounced in wild-type (+/+) compared to PACAP-deficient mice (-/-). These results confirm our qRT-PCR data and show that GAL mRNA is induced throughout the adrenal medulla in response to stress (Figure 11, following page).

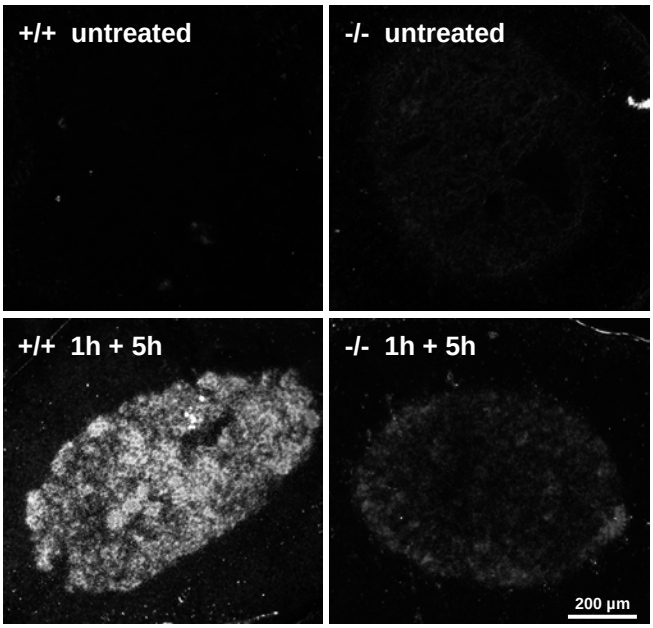

Figure 11. Localization of GAL mRNA in mouse adrenal glands after transient hypoglycemia. Complementary RNA probes labeled with ^{35}S-UTP were added to 14 µm-thick frozen sections of adrenal glands. Sections were coated with autoradiography emulsion, developed after 50 hours of exposure, and counterstained with cresyl violet. Images were captured under darkfield illumination to visualize silver grains representing specific hybridization signals. Six hours after insulin injection, adrenals from wild-type (+/+) and knock-out mice (-/-) show a significant increase in GAL hybridization signal throughout the medulla, and this increase is clearly more pronounced in wild-types. Scale bar = 200 µm.

The adrenal cortex did not show any detectable expression, and hybridizations with GAL sense cRNA probe (negative control) yielded no signals (data not shown).

6.7.2. Induction of catecholamine-synthesizing enzymes is PACAP-dependent in response to processive and systemic stressors

PACAP is known to be required for adrenomedullary catecholamine secretion in response to systemic stress (Hamelink et al., 2002). To investigate whether the catecholaminergic system is also subject to PACAP-dependent transcriptional regulation, expression of transcripts encoding tyrosine hydroxylase (TH) and phenylethanolamine N-methyltransferase (PNMT) was measured in the adrenal glands after exposure of wild-type and PACAP-deficient mice to hypoglycemia- and restraint-induced stress. TH and PNMT are the rate-limiting and final enzyme, respectively, required for the biosynthesis of epinephrine. First, effects of transient versus prolonged restraint were compared. TH was found to be upregulated 2.2-fold only in wild-types (not statistically significant), and levels were significantly lower in PACAP-deficient mice (Figure 12A, following page). In a second experiment, both genotypes showed significant upregulation, and TH mRNA was again more abundant in wild-types (Figure 12B, following page). Results for PNMT were practically identical in both experiments, such that a small but significant increase occurred in PACAP-deficient mice, with a larger increase observed in wild-types (Figure 12A and B). Thus, TH and PNMT mRNAs were found to be clearly PACAP-dependent, with maximal expression levels in wild-type being significantly higher than in PACAP-deficient mice.

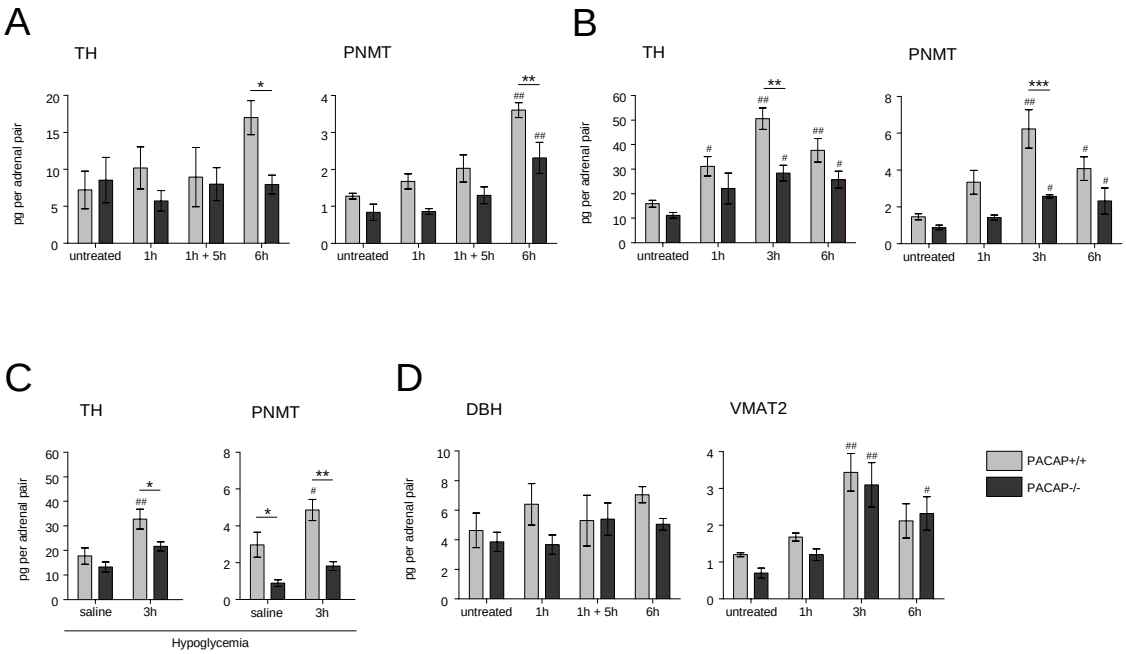

Figure 12. Regulation of adrenomedullary catecholaminergic factors after restraint and hypoglycemia. (A, B, D) Restraint. Male mice (average age: 4.8 months; N = 4-6 per group) were restrained for different durations. Data from qRT-PCR are displayed as means +/- SEM. Pound signs indicate significant difference from controls (one-way ANOVA with Dunnett's Multiple comparison test; $^{\#}p<0.05$, $^{\#\#}p<0.01$). Asterisks indicate significant difference between genotypes (two-way ANOVA with Bonferroni post-test; *p<0.05, **p<0.01, ***p<0.001). (C) Hypoglycemia. Male mice (average age: 5.9 months; N = 4-6 per group) were injected with insulin (2 U/kg, i.p.) and killed 3h later. Controls were injected with saline. Data from qRT-PCR are displayed as means +/- SEM. Pound signs indicate significant difference from the respective genotype's saline control group ($^{\#}p<0.05$, $^{\#\#}p<0.01$). Asterisks indicate differences between genotypes (*p<0.05, **p<0.01). One-way ANOVA with Newman-Keuls Multiple comparison test.

Results for both transcripts were similar in response to systemic stress. After 3h of prolonged hypoglycemia, TH and PNMT were PACAP-dependently upregulated, with levels in wild-type significantly exceeding those in PACAP-deficient mice. In contrast to all other control conditions, we found PNMT mRNA abundance in saline-treated mice from the sustained hypoglycemia experiments to be significantly higher in wild-types, possibly attributable to fasting or mild injection-related stress (Figure 12C).

Transcript levels of dopamine beta-hydroxylase (DBH), the enzyme converting dopamine into norepinephrine, were unaffected by stress and equivalent in both genotypes. Abundance of mRNA encoding the vesicular monoamine transporter 2 (VMAT2) was significantly increased in wild-type and PACAP-deficient mice (Figure 12D). Taken together, our results therefore suggest that PACAP-dependent effects on expression of catecholaminergic factors during stress are restricted to specific target genes, namely the first and the final enzyme required for epinephrine biosynthesis.

6.7.3. Transcription factors implicated in control of adrenomedullary TH and PNMT expression are PACAP-dependently induced in response to restraint

Transcripts encoding Egr1, Fos and Nurr1, inducible transcription factors (ITF) implicated in control of TH and PNMT expression, were PACAP-dependently upregulated in the adrenal glands in response to restraint. Within 1h, transcript abundance robustly increased in both genotypes, but the response in PACAP-deficient mice was significantly impaired, such that mRNA levels were up to <50% relative to wild-types (Figure 13). Upregulation was transient, and there was no statistically significant difference between prolonged (group 6h) and transient restraint (group 1h + 5h), although a trend towards higher expression levels after prolonged exposure was evident for Egr1 and Fos.

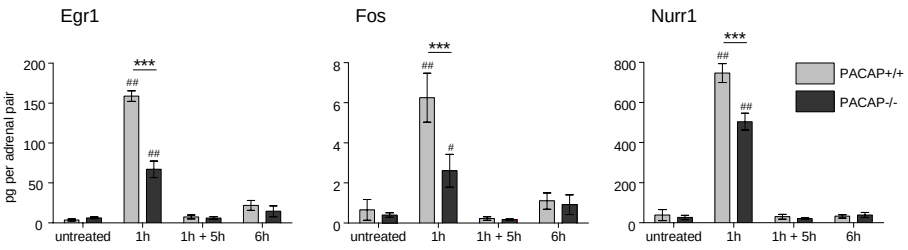

Figure 13. Inducible transcription factors are PACAP-dependently upregulated in mouse adrenal glands in response to restraint. Data from qRT-PCR are displayed as means +/- SEM (N = 4-6 male mice per time point; average age: 4.1 months). Pound signs indicate significant difference between untreated and post-treatment time points within each genotype (one-way ANOVA with Dunnett's multiple comparison test; $^{\#}p<0.05$, $^{\#\#}p<0.01$). Asterisks indicate significant difference between genotypes (two-way ANOVA with Bonferroni post-test; ***p<0.001).

6.8. Stress induces PACAP-dependent expression of potential cytoprotectants in the adrenal glands, but not the hypothalamus

Most of the rapid response genes we tested, such as Egr1 and Fos, displayed a stressor-specific expression pattern, with maximal induction in the adrenal glands following hypoglycemia and restraint being PACAP-independent and -dependent, respectively. In contrast, Ier3 and Stc1 (stanniocalcin 1), encoding putative cytoprotective factors, were found to be PACAP-dependent in both paradigms. Upregulation occurred within 1h and was significantly blunted in PACAP-deficient adrenal glands (Figure 14A and B, following page). Interestingly, restraint-induced expression levels of Stc1 mRNA returned to baseline within 5h after termination of stressor exposure (group 1h + 5h), while they remained elevated in the continued presence of the stressor (group 6h; Figure 14B).

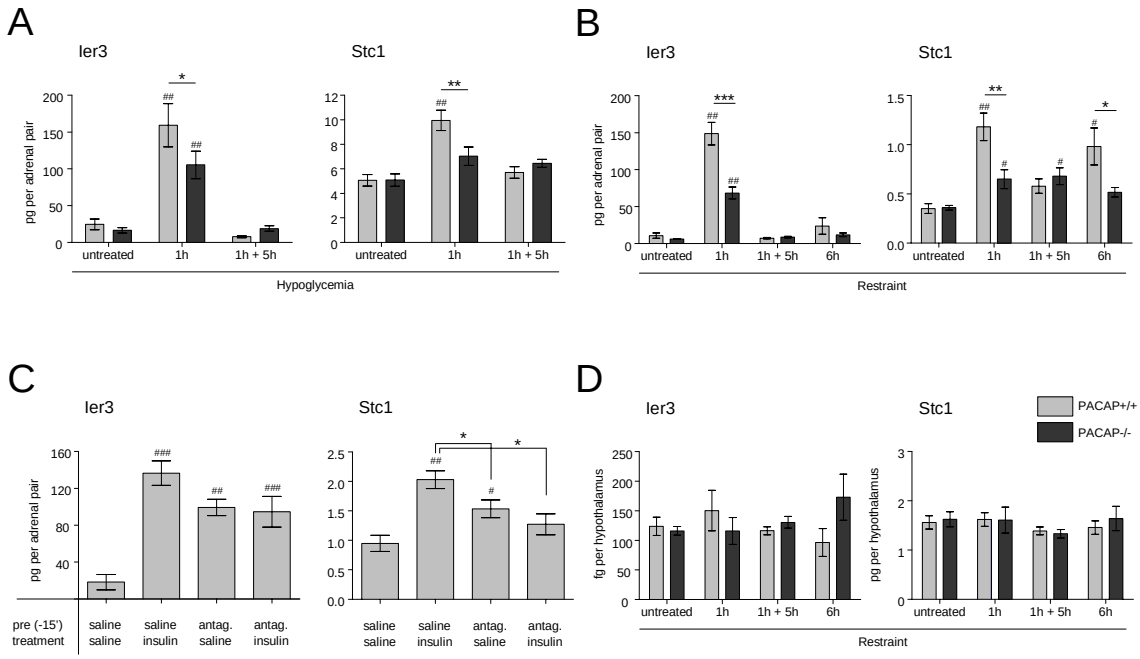

Figure 14. PACAP-dependent expression of potential cytoprotectants is induced by stress in the adrenal glands, but not the hypothalamus. (A) Hypoglycemia (N = 11-13 male mice per time point; average age: four months) and (B) restraint (N = 4-6 male mice per time point; average age: four months) induce expression of Ier3 and Stc1 in mouse adrenal glands. Data from qRT-PCR are displayed as means +/- SEM. Pound signs indicate significant difference between untreated and post-treatment time points within each genotype (one-way ANOVA with Dunnett's multiple comparison test; $^{\#}p<0.05$, $^{\#\#}p<0.01$). Asterisks indicate significant difference between genotypes (two-way ANOVA with Bonferroni post-test; *p<0.05, **p<0.01, ***p<0.001). (C) Effects of ganglionic blockade on adrenal gene expression in wild-type mice (N = 4 male mice per time point; average age: 5.5 months). Pound signs indicate significant difference from the control group (saline + saline). One-way ANOVA with Newman-Keuls multiple comparison test ($^{\#}p<0.05$, $^{\#\#}p<0.01$, $^{\#\#\#}p<0.001$). Asterisk indicates difference from the group exposed to hypoglycemia (saline + insulin; *p<0.05). (D) Expression in hypothalamus (N = 5-6 male mice per time point; average age: four months). Statistics are the same as for A and B.

Similar to what we observed in the case of Egr1 and Nur77 mRNA, Ier3 and Stc1 were elevated above control levels after treatment with cholinergic antagonists (chlorisondamine plus atropine). Pretreatment with antagonists alone resulted in Ier3 expression levels that were almost identical to those elicited by hypoglycemia, and pretreatment with antagonists followed by hypoglycemia was not different (Figure 14C). Stc1 displayed a similar pattern, although hypoglycemia-induced mRNA abundance significantly exceeded all other conditions, and pretreatment with antagonists followed by hypoglycemia was not different from saline controls (Figure 14C).

In the hypothalamus, transcripts encoding Ier3 and Stc1 were unaffected by restraint stress and equally abundant in both genotypes (Figure 14D). This suggests that the PACAP-dependent upregulation of these two rapid response genes is tissue-specific, occurring after exposure to hypoglycemia and restraint in the adrenal glands, but not the hypothalamus. This is in contrast to the stressor-specific regulation of genes such as Egr1 and Fos, whose induction depends on PACAP in adrenal glands (see above) and hypothalamus (see section 6.9.4) during restraint, but not hypoglycemia.

6.9. PACAP is required for responses of the HPA axis to restraint

6.9.1. Volumes of serum obtained from mice after stress exceed those obtained from untreated mice

For measurements of stress-induced secretion of the HPA axis hormones ACTH and corticosterone, trunk blood was collected immediately after decapitation, and the serum was separated. Volumes of serum obtained from wild-type and PACAP-deficient mice were identical at all time points, i.e. in untreated mice as well as after 1h and 6h of restraint. However, when sorting values by time point rather than genotype, we found that volumes of serum obtained from stressed animals were significantly higher than those from untreated controls (Figure 15).

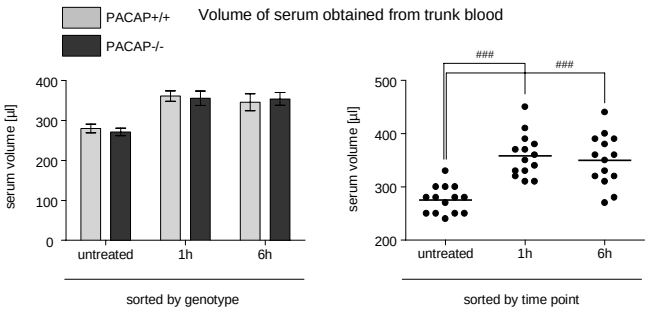

Figure 15. Yields of serum are higher after stress compared to controls, but not different between PACAP genotypes. Serum was obtained from trunk blood after decapitation. Data are displayed as means +/- SEM. Left panel: samples sorted by genotype (N = 7 per time point). No difference was found between genotypes at any time point. Right panel: samples from both genotypes sorted by time point (N = 14 per group). Pound signs indicate significant difference between untreated and post-treatment time points (one-way ANOVA with Newman-Keuls multiple comparison test; $^{###}p<0.001$).

6.9.2. Secretion of ACTH and corticosterone during stress is blunted in PACAP-deficient mice

Stress elicited marked activation of the HPA axis (Figure 16, following page). Serum concentrations of ACTH and corticosterone were increased in both genotypes after 1h of restraint. After 6h, ACTH had normalized and was no longer significantly elevated, whereas corticosterone concentrations remained higher than in untreated animals (Figure 16A). Peak responses of ACTH and corticosterone were significantly blunted in PACAP-deficient mice, as was the sustained phase of corticosterone secretion. Concentrations of ACTH (+/+ 152 vs. -/- 38 pg/ml) and corticosterone (+/+ 282 vs. -/- 163 ng/ml) were 75% and 42% lower, respectively, compared to wild-types after 1h of restraint. The difference in serum corticosterone became even more pronounced after 6h of restraint, with concentrations in PACAP-deficient mice diminished by more than 60% relative to wild-types (+/+ 188 vs. -/- 74 ng/ml; Figure 16A).

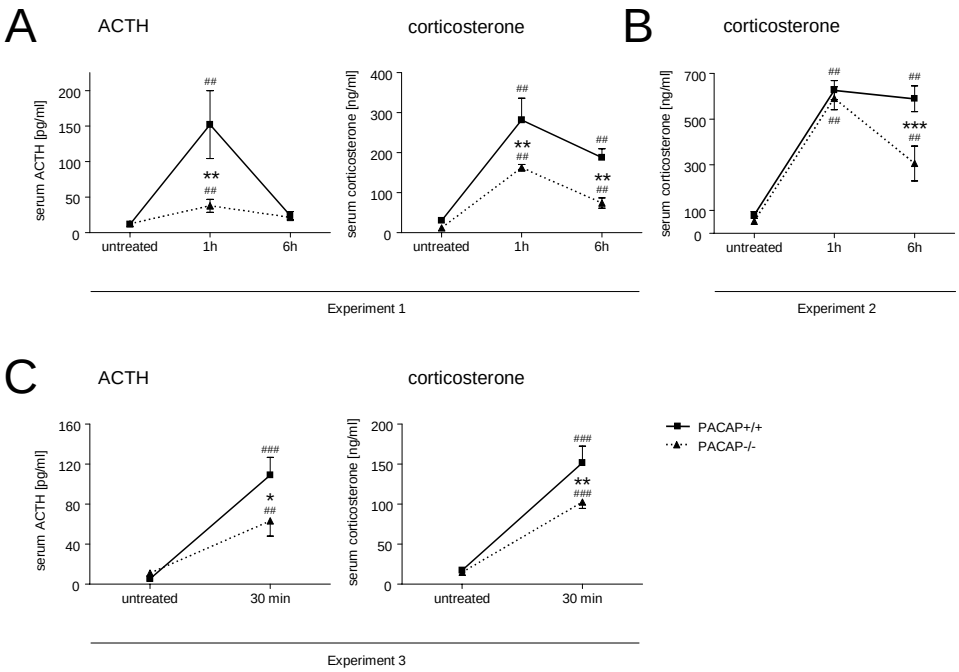

Figure 16. Secretion of ACTH and corticosterone in response to restraint is impaired in PACAP-deficient mice. (A, B) Hormone concentrations in serum were measured after 1h and 6h of restraint in PACAP-deficient and wild-type mice (N = 5-7 per time point) in two separate experiments. Values are means +/- SEM. Pound signs indicate significant difference from the respective genotype's control (untreated). One-way ANOVA with Dunnett's multiple comparison test ($^{\#\#}p<0.01$). Asterisks indicate significant difference between genotypes. Two-way ANOVA with Bonferroni post-test (**p<0.01, ***p<0.001). (C) The early phase of secretion was assessed by measuring serum hormone concentrations after 30 minutes of restraint (N = 8-10 per time point). Values are means +/- SEM. Pound signs indicate significant difference from the respective genotype's untreated control ($^{\#\#}p<0.01$, $^{\#\#\#}p<0.001$). Asterisks indicate significant difference between genotypes (*p<0.05, **p<0.01). One-way ANOVA with Newman-Keuls multiple comparison test.

In order to confirm PACAP-dependent hormone secretion during restraint stress, we conducted a second experiment using the same conditions as before (Figure 16B). This time, the peak of corticosterone secretion in response to restraint was unaffected in PACAP-deficient mice, such that serum concentrations after 1h were not different compared to wild-types. However, as in the first experiment, prolonged restraint resulted in a marked difference between genotypes, to the effect that corticosterone concentrations were about 50% lower in PACAP-deficient mice after 6h (Figure 16B). To clarify whether early secretory responses are intact, i.e. ACTH and corticosterone concentrations are normal after briefer stressor exposure, a third experiment was conducted. Using a larger number of animals in each group, PACAP-deficient and wild-type mice were restrained for 30 minutes and compared to untreated controls. As in the first experiment, serum concentrations of both hormones were lower in PACAP-deficient mice, although the differences were clearly less pronounced compared to prolonged restraint (ACTH 42% lower, corticosterone 33% lower; Figure 16C).

In summary, our results indicate that basal concentrations of ACTH and corticosterone are independent of genotype. However, restraint-induced concentrations of corticosterone in PACAP-deficient mice are 33% (30 min), 42% (1h) and >60% (6h) lower compared to wild-types. Thus, immediately after stressor exposure, output of the HPA axis is relatively mildly impaired, while differences become more pronounced with persistent stressor exposure.

6.9.3. Stress-induced upregulation of CRH mRNA in the paraventricular nucleus of the hypothalamus is PACAP-dependent

Since we found hormonal responses of the HPA axis to restraint significantly blunted in PACAP-deficient mice, and regulation of the axis is known to occur chiefly at the level of the central nervous system, we measured changes in gene expression in the hypothalamus by qRT-PCR and ISH. In response to restraint, mRNA encoding corticotropin-releasing hormone (CRH) was upregulated in a PACAP-dependent pattern. After 1h and 6h of restraint, abundance was significantly higher in wild-type mice, and no upregulation at all was found in hypothalamus from PACAP-deficient animals (Figure 17). Interestingly, our experiment revealed that sustained stressor exposure is required to elicit PACAP-dependent upregulation of CRH. Thus, after 1h of stress followed by 5h of rest (group 1h + 5h), abundance of CRH mRNA was not different from untreated controls, whereas 6h of stress resulted in a 2.2-fold increase in expression. In a second experiment, these findings were confirmed. After 1h, 3h and 6h of restraint, CRH expression levels were about 2-fold higher compared to untreated controls, and no induction at all was observed in PACAP-deficient mice (Figure 17). Thus, restraint-induced upregulation of hypothalamic CRH is completely PACAP-dependent, whereas basal expression levels appear to be unaffected by genotype (no statistically significant differences observed between wild-type and PACAP-deficient mice).

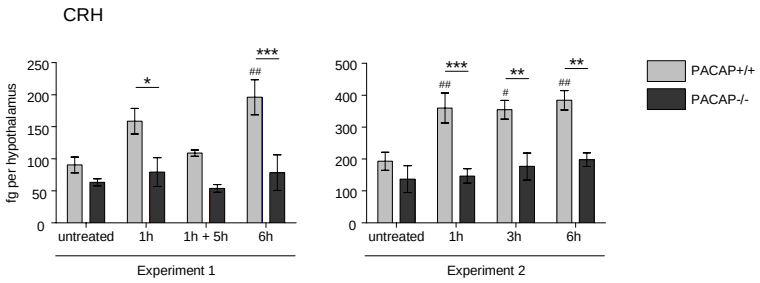

Figure 17. Restraint-induced upregulation of CRH in the hypothalamus is completely abolished in PACAP-deficient mice. Transcript levels were measured by qRT-PCR. Data are displayed as means +/- SEM (N = 5-6 male mice per time point; average age: 4.8 months). Pound signs indicate significant difference from the respective genotype's control (untreated). One-way ANOVA with Dunnett's multiple comparison test ($^{\#}p<0.05$, $^{\#\#}p<0.01$). Asterisks indicate significant difference between genotypes. Two-way ANOVA with Bonferroni post-test (*p<0.05, **p<0.01, ***p<0.001).

In situ hybridization confirmed that our qRT-PCR results reflect regulation of CRH in the paraventricular nucleus (PVN) of the hypothalamus, where hypophysiotropic neurons controlling the HPA axis are located. Specific expression of CRH mRNA was readily apparent in the PVN of untreated wild-type and PACAP-deficient mice. After 1h of restraint, hybridization signals increased significantly only in wild-types, confirming that CRH regulation during stress is fully PACAP-dependent (Figure 18, following page; also see Figure 20 in next section). Hybridization signals for CRH also appeared in the amygdala and scattered in the cerebral cortex, but no genotype differences or effects of treatment were found.

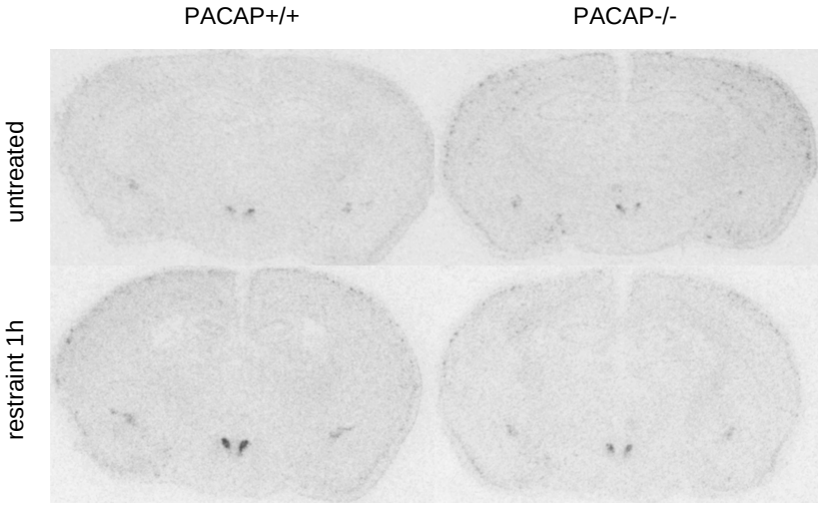

Figure 18. Autoradiographic detection of PACAP-dependent CRH mRNA expression in the paraventricular nucleus (PVN) of the hypothalamus. In situ hybridization with a ^{35}S-labeled cRNA probe for CRH was carried out on 14 µm-thick coronal sections of mouse brain encompassing the PVN. Sections were exposed to autoradiographic film, which was scanned and digitized after development. Images clearly show specific hybridization signals in the PVN, the abundance of which increases after stress (restraint 1h) only in wild-type (PACAP+/+), but not in PACAP-deficient (PACAP-/-) mice. Hybridization is also observed in the amygdala and in scattered cells of the cerebral cortex.

6.9.4. Stimulus-transcription coupling in the hypothalamus and PVN triggered by restraint is attenuated in PACAP-deficient mice

Activity-regulated transcription factors such as Egr1 and Fos have been widely used to trace responses of neural circuitry to incoming stimuli. In response to restraint, we found hypothalamic expression of Egr1 and Fos mRNA to be rapidly and transiently induced. Further corroborating PACAP-dependent stimulation of the HPA axis at the level of the hypothalamus, induction of both factors was significantly attenuated in PACAP-deficient mice (Figure 19A, following page). Expression peaked at 1h, reaching levels significantly greater than in untreated mice, and returned to baseline thereafter. No difference was found between mice that were continuously restrained (group 6h) or restrained and released (group 1h + 5h), indicating that the induction of Egr1 and Fos expression is inherently transient, even in the continued presence of the stressor (Figure 19A).

In addition to Egr1 and Fos, mRNAs encoding ITF from the Nr4a family of orphan nuclear receptors were differentially upregulated in the hypothalamus. The expression pattern was very similar, in that induction was rapid, transient, and significantly attenuated in PACAP-deficient mice. Nur77 and Nor1 were induced after 1h of restraint, while Nurr1 was unaffected by treatment and equally abundant in both genotypes (Figure 19B, following page).

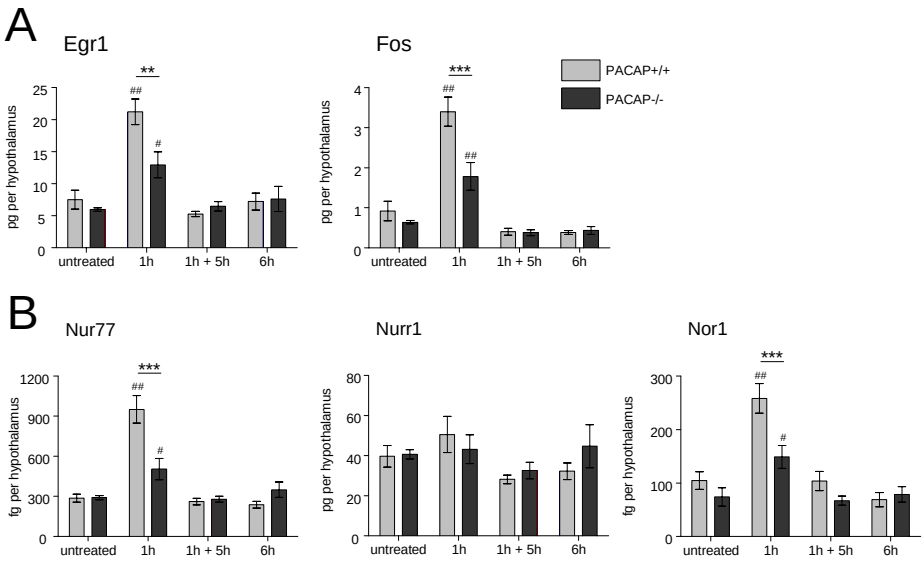

Figure 19. Upregulation of inducible transcription factors (ITF) in the hypothalamus in response to restraint is PACAP-dependent. (A) "Promiscuous" ITF. (B) Nr4a family of orphan nuclear receptors. Data from qRT-PCR are displayed as means +/- SEM (N = 5-6 male mice per time point; average age: four months). Pound signs indicate significant difference between untreated controls and post-treatment time points within each genotype (one-way ANOVA with Dunnett's multiple comparison test; $^{\#}p<0.05$, $^{\#\#}p<0.01$). Asterisks indicate significant difference between genotypes (two-way ANOVA with Bonferroni post-test; $^{**}p<0.01$, $^{***}p<0.001$).

To determine the localization of PACAP-dependent Nur77 and Nor1 mRNA expression after stress, and to see whether it occurs in the same neurons that express CRH, in situ hybridization was carried out on brain sections encompassing the hypothalamus including PVN. Sense probes were used as negative controls and yielded no specific signal (data not shown). As expected, labeling of serial sections with cRNA probes for CRH, Nur77 and Nor1 revealed overlapping expression patterns, suggesting that cell groups in the PVN expressing CRH also express Nur77 and Nor1 (Figure 20, following page). Hybridization signals increased after restraint and were clearly more abundant in wild-type mice. In contrast to CRH and Nur77, Nor1 cRNA probes also labeled the suprachiasmatic nucleus of the hypothalamus (data not shown) and cells lining the third ventricle, with the latter occurring only in stressed wild-type mice. CRH hybridization signals were restricted to the PVN and relatively intense per cell, whereas Nur77 and Nor1 mRNA expression in the hypothalamus appeared somewhat diffuse (Figure 20).

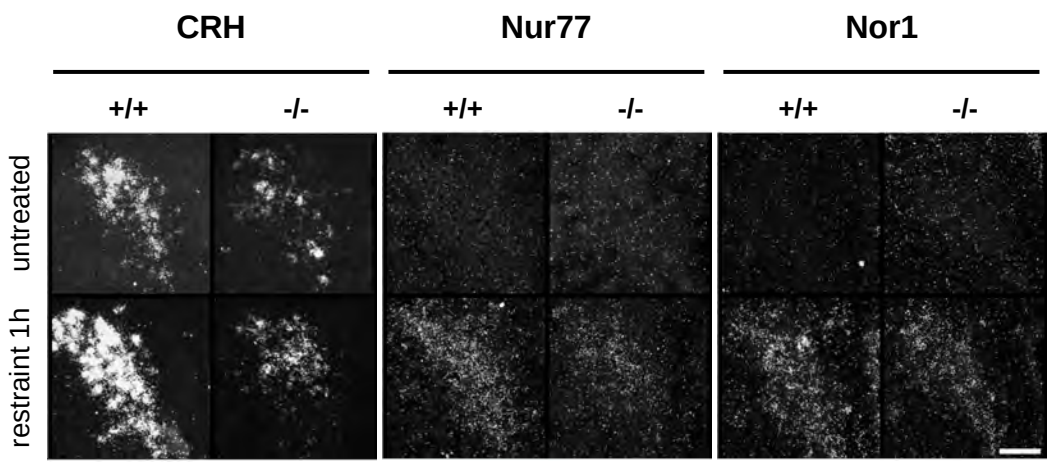

Figure 20. Restraint-induced expression of Nr4a transcription factors overlaps with CRH mRNA in the hypothalamic paraventricular nucleus. 14 µm-thick frozen coronal sections of brains from wild-type (+/+) and PACAP-deficient (-/-) mice were incubated with ^{35}S-labeled cRNA probes for CRH, Nur77 and Nor1, and coated with autoradiographic emulsion. After exposure (68 h for CRH, 92 h for Nur77, 90 h for Nor1) and development, specific hybridization signals (white speckles = silver grains) were visualized using darkfield microscopy. Note expression of Nor1 in cells lining the third ventricle, which was only observed in stressed (restraint 1 h) wild-type mice. Scale bar = 100 µm.

6.9.5. Stress-induced activation of the pituitary gland requires PACAP

As in the hypothalamus, expression of Nr4a transcription factors in the pituitary gland was rapidly and robustly induced by restraint. In wild-type mice, abundance of Nur77 and Nurr1 mRNA significantly increased within 1h, whereas no induction occurred in PACAP-deficient mice. After this initial peak, expression returned to baseline. Nor1 was not statistically significantly upregulated in either genotype, but more abundant in pituitaries from PACAP-deficient mice after 6h of restraint (Figure 21A, following page). Although not statistically significant, a modest 1.5-fold increase in proopiomelanocortin (POMC) mRNA expression was observed in wild-types. Expression in untreated PACAP-deficient mice appeared variable, with two out of six pituitary samples showing mRNA levels far above this group's average. Overall, POMC was more abundant in pituitaries from wild-type mice, significantly so after 6h of restraint (Figure 21B, following page). In a second experiment, a larger number of untreated mice were used to measure pituitary gene expression, and POMC mRNA in samples from PACAP-deficient mice was found to be 90% lower than in wild-types, confirming the trend from the previous cohort (Figure 21C, following page).

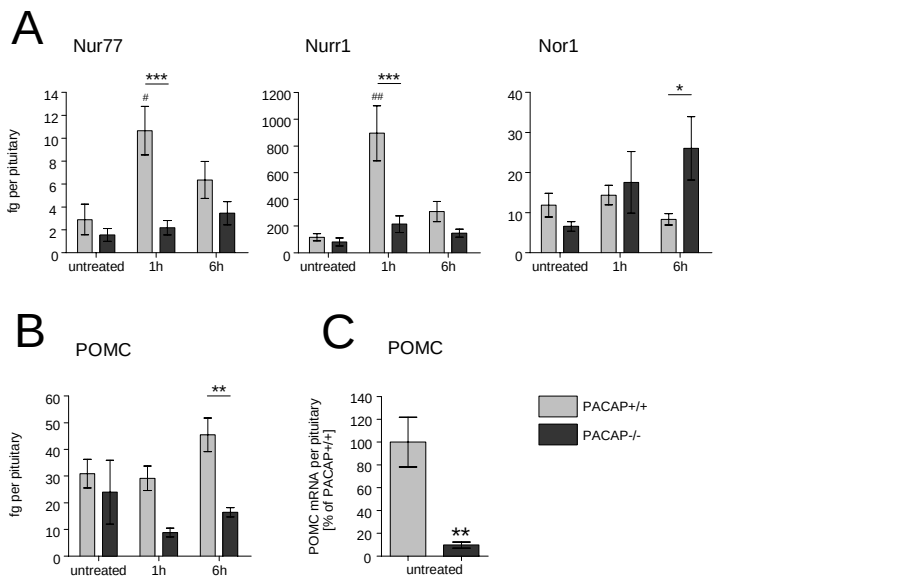

Figure 21. Restraint-induced stimulus-transcription coupling in the pituitary gland depends on PACAP. Data from qRT-PCR are displayed as means +/- SEM (N = 5-6 male mice per time point; average age: 5 months). (A, B) Restraint-induced upregulation of Nr4a factors precedes PACAP-dependent expression of POMC mRNA. Pound signs indicate significant difference from the respective genotype's control (untreated). One-way ANOVA with Dunnett's multiple comparison test ($^{\#}p<0.05$, $^{\#\#}p<0.01$). Asterisks indicate significant difference between genotypes. Two-way ANOVA with Bonferroni post-test (*p<0.05, **p<0.01, ***p<0.001). (C) Basal expression of pituitary POMC mRNA is lower in PACAP-deficient mice (N = 8-10 male mice per time point; average age: 5 months). Asterisks indicate difference between genotypes (**p=0.001; unpaired t-test).

6.9.6. Stimulus-transcription coupling in the adrenal cortex triggered by restraint is attenuated in PACAP-deficient mice

In the adrenal glands, all three Nr4a transcription factors were PACAP-dependently induced, as measured by qRT-PCR. Peak levels of mRNA expression after 1h of restraint were about 50% lower in PACAP-deficient compared to wild-type mice. While expression of Nurr1 and Nor1 returned to baseline after the initial peak, Nur77 was still elevated after 3h of restraint in wild-type and significantly higher than control after 6h in PACAP-deficient mice (Figure 22).

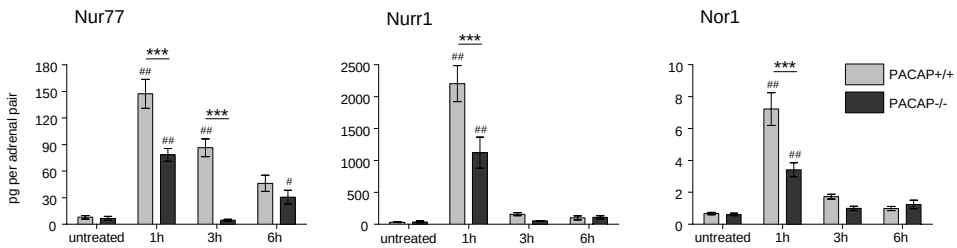

Figure 22. Upregulation of inducible transcription factors in response to restraint is significantly blunted in adrenal glands from PACAP-deficient mice. Transcript levels were measured by qRT-PCR using both glands per animal. Data are displayed as means +/- SEM (N = 5 male mice per time point). Pound signs indicate significant difference from the respective genotype's control (untreated). One-way ANOVA with Dunnett's multiple comparison test ($^{\#}p<0.05$, $^{\#\#}p<0.01$). Asterisks indicate significant difference between genotypes. Two-way ANOVA with Bonferroni post-test (***p<0.001).

In situ hybridization revealed that all three Nr4a family members were upregulated in the adrenocortical compartment, with some degree of zonal differences. Nur77 was strongly induced throughout the cortex, whereas Nurr1 and Nor1 were most prominently expressed in the outer layers (Figure 23).

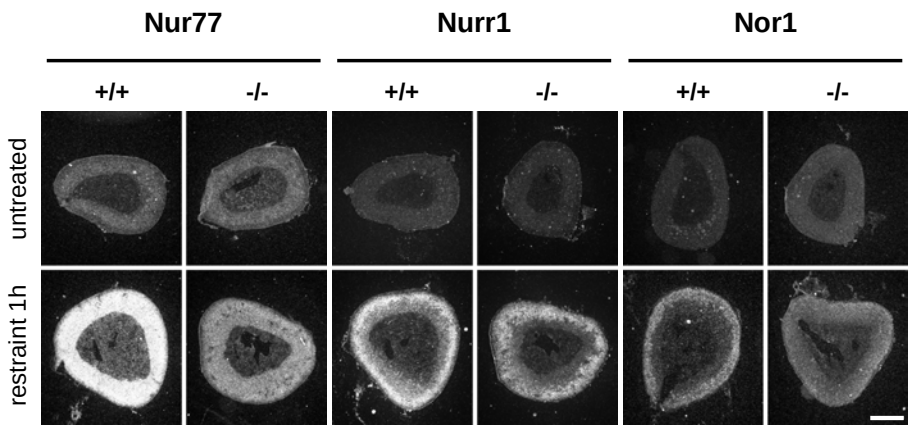

Figure 23. Restraint-induced upregulation of PACAP-dependent Nr4a transcription factors occurs in the adrenal cortex. 14 µm-thick frozen sections of adrenal glands from wild-type (+/+) and PACAP-deficient mice (-/-) were incubated with ^{35}S-labeled cRNA probes for Nur77, Nurr1 and Nor1. Sections were coated with autoradiographic emulsion, and after exposure (44 h for Nur77, 48 h for Nurr1, 68 h for Nor1) and development, specific hybridization signals (white speckles = silver grains) were visualized using darkfield microscopy. Scale bar = 500 µm.

Although far less pronounced than in the cortex, hybridization signals for Nur77 and Nurr1 also appeared to increase after restraint in the adrenal medulla (see Figure 24 for examples of Nur77). While bona fide quantification would require densitometry or grain counting, carried out systematically on larger series of sections, our preliminary results suggest that adrenomedullary induction of Nur77 is PACAP-dependent.

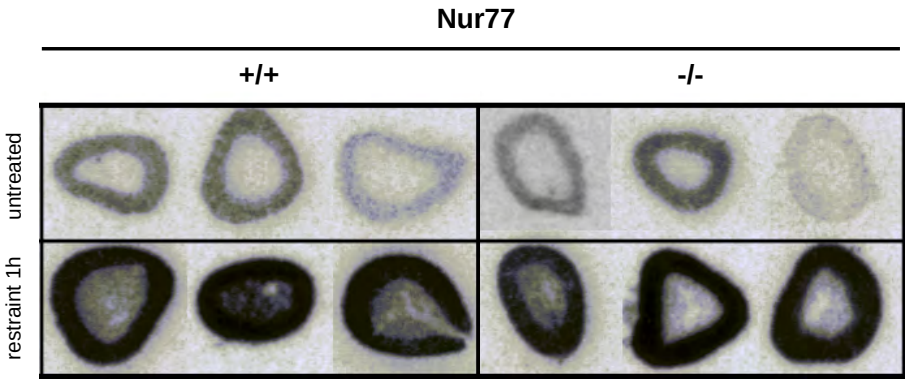

Figure 24. Restraint-induced upregulation of Nur77 mRNA in the adrenal cortex and medulla. 14 µm-thick frozen sections of adrenal glands from wild-type (+/+) and PACAP-deficient (-/-) mice were incubated with ^{35}S-labeled cRNA probes for Nur77. Sections were apposed to autoradiographic film, on which hybridization signals appear as black spots. Films were scanned at 2400 dpi on a conventional flatbed scanner. Resulting digital images were cropped and compiled.

6.9.7. Steroidogenic factors and biosynthetic enzymes of the adrenal cortex are induced during stress in a PACAP-dependent fashion

Steroidogenic factor 1 (SF-1; Nr5a1), the most important adrenocortical transcription factor, also exhibited a PACAP-dependent expression pattern in response to restraint, providing further evidence for PACAP-dependent stimulus-transcription coupling in the adrenal cortex. Like the Nr4a factors, SF-1 belongs to the family of orphan nuclear receptors. Its expression in the adrenal glands was robustly elevated after 1h of restraint. Expression in wild-type mice was maximal after 3h, whereas PACAP-deficient mice displayed only a modest increase at 1h that was maintained throughout the time course of the experiment. Thus, peak expression levels of SF-1 mRNA were more than 50% lower compared to wild-types (Figure 25A).

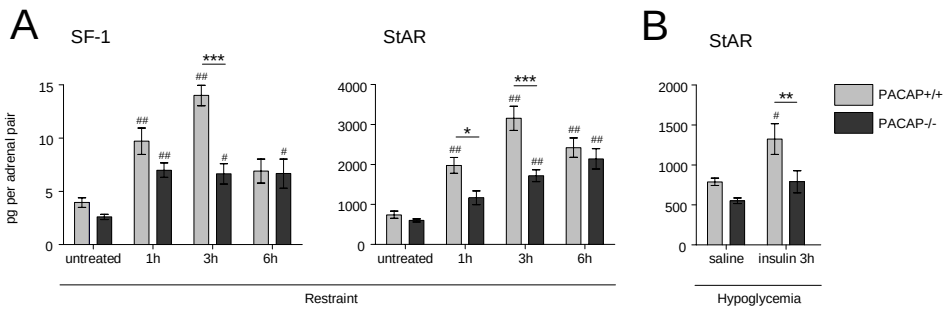

Figure 25. Stressor-induced upregulation of mRNA encoding steroidogenic factor 1 (SF-1) and steroidogenic acute regulatory protein (StAR) in the adrenal glands is PACAP-dependent. Data from qRT-PCR are displayed as means +/- SEM. (A) Restraint (N = 5-6 male mice per time point; average age: 5.5 months). Pound signs indicate significant difference from the respective genotype's control (untreated). One-way ANOVA with Dunnett's multiple comparison test ($^{\#}p<0.05$, $^{\#\#}p<0.01$). Asterisks indicate significant difference between genotypes. Two-way ANOVA with Bonferroni post-test (*p<0.05, **p<0.01, ***p<0.001). (B) Hypoglycemia (N = 6 male mice per time point; average age: 5.9 months). Pound sign indicates significant difference from the respective genotype's control (saline). Asterisks indicate difference between genotypes. One-way ANOVA with Newman-Keuls multiple comparison test ($^{\#}p<0.05$, **p<0.01).

Strikingly, mRNA encoding steroidogenic acute regulatory protein (StAR) was significantly induced after restraint in a PACAP-dependent fashion. StAR protein mediates the transfer of cholesterol to the inner mitochondrial membrane, thus being the limiting factor for all steroidogenic processes. At all time points tested, StAR mRNA was significantly elevated in wild-type mice, reaching a maximum at 3h. Although a modest upregulation was also observed in PACAP-deficient adrenal glands, abundance of StAR in wild-types was significantly higher after 1h and 3h of restraint (Figure 25A). Hypoglycemia elicited a similar expression pattern, leading to a significant difference between genotypes 3h after i.p. injection of 2 U/kg insulin. Compared to restraint, induction of StAR appeared somewhat less pronounced in this stress model (Figure 25B).

To determine the potential contribution of steroid hydroxylase gene regulation to PACAP-dependent corticosterone synthesis, we measured transcript levels of all enzymes from the adrenocortical steroidogenic pathway (Figure 26, following page).

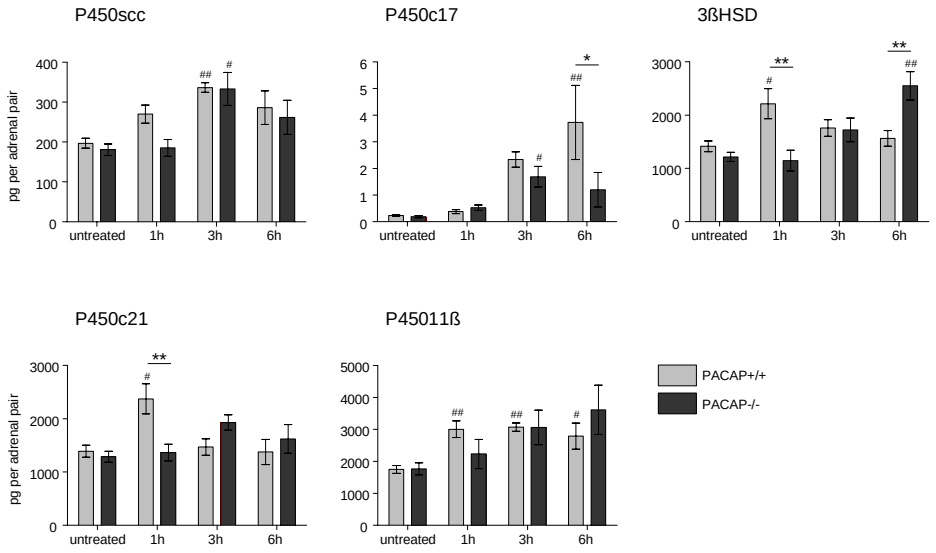

Figure 26. Transcripts encoding adrenocortical steroidogenic enzymes are induced by restraint stress, some of which display a PACAP-dependent pattern. Data from qRT-PCR are displayed as means +/- SEM (N = 5 male mice per time point; average age: 5.5 months). Pound signs indicate significant difference from the respective genotype's untreated control (one-way ANOVA with Dunnett's multiple comparison test; $^{\#}p<0.05$, $^{\#\#}p<0.01$). Asterisks indicate significant difference between genotypes (two-way ANOVA with Bonferroni post-test; $*p<0.05$, $**p<0.01$).

P450scc, encoding cholesterol side-chain cleavage enzyme (the first and rate-limiting enzyme in steroid biosynthesis), was modestly upregulated in wild-type and PACAP-deficient mice after 3h of restraint. No difference in abundance was found when comparing the two genotypes. Expression of P450c17 mRNA (steroid 17-alpha-hydroxylase) was upregulated in both genotypes, but peak levels in wild-types at 6h were more than 3-fold higher compared to PACAP-deficient adrenal glands. Transcripts encoding 3ßHSD (hydroxy-delta-5-steroid dehydrogenase, 3 beta- and steroid delta-isomerase 1) were induced in both genotypes to a similar extent, but the time course in PACAP-deficient mice was shifted relative to wild-types. Thus, while expression in the latter group of mice was transiently elevated after 1h of restraint, induction in PACAP-deficient mice first occurred after 6h. P450c21 mRNA (steroid 21-hydroxylase) was rapidly induced in wild-type mice after 1h of restraint, subsequently returning to baseline. No induction occurred in PACAP-deficient mice. Finally, no differences were observed for P45011ß (steroid 11-beta-hydroxylase), which catalyzes the last step in the synthesis of corticosterone, although statistically significant induction occurred only in wild-type mice (Figure 26).

Overall, we found a complex expression pattern of steroid hydroxylases in the adrenal glands, with some PACAP-dependent components. The magnitude of regulation was modest except in the case of P450c17. On the other hand, stress-induced upregulation of SF-1 and StAR mRNA was clearly and robustly PACAP-dependent, suggesting that these two factors are more likely to be involved in the PACAP-dependent corticosterone biosynthesis reported here.

6.10. Preliminary findings

Over the course of our experiments, preliminary data were obtained whose further analysis will be the subject of future studies. These data pertain to PACAP-dependent gene expression in the adrenal glands and brain, as well as potential effects of PACAP on development of the pituitary gland.

6.10.1. Basal expression levels of hypothalamic vasopressin are attenuated in PACAP-deficient mice

Basal levels of mRNA encoding vasopressin (AVP) in the hypothalamus were found to be highly significantly PACAP-dependent, with abundance in PACAP-deficient mice being <50% relative to wild-types (Figure 27).

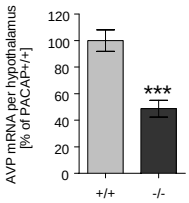

Figure 27. AVP mRNA is less abundant in hypothalamus from PACAP-deficient mice. Data from qRT-PCR are displayed as means +/- SEM (N = 10 male mice per genotype) and were compared by unpaired t-test (***p<0.0001). Data are expressed as percentage of abundance in hypothalamus from wild-type mice (+/+). Abundance in PACAP-deficient mice (-/-) is >50% lower.

Based on our dissection procedure, this difference most likely reflects differences in the PVN, as the supraoptic nucleus of the hypothalamus is largely, if not completely, excluded from the tissue sample.

6.10.2. RNA yields from the pituitary glands of PACAP-deficient mice are low compared to wild-type mice

Throughout our experiments, RNA yields from all tissue samples were monitored as a means of quality-controlling the extraction procedure. We noticed that pituitary glands from PACAP-deficient mice consistently yielded less RNA than pituitary glands from wild-types. This was true for untreated mice as well as those exposed to various durations of restraint. As an example, Figure 28 illustrates values from a group of untreated animals, in which RNA yields from PACAP-deficient pituitary glands were 23% lower compared to wild-types.

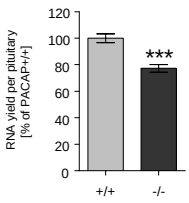

Figure 28. Pituitary glands from untreated PACAP-deficient mice contain significantly lower amounts of RNA. Yields of total RNA obtained from pituitary glands (N = 15 per genotype) were compared by unpaired t-test (***p<0.0001). Data are expressed as percentage of yield from wild-type mice (+/+). Yields from PACAP-deficient mice (-/-) are 23% lower.

6.10.3. Abundance of mRNA encoding the hop variant of the PAC1 receptor (PAC1hop) tends to be lower in adrenal glands from PACAP-deficient compared to wild-type mice

Mouse adrenal glands express all three variants of the third intracellular loop of the PACAP-specific PAC1 receptor (Figure 29A). PAC1hop mRNA expression levels in adrenal glands from PACAP-deficient mice were found to be more than 30% lower compared to wild-types, although this did not reach statistical significance (Figure 29B). Given the fact that PAC1hop appears to be the most abundant isoform in mouse adrenal glands (Figure 29A), and given the importance of PAC1hop in mediating secretion from adrenomedullary chromaffin cells (Mustafa et al., 2007), analysis of basal and stress-induced expression in a larger cohort of mice is clearly warranted. In addition, it remains to be determined whether other variants of the PAC1 receptor (null, hip) are affected by PACAP knock-out.

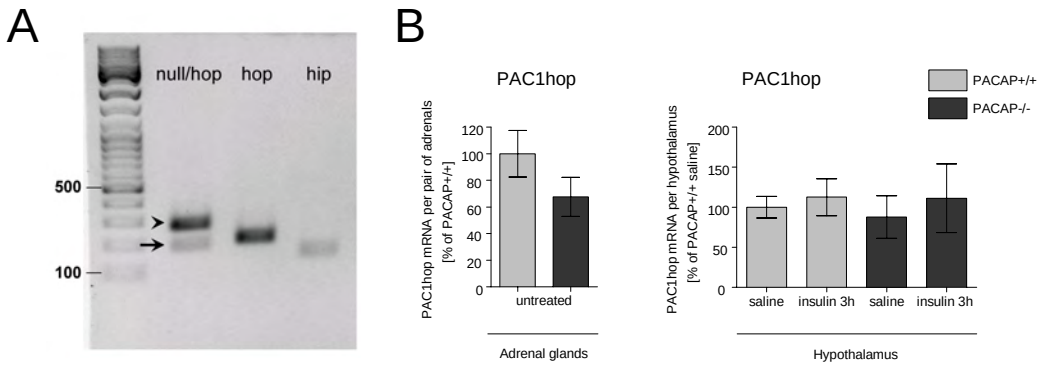

Figure 29. Expression of transcripts encoding the PACAP-specific PAC1 receptor in mouse adrenal glands and hypothalamus. (A) RT-PCR analysis of PAC1 receptor variant expression in mouse adrenal glands (PACAP-deficient animal). All three isoforms of the third intracellular loop of the PAC1 receptor are expressed, with PAC1hop being the most abundant. PAC1null and PAC1hip are also detected, but levels are clearly lower. Results in adrenal glands from wild-type mice are qualitatively similar. In lane 1, variants null and hop are indicated by an arrow and arrowhead, respectively. Size marker = 100 bp DNA ladder. (B) Although a trend towards lower expression in PACAP-deficient mice is evident, PAC1hop mRNA abundance in the adrenal glands is not statistically significantly different between genotypes (left panel). PAC1hop mRNA expression in the hypothalamus is unaffected by systemic stress and equally abundant in wild-type and PACAP-deficient mice (right panel). Data from qRT-PCR are displayed as means +/- SEM (N = 4-5 male mice per group) and expressed as percentage of abundance in untreated or saline-treated wild-types.

Abundance of PAC1hop mRNA in the hypothalamus appeared unaffected by systemic stress and not different between PACAP genotypes.

6.10.4. Chemokine expression in response to hypoglycemia is enhanced in PACAP-deficient adrenal glands

Microarray analysis after 3h of prolonged hypoglycemia had indicated that factors involved in inflammatory responses were PACAP-repressed in the adrenal glands. Thus, transcripts encoding Ccl2, Ccl7, Cxcl1 and IL6 were more abundant compared to wild-type, and/or upregulated exclusively in adrenal glands from PACAP-deficient mice (Tables 5-7, appendix).

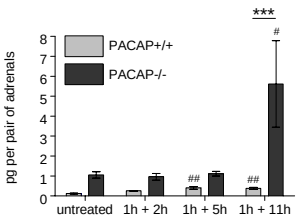

Figure 30. Ccl2 mRNA is induced by hypoglycemia and far more abundant in adrenal glands from PACAP-deficient mice. Data from qRT-PCR are displayed as means +/- SEM (N = 4-5 male mice per time point; average age: 4 months). Pound signs indicate significant difference from the respective genotype's untreated control (one-way ANOVA with Dunnett's multiple comparison test; $^{\#}p<0.05$, $^{\#\#}p<0.01$). Asterisks indicate significant difference between genotypes (two-way ANOVA with Bonferroni post-test; ***p<0.001). Note that Ccl2 mRNA abundance is higher in PACAP-deficient mice at all time points, although a statistically significant difference is only observed after 12h.

Selecting Ccl2 as an example, we confirmed this microarray-derived result in a time course experiment after transient hypoglycemia, measuring Ccl2 mRNA by qRT-PCR. As shown in Figure 30, Ccl2 mRNA was induced in both genotypes, with maximal levels in PACAP-deficient mice 12h after insulin injection being 15-fold higher than in wild-types. Although not statistically significant due to the large induction and variability at the 12h time point, it is worth noting that Ccl2 mRNA abundance in untreated mice was already 8-fold higher in PACAP-/- compared to PACAP+/+ adrenal glands, and higher at all other time points as well.

6.10.5. Vesicular glutamate transporter 2 mRNA is significantly more abundant in hippocampus from PACAP-deficient compared to wild-type mice

Preliminary analysis of gene expression was carried out by qRT-PCR using samples of hippocampus from one hemisphere per mouse. Transcripts encoding the vesicular glutamate transporter isoform 2 (VGluT2) were found to be significantly more abundant in hemi-hippocampus from PACAP-deficient compared to wild-type mice (Figure 31).

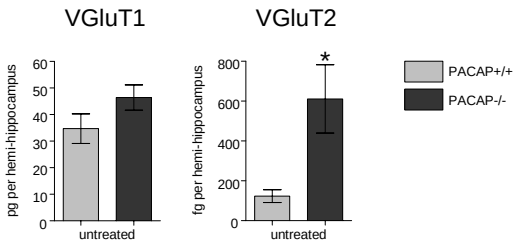

Figure 31. VGluT2 mRNA expression is higher in PACAP-deficient hippocampus. Hippocampal tissue was obtained from one hemisphere per animal, and mRNA expression levels were measured by qRT-PCR. Data are displayed as means +/- SEM (N = 5-6 male mice per time point; average age: 3 months). Asterisk indicates significant difference between genotypes (unpaired t-test; *p<0.05).

A similar trend was observed for VGluT1 mRNA, but this was much less pronounced and not statistically significant (Figure 31).

7. Discussion

7.1. The PACAP knock-out mouse is a useful model for acute stress responses

To study the impact of stress on an organism, and to dissect the functional role of particular peptides or proteins in stress responses and subsequent disease states, it is desirable to have access to animal models in which detailed analyses can be carried out on the behavioral, physiological, cellular and molecular levels. To that end, transgenic mice have been used very successfully in biological research, confirming the function of factors already known to be critical for stress responses, and uncovering important new candidates (Chourbaji et al., 2008; Muller et al., 2004). However, there are limitations to the usefulness of such models, especially when the gene of interest is mutated in every cell at every stage of development, such as in a "conventional" germline knock-out. Ideally, mouse models for stress would display little or no phenotypic differences when compared to their wild-type counterparts under basal or resting conditions, while showing distinct reactions when exposed to particular stressors. This would allow dissection of the specific pathways and factors that contribute to altered stress responses, based on an individual strain being more susceptible or more resilient to stress than a wild-type strain. A pronounced phenotype in the absence of stress, due only to the genetic mutation in all cells of the organism, provides a relatively unfavorable background against which stressor-induced mechanisms could be difficult to discern.

The mouse strain used in the present work was created using a conventional gene knock-out approach, where the PACAP-coding region was replaced with a selectable marker via homologous recombination in embryonic stem cells (Hamelink et al., 2002). Mice from this strain do not express PACAP at any time in any cell, thus being completely PACAP-deficient. In the absence of challenge, they are healthy and appear mostly normal, i.e. show no gross differences from the C57BL/6 strain into which the PACAP knock-out allele has now been fully backcrossed. However, several features of PACAP-deficient mice have been reproducibly detected by different laboratories using independently created strains. Compared with wild-type mice, breeding deficits (Isaac and Sherwood, 2008; Shintani et al., 2002) and a leaner phenotype were observed (Adams et al., 2008; Tomimoto et al., 2008), both of which we confirmed during our present studies. Also, genetic disruption of PACAP or its specific PAC1 receptor alters behavior, affecting the social, emotional and psychomotor phenotype (Girard et al., 2006; Hashimoto et al., 2001; Nicot et al., 2004; Otto et al., 2001a; Otto et al., 2001b). Nonetheless, for the purpose of our present studies, which are mainly concerned with PACAP's role during acute neuroendocrine stress responses, PACAP-deficient mice are a useful model. The reasons for this view are presented in the following paragraphs.

7.1.1. Function of stressor-responsive systems is normal in PACAP-deficient mice in the absence of stimulation

The first experiments with the PACAP-deficient strain generated in our laboratory were concerned with the role of PACAP at the sympathoadrenal synapse, where it is released as a transmitter from the splanchnic nerve and responsible for catecholamine synthesis and secretion during hypoglycemia-induced stress (Hamelink et al., 2002). These experiments showed that adrenal morphology and adrenomedullary chemical neuroanatomy are unaltered in PACAP-deficient mice, suggesting that development and basal function of the glands are normal, further supported by the fact that adrenal epinephrine content and circulating corticosterone concentrations do not differ between genotypes. In our present experiments, these findings were confirmed and extended. There were no significant differences in serum concentrations of ACTH or corticosterone between untreated PACAP-deficient and wild-type mice (Figure 16), clearly suggesting that activity and output of the HPA axis are normal in the absence of stimulation.

7.1.2. Basal transcriptome profiles are largely unaffected by PACAP knock-out

Microarray analyses provided further evidence for the notion that, in the absence of stimulation or challenge, tissues involved in neuroendocrine stress responses function normally in PACAP-deficient mice. Global expression profiles of the adrenal glands yielded few differentially expressed genes, and the magnitude of differences between genotypes was only modest. The transcriptome of the cerebral cortex provided similar results (see Tables 3 and 4, appendix). More detailed expression analysis of specific genes by qRT-PCR corroborated these findings, showing that key genes involved in adrenomedullary hormone production (TH, DBH, PNMT) and function of the HPA axis (CRH, StAR, steroidogenic enzymes) are equally abundantly expressed in untreated wild-type and PACAP-deficient mice. Expression of mRNA encoding adrenomedullary PNMT and hypothalamic CRH tended to be slightly lower in PACAP-deficient mice, but this was not statistically significant. Notable exceptions to this overall pattern are pituitary POMC and hypothalamic AVP (lower in PACAP-/-), and hippocampal VGluT2 (higher in PACAP-/-).

Taken together, the aforementioned data support our use of PACAP-deficient mice in experimental models of acute stress in vivo. Neither secretory activity nor gene expression patterns of the sympathoadrenal system and HPA axis are distorted by disruption of the gene encoding PACAP, providing a useful background for the study of stressor-induced responses and their underlying mechanisms.

7.2. Global gene expression patterns in mouse adrenal glands after prolonged systemic stress are difficult to interpret – sustained hypoglycemia in PACAP-deficient mice as a confounding factor

Our microarray analyses of gene expression in whole adrenal glands after hypoglycemia revealed several interesting candidate transcripts, whose regulation was validated by qRT-PCR and investigated further in subsequent experiments. The overall pattern emerging from microarray Experiment 1 and 2 was that *PACAP-repressed* genes (i.e. genes induced only or more strongly in PACAP-deficient adrenal glands after stress) were much more numerous than *PACAP-dependent* genes (i.e. genes induced only or more strongly in wild-types; see Tables 5-7, appendix). Somewhat surprisingly, the union of the gene lists derived from Experiment 1 and 2 included a large number of genes (14/36 or 39%) that we had recently characterized as being *PACAP-responsive*, i.e. induced in cultured PC12 pheochromocytoma cells after treatment with PACAP (Eiden et al., 2008). Three examples of these were followed up in a time course experiment and measured by qRT-PCR after 1h, 2h, 4h and 6h of hypoglycemia. Egr1, Ier3 and Nurr1 mRNAs were all found to increase rapidly in both genotypes, with expression levels returning to baseline in wild-type but persisting in PACAP-deficient mice, thus confirming the pattern observed by microarray after 3h of hypoglycemia (Figure 5). Stress-induced expression of Egr1 was further characterized by in situ hybridization and found to occur in the adrenal cortex and medulla in both genotypes (Figure 8).

Two main reasons prompted us to reconsider prolonged hypoglycemia as a model in the context of global expression analysis. First, the numbers of PACAP-deficient mice dying after insulin injection were far higher than previously reported (Hamelink et al., 2002). In our experiments, mortality rates were up to 40% per cohort, compared to 0% in wild-type. During all of our experiments, wild-type mice never showed obvious symptoms of insulin shock after i.p. administration of 2 U/kg, while PACAP-deficient mice invariably displayed lower breathing rates, hyporesponsiveness to touch, and mild to massive convulsions. Hypothermia, which is a survival response during prolonged hypoglycemia (Buchanan et al., 1991), was also observed predominantly in knock-out animals. Second, our microarray experiments suggested that the gene expression changes seen after 3h are largely due to prolonged hypoglycemia-induced cellular stress, rather than directly reflecting lack of PACAPergic signaling at the sympathoadrenal synapse. For example, metallothionein 1 and 2 (Mt1, Mt2), genes known to be induced by oxidative stress (Formigari et al., 2007; Haq et al., 2003), and sulfiredoxin (Srxn1), a target and regulator of peroxide (H_2O_2)-mediated signaling (Rhee et al., 2005), were upregulated in the adrenal glands after hypoglycemia. Mt1 (8.15 vs 2.29-fold) and Srxn1 (5.51 vs 3.44-fold) showed more pronounced induction in knock-out compared to wild-type mice, and Mt2 was induced only in the former (microarray Experiment 2). Mt1 was also found to be more abundant in knock-out compared to wild-type adrenal glands after 3h of sustained hypoglycemia (microarray Experiment 1). Given that decreased availability of glucose is well known to cause oxidative stress (Moley and Mueckler, 2000), it appears reasonable to assume

that sustained and more profound hypoglycemia in PACAP-deficient mice would exacerbate oxidative stress in cells of the adrenal glands. In fact, PACAP-deficient mice have very recently been proposed to be more susceptible to oxidative stress (Ohtaki et al., 2010). Thus, transcriptome patterns after 3h of hypoglycemia seem to reflect a secondary effect (e.g. oxidative stress) rather than the primary effect (reduced synaptic transmission) of lack of PACAP at the sympathoadrenal synapse. Furthermore, the extreme physiological symptoms of insulin shock in these animals, such as severe convulsions, possibly precipitate a whole range of other confounding factors, making global transcriptome analysis of peripheral tissues after several hours of hypoglycemia impractical. A stressor circumventing direct metabolic manipulation, such as restraint, would provide a more unbiased approach.

7.3. PACAP controls the sympathoadrenal hormonal system during stress

7.3.1. Secretory activity is coupled to expression of catecholaminergic enzymes and release-modulating neuropeptides

PACAP-dependent production and secretion of adrenomedullary catecholamines (chiefly epinephrine) during systemic stress are a matter of life and death. Due to insufficient activation of tyrosine hydroxylase (TH), the enzyme that catalyzes the rate-limiting step in catecholamine biosynthesis, PACAP-deficient mice dose-dependently succumb to insulin-induced hypoglycemia (Hamelink et al., 2002). Our present experiments indicate that, in addition to the previously described catecholamine secretion and posttranslational control of TH, PACAP is required for stimulus-transcription coupling in the adrenal glands, leading to regulation of genes encoding catecholamine biosynthetic enzymes. In response to hypoglycemia and restraint, transcripts encoding TH and PNMT were PACAP-dependently upregulated in our studies [(Stroth and Eiden, 2010) and present results; see Figure 12]. Regulation of TH and PNMT during stress has been studied in great detail [reviewed in (Kvetnansky et al., 2009; Sabban and Kvetnansky, 2001)] and suggested to sustain adrenomedullary function during periods of increased secretory demand (Tai et al., 2007),

PACAP-dependent signaling during stress was also found to increase expression of GAL mRNA in the adrenal medulla, both in response to hypoglycemia and restraint (Figures 9-11). Galanin mRNA and peptide have previously been shown to be upregulated after hypoglycemia-induced reflex activation of the splanchnic nerve in the rat, with peptide levels robustly elevated for up to two weeks (Anouar and Eiden, 1995; Fischer-Colbrie et al., 1992). This suggests that the PACAP-dependent changes we observed after exposure of mice to two different stressors are indeed part of a specific adrenomedullary response pattern. Interestingly, a previous study in rats demonstrated that galanin potentiates epinephrine responses to a psychosocial stressor, without affecting epinephrine levels in unstressed animals (Ceresini et al., 1998). Transcript levels of VIP were also PACAP-dependent in the adrenal glands. While the 2.5-fold upregulation in response to hypoglycemia was not statistically significant, mRNA abundance was clearly higher in wild-type compared to PACAP-deficient mice (Figure 10). In

the perfused rat adrenal gland, VIP has been shown to stimulate secretion of catecholamines (Malhotra and Wakade, 1987; Wakade et al., 1991).

In summary, it appears that PACAP, in addition to regulating the catecholaminergic system directly, controls expression of adrenomedullary neuropeptides that modulate catecholamine secretion. This could provide a mechanism for functional plasticity of the sympathoadrenal hormonal system, recruited specifically in response to stressful stimuli.

7.3.2. The PAC1hop receptor is most likely responsible for PACAP's effects

The receptor through which PACAP controls adrenomedullary function is most likely the PAC1 receptor, specifically the PAC1hop splice variant, based on the following observations. While all three PACAP receptors (PAC1, VPAC1, VPAC2) are expressed in the adrenal medulla of the rat (Mazzocchi et al., 2002), in situ hybridization and receptor autoradiography show that patterns of PAC1 mRNA expression and ^{125}I-PACAP-27 binding are practically identical (Moller and Sundler, 1996). It is generally agreed that adrenomedullary effects of PACAP are largely mediated through PAC1 [reviewed in (Conconi et al., 2006)], and PAC1hop appears to be the predominant splice variant in the rat (Nogi et al., 1997) and mouse (Ushiyama et al., 2007). A recent study found PAC1 expression at the plasma membrane of mouse adrenomedullary chromaffin cells, in close apposition to PACAP-positive splanchnic nerve terminals, and demonstrated PACAP-evoked catecholamine secretion from mouse adrenal slices in response to direct electrical stimulation of the splanchnic nerve (Kuri et al., 2009). Finally, the hop cassette has been shown to couple calcium signaling to catecholamine secretion in cultured cells (Mustafa et al., 2007). Our present RT-PCR analysis clearly suggests that PAC1hop is the most abundant splice variant in mouse adrenal glands, confirming and extending the aforementioned findings. While not statistically significant, we found a trend for PAC1hop mRNA levels in adrenal glands from PACAP-deficient mice to be lower compared to wild-types (Figure 29). This preliminary result warrants further investigation into the role of PAC1hop in the adrenal glands, and how it is affected by PACAP knock-out.

7.4. Rapid upregulation of inducible transcription factors in the adrenal glands in response to hypoglycemia – PACAP and ACh are not required

In our experiments with insulin-induced hypoglycemia, we observed rapid upregulation of ITF in the adrenal glands. Within 1h of insulin injection, expression of Egr1, Fos, Fosl1, Nur77 and Nurr1 increased robustly in both genotypes. Only Nurr1 was affected by PACAP knock-out, with peak levels being about 40% lower compared to wild-type mice (Figure 6). When stressor exposure was transient, i.e. animals received a glucose injection 1h after insulin, ITF expression levels returned to baseline after the initial peak (Fosl1 being an exception). When stressor exposure was prolonged, expression remained elevated only in PACAP-deficient mice, which we confirmed by microarray and qRT-PCR analysis (see above). In both cases, as mentioned, rapid induction of these genes was largely unaffected by knock-out of PACAP. This

was somewhat surprising, as we had recently shown that all factors are PACAP-responsive in cell culture, i.e. upregulated after exposure of PC12 cells to PACAP (Eiden et al., 2008).

To determine whether PACAP-independent gene regulation is mediated by acetylcholine (ACh), hypoglycemia was initiated in wild-type mice after pretreatment with nicotinic and muscarinic ACh receptor antagonists. Chlorisondamine (5 mg/kg) and atropine (1 mg/kg) were co-administered at doses previously shown to block elevation of adrenal neuropeptide expression caused by hypoglycemia in rats (Kanamatsu et al., 1986). Surprisingly, we found that this did not appear to inhibit hypoglycemia-induced regulation of PACAP-independent, i.e. potentially ACh-dependent transcripts. In fact, mRNA abundance of Egr1 and Nur77 was robustly elevated above control values when antagonist pretreatment was followed by saline injection (group “antagonist control”; see Figure 7). Maximal values were almost identical in all groups that received cholinergic antagonists and/or insulin. Chlorisondamine (Santajuliana et al., 1996; Schiltz et al., 1997; Singewald et al., 1993) and atropine (Hamel and Ford-Hutchinson, 1985) are known to cause hypotension, which in turn evokes splanchnic nerve reflex activation (Donnerer, 1988; Jordan and Miller, 1991; Vollmer et al., 2000). Therefore, it appeared possible that PACAP release at the sympathoadrenal synapse, elicited by hypotension-induced splanchnic neural activity, caused adrenal gene regulation in the absence of cholinergic signaling in wild-type mice. This suggested that genetic disruption of PACAP, in combination with pharmacological inhibition of ACh, should abolish all sympathoadrenal transsynaptic effects. However, repetition of the above experiment in PACAP-deficient mice yielded practically identical results, both in terms of response magnitude and pattern (Figure 7). The exception was Egr1, where the two insulin-treated groups showed higher expression levels than the antagonist control group.

Taken together, our results indicate that neither PACAP nor ACh are necessary for upregulation of ITF such as Egr1 and Nur77 in the adrenal glands during hypoglycemia. Since hemodynamic manipulations such as hemorrhage can activate the HPA axis (Plotsky et al., 1985), it is possible that hypotension caused by ganglionic blockade (Hamel and Ford-Hutchinson, 1985; Santajuliana et al., 1996; Schiltz et al., 1997; Singewald et al., 1993) increases ITF expression via this pathway when PACAPergic and cholinergic neural transmission is blocked. Alternatively, unknown neurotransmitters might stimulate adrenal gene expression. Although section of the splanchnic nerve could provide additional insight, there are precedents for stress-induced effects on gene expression in the adrenal glands that require neither the pituitary (ruling out involvement of the HPA axis), nor cholinergic signaling, nor the splanchnic nerve (ruling out the neural pathway) (Kvetnansky et al., 1996; Nankova et al., 1994). Also, it is important to note that administration of cholinergic antagonists affected the phenotype of both wild-type and PACAP-deficient mice. Most remarkably, when pretreatment with antagonists was followed by insulin injection, wild-type mice displayed clear signs of hypoglycemia-induced stress, which had never been the case in experiments with insulin alone. Therefore, dissection of the mechanism controlling ITF expression in the absence of cholinergic and PACAPergic signaling might ultimately prove to be very difficult.

7.5. Rapid upregulation of inducible transcription factors in the adrenal glands during restraint – responses in PACAP-deficient mice are attenuated

Expression of ITF rapidly increased in the adrenal glands in response to restraint, with maximal mRNA abundance of each being very similar to what was observed in response to hypoglycemia. However, in contrast to the latter stressor, upregulation after exposure to restraint was significantly blunted in PACAP-deficient mice (Figures 13 and 22). At 1h, peak expression of transcripts such as Egr1, Fos, Nur77, Nurr1 and Nor1 was reduced by approximately 50% compared to wild-type mice. With the exception of Nur77, where significantly elevated expression persisted in wild-types up to 3h after onset of restraint, mRNA abundance returned to baseline after the initial peak.

Our data thus show that PACAP-dependent regulation of ITF in the adrenal glands is stressor-specific, i.e. occurs in response to restraint, but not hypoglycemia. This is in contrast to some of their putative target genes, such as GAL, TH and PNMT, all of which are PACAP-dependently upregulated in response to both stressors. If factors such as Egr1 and Fos were critically involved in PACAP-dependent regulation of GAL, TH and PNMT, expression patterns in response to different stressors would have to correlate with the expression patterns of their putative target genes. However, as shown in our present results, this is not the case.

7.6. What are the mechanisms underlying PACAP-dependent expression of adrenomedullary neuropeptides and catecholaminergic enzymes?

There is evidence for PACAP-induced regulation of galanin (Anouar et al., 1999) and catecholaminergic enzymes (Choi et al., 1999; Corbitt et al., 2002; Tonshoff et al., 1997; Wong et al., 2002) in primary cultures of bovine adrenomedullary cells and in PC12 cells. Transcription factors including Egr1 and Fos have been implicated in controlling their expression in vitro and in vivo (Anouar et al., 1999; Kvetnansky et al., 2009; Morita et al., 1996; Sabban and Kvetnansky, 2001; Tai et al., 2001), and these transcription factors (among others) are PACAP-responsive in PC12 cells (Eiden et al., 2008). Therefore, it can not be completely excluded that ITF participate in stress-induced upregulation of GAL, TH and PNMT, although their PACAP-dependent expression patterns after hypoglycemia and restraint do not match (see above). To further address this issue, detailed in situ hybridization is required to localize expression of all ITF. Our experiments with hypoglycemia show that regulation of Egr1 occurs both in the adrenal cortex and medulla, and it remains to be determined whether the cortical and/or medullary compartment is the source of PACAP-dependent increases measured by qRT-PCR after exposure to restraint.

Our studies concerning the adrenal glands revealed one case in which expression patterns of transcription factor and putative target gene largely matched across stressors. Thus, both Nurr1 and TH were PACAP-dependently upregulated in response to hypoglycemia (some

experiments) and restraint (all experiments). Nurr1 is known to control TH in vitro and in vivo (Eells et al., 2006; Kim et al., 2003; Sakurada et al., 1999), and its potential role in PACAP-dependent TH expression clearly warrants further investigation, even though our present results (see ISH, Figure 23) suggest that upregulation of its mRNA in the adrenal medulla after 1h of restraint is relatively modest. Interestingly, Nurr1 could also be involved in the PACAP-dependent expression of VIP mRNA reported here, as the mouse VIP gene is a transcriptional target of Nurr1 (Luo et al., 2007).

There are other mechanisms that could account for the apparent discrepancy between expression of ITF and their putative target genes. For example, it has been proposed that stability and DNA binding activity of Egr1 are modulated via its phosphorylation state (Cao et al., 1992; Cao et al., 1993). Similarly, posttranslational control has been shown to affect the activities of Nr4a factors such as Nur77 and Nurr1 (Sacchetti et al., 2006; Wingate and Arthur, 2006), and specific intracellular signaling pathways regulate translocation of Nur77 to the nucleus (Klopotowska et al., 2005). It is possible that such mechanisms are differentially recruited for target gene expression in response to specific stressors, independent of transcriptional regulation of ITF. Thus, protein abundance, phosphorylation status and cellular localization of the ITF would have to be determined. In the case of PNMT, PACAP-dependent corticosterone production is most likely responsible for the PACAP-dependent increase in mRNA expression during stress, activating transcription via the glucocorticoid receptor.

7.7. Rapid upregulation of putative cytoprotectants in the adrenal glands is PACAP-dependent in response to different stressors

The present study identified two rapid response transcripts whose expression in the adrenal glands was PACAP-dependently elevated by hypoglycemia and restraint (Figure 14). Ier3 has been implicated in regulation of apoptosis (Wu, 2003), with recent data suggesting that positive effects on cell survival are due to Ier3-mediated inhibition of intracellular reactive oxygen species (Shen et al., 2006). Stc1 has been shown to be neuroprotective, presumably by regulating cellular calcium homeostasis (Westberg et al., 2007; Zhang et al., 2000). Notably, levels of Stc1 remained elevated in the continued presence of a stressor (restraint), while subsiding within 5h of rest, indicating that Stc1 might be a marker for ongoing cellular stimulation (Figure 14B). Although it remains to be determined whether PACAP-dependent upregulation of Ier3 and Stc1 occurs in the adrenal cortex and/or medulla, it is tempting to speculate that their protein products provide protection of adrenal cells during periods of high secretory demand. In other words, PACAP might counter cellular stress by inducing cytoprotective factors. In contrast to the adrenal glands, stress-induced upregulation of both transcripts did not occur in the hypothalamus, suggesting that it is a tissue-specific response.

7.8. Responses of the HPA axis to hypoglycemia – expression of adrenal "index genes" suggests that PACAP-deficient mice secrete less ACTH and corticosterone during insulin-induced stress

Early experiments with the PACAP-deficient mouse strain developed in our laboratory had indicated that its HPA axis is intact. Plasma concentrations of corticosterone were identical in both PACAP genotypes, at rest and in response to 2h of insulin-induced hypoglycemia (Hamelink et al., 2002). However, our present studies reveal that "index genes" of increased HPA activity are PACAP-dependently induced in response to restraint and hypoglycemia. In the former stress model, expression of these index genes clearly correlates with PACAP-dependent secretion of ACTH and corticosterone. Thus, it appears that the HPA axis response to hypoglycemia, although initially thought to be unperturbed in PACAP-deficient mice, should be reexamined.

7.8.1. Index gene 1 – StAR

Steroidogenic acute regulatory protein (StAR) is the limiting factor for all steroidogenic processes. Its production is tightly linked with steroid biosynthesis in steroidogenic cells, and ACTH is the main hormonal stimulus for its transcriptional induction [reviewed in (Lavoie and King, 2009; Manna et al., 2009; Sewer and Waterman, 2003)]. The experiments presented here indicate PACAP-dependent upregulation of StAR mRNA in response to hypoglycemia (Figure 25B), suggesting that ACTH (upstream of StAR) and corticosterone (downstream of StAR) are also PACAP-dependently increased during insulin-induced stress.

7.8.2. Index gene 2 – PNMT

The PNMT gene is regulated by several transcription factors [reviewed in (Kvetnansky et al., 2009; Sabban and Kvetnansky, 2001; Wong et al., 2008)]. In vivo, glucocorticoids play a major role in stimulating PNMT expression (Wong et al., 1992), and stress-induced increases in PNMT mRNA abundance are completely abolished when the HPA axis is disrupted by hypophysectomy in rats (Viskupic et al., 1994). Furthermore, mice with targeted deletions of the glucocorticoid receptor express no PNMT (Finotto et al., 1999). Our present results show PACAP-dependent PNMT mRNA upregulation in response to hypoglycemia (Figure 12C), suggesting reduced HPA axis activity and diminished corticosterone secretion in PACAP-deficient compared to wild-type mice. Since adrenal denervation is ineffective in blocking stress-induced increases in PNMT mRNA expression (Viskupic et al., 1994), it is unlikely that PACAP release from the splanchnic nerve is involved.

Based on the aforementioned considerations, our PACAP-deficient mouse strain, now completely backcrossed, is going to be reexamined. Experiments are currently underway to compare responses of the HPA axis to hypoglycemia, lipopolysaccharide injection (systemic immunological stressor) and restraint.

7.9. Responses of the HPA axis to restraint are markedly PACAP-dependent

The most extensive part of our present results deals with restraint-induced activation of the HPA axis, and how it is affected by disruption of the gene encoding PACAP in mice. PACAP-dependent phenomena were observed at all three levels (hypothalamus, pituitary gland, adrenal cortex), suggesting a link between neuronal activation, stimulus-transcription coupling, as well as production and secretion of hormones throughout the HPA axis. The following paragraphs will discuss these phenomena in detail.

7.9.1. Expression of CRH in the paraventricular nucleus in response to stress – evidence for PACAP mediating central control of the HPA axis

Coordination of mammalian stress responses is achieved through complex circuitry that senses stressors, signals to the central nervous system, integrates afferent information and generates adequate output. Although different stressors elicit different patterns with relatively specific neurochemical and neuroendocrine “signatures” (Goldstein and Kopin, 2008; Pacak and Palkovits, 2001), the hypothalamic PVN is invariably involved in the generation of these responses. With respect to activation of the HPA axis, specialized neurons in the PVN that express and release CRH represent the central relay station. These neurons summate excitatory and inhibitory inputs from a multitude of sources into a hypophysiotropic secretory signal, which in turn dictates the magnitude and duration of pituitary and adrenocortical activation (Herman and Cullinan, 1997; Herman et al., 2003).

PACAP emerged as a potential regulator at this very central locus, based on several important findings. First, PACAP-containing nerve terminals form synaptic contacts with CRH-immunoreactive neurons in the PVN (Legradi et al., 1998). Second, intracerebroventricular (i.c.v.) administration of PACAP causes upregulation of CRH mRNA (Grinevich et al., 1997) and secretion of corticosterone (Agarwal et al., 2005; Yi et al., 2010). Providing direct in vivo evidence for the significance of these findings and the functional relevance of the endogenous PACAPergic system, we recently showed that CRH mRNA induction is completely abolished, and sustained corticosterone secretion is diminished, in PACAP-deficient mice exposed to restraint (Stroth and Eiden, 2010). We subsequently confirmed these crucial results and significantly expanded them, proposing potential mechanisms for PACAP-dependent control of hypophysiotropic neurons.

In two independent experiments, we quantified CRH mRNA in hypothalamic extracts from wild-type and PACAP-deficient mice, using qRT-PCR. In response to varying durations of prolonged restraint, transcript abundance increased compared to untreated controls, exclusively in wild-type mice (Figure 17). This was very reproducible, varying only within a narrow range of 1.75-fold to 2.15-fold induction, suggesting that there is a maximum level of CRH mRNA expression in the PVN, which is not exceeded by the particular stressor employed in our studies. Interestingly, expression of CRH was not maintained when stressor exposure was only transient, such that transcript abundance had returned to baseline 5h after a 1h period

of restraint. An additional experiment confirmed, by in situ hybridization, that the change in CRH expression indeed occurred exclusively in the PVN of the hypothalamus.

7.9.2. Restraint-induced pituitary function is attenuated

Our present experiments show that output of the pituitary gland is normal in unstressed PACAP-deficient mice, as indicated by serum concentrations of ACTH being identical with those in wild-types. However, after exposure to restraint, increases in ACTH secretion are markedly blunted, and this effect becomes more pronounced with increasing duration of the stressor (Figure 16). Together with the pituitary expression pattern of Nur77 and Nurr1, this clearly shows that stimulation of the gland is strongly diminished (Figure 21). The most obvious potential explanation is that CRH, the principal hypophysiotropic factor (Denver, 2009), is PACAP-dependently regulated during stress, for which our experiments provide important evidence. Thus, stored CRH peptide appears initially sufficient for causing ACTH secretion, but as stressor exposure is sustained, and no compensatory CRH biosynthesis occurs in PACAP-deficient mice [(Stroth and Eiden, 2010), and present results], pituitary output becomes increasingly PACAP-dependent. In rats, it has been shown that PACAP is released into the hypophyseal portal blood (Dow et al., 1994), and about 50% of ACTH-producing cells bind PACAP (Vigh et al., 1993), suggesting that PACAP could also directly stimulate anterior pituitary hormone secretion in vivo (Rawlings and Hezareh, 1996), perhaps acting in parallel with CRH. PACAP-induced secretion of ACTH also occurs in cultured anterior pituitary cell lines (Aoki et al., 1997; Boutillier et al., 1994; Braas et al., 1994; Koch and Lutz-Bucher, 1992; Propato-Mussafiri et al., 1992), although doubts have been raised with respect to the in vivo relevance of these findings (Rawlings and Hezareh, 1996).

Despite normal basal ACTH output, two pieces of evidence from our experiments suggest that the pituitary gland in PACAP-deficient mice is itself predisposed towards responding insufficiently to stressors. First, RNA yields from pituitaries are >20% lower in PACAP-deficient mice, suggesting that the glands are smaller in size (Figure 28). Second, abundance of POMC mRNA, the precursor from which ACTH is ultimately derived, is significantly diminished (Figure 21). While neither result can automatically be attributed to the anterior pituitary, i.e. the compartment most relevant for the HPA axis, it is clearly warranted to further investigate whether pituitary weight, size and cellular composition differ between PACAP genotypes, and whether expression of the POMC or ACTH peptides is reduced. Given that PACAP is known to stimulate POMC promoter activity as well as hnRNA and mRNA expression in pituitary cells and pituitary-derived cell lines (Aoki et al., 1997; Boutillier et al., 1994; Braas et al., 1994; Rene et al., 1996), our results may suggest that tonic PACAP release is required for normal POMC expression levels in vivo, and perhaps for completely normal development of the pituitary gland.

7.9.3. Restraint-induced corticosterone production and secretion is blunted

Historically, it was thought that the adrenal cortex stores little of its secretory products (Holzbauer, 1957; Vogt, 1943), whereas recent functional and ultrastructural data suggest that some form of storage may occur (Mohn et al., 2005). Our results clearly indicate that inducible and sustained adrenocortical steroidogenesis is required for a fully intact response to stressors such as restraint. This inducible steroidogenic response is impaired in PACAP-deficient mice, whereas basal corticosterone concentrations in serum are normal (Figure 16). Although steroid production and secretion in the adrenal cortex are chiefly mediated through ACTH via the HPA axis, there is evidence for functional innervation of the adrenal cortex by the sympathetic splanchnic nerve (Engeland, 1998). Specifically, it appears that the splanchnic nerve modulates adrenocortical responses during stress by increasing adrenal sensitivity to ACTH (Ulrich-Lai and Engeland, 2002).

Our results clearly indicate that PACAP-dependent corticosterone secretion in response to prolonged restraint is controlled far upstream of the adrenal cortex. Activation of the hypophysiotropic PVN is diminished in PACAP-deficient mice, including insufficient CRH biosynthesis. This in turn causes the pituitary response to fail, resulting in strongly attenuated secretion of ACTH. Consequently, the expression of adrenocortical transcription factors (SF-1, Nur77, Nurr1 and Nor1) and StAR, important for regulation of steroidogenic enzyme expression and steroid biosynthesis, respectively, is inadequately stimulated (Figures 22, 23 and 25), and corticosterone production is impaired. The expression patterns of Nur77 and Nurr1 observed in our experiments are in exact agreement with those elicited by ACTH injection (Davis and Lau, 1994), further strengthening our notion that the impaired adrenocortical response of PACAP-deficient mice is indeed due to impaired activation of the HPA axis.

7.10. Nr4a orphan nuclear receptors – inducible transcription factors with important potential roles throughout the HPA axis

The Nr4a family of orphan nuclear receptors has been implicated in regulation of the HPA axis, mostly based on their function as transcription factors. For example, Nur77 and Nurr1 enhance transcriptional activity of the CRH and POMC gene promoters, while also being induced by CRH treatment in pituitary cells, thereby mediating expression of hypothalamic and pituitary stress hormones (Kovalovsky et al., 2002; Murphy and Conneely, 1997; Philips et al., 1997a; Philips et al., 1997b). In addition, induction of Nur77 and Nurr1 has been observed in the adrenal glands in response to stress or ACTH injection (Davis and Lau, 1994; Honkaniemi et al., 2000), showing that all three compartments of the HPA axis are likely targets of Nr4a-mediated effects. Our present results provide important new insights into the expression of Nr4a factors during stress in vivo.

7.10.1. Potential role in PACAP-dependent expression of CRH in the PVN

When CRH is released during stress responses, compensatory biosynthesis is achieved primarily through enhanced CRH gene transcription (Aguilera et al., 2007). The CRH promoter is highly conserved across species and contains a number of response elements for different transcriptional regulators, including an NGFI-B response element (NBRE) (Yao and Denver, 2007) that can be bound by the Nr4a family of orphan nuclear receptors. Via ligand-independent, monomeric and homo- or heterodimeric binding to their shared DNA response elements (NBRE and NurRE), Nr4a factors activate target gene promoters, with specific combinations effecting gene- and sequence-specific response patterns (Maira et al., 1999). The CRH promoter also includes binding sites for the glucocorticoid receptor (Yao and Denver, 2007). The glucocorticoid receptor (GR) is a nuclear receptor that binds corticosterone and controls negative feedback within the HPA axis, required for appropriate termination of acute stress responses, partly via repression of CRH transcription (Aguilera et al., 2007).

A number of studies have shown that within the rodent hypothalamus in vivo, stress induces increases in Nur77 expression that occur in the paraventricular nucleus (PVN), where CRH-containing neuroendocrine neurons are located (Chan et al., 1993; Honkaniemi et al., 1994; Imaki et al., 1996; Kovacs and Sawchenko, 1996b; Umemoto et al., 1994; Umemoto et al., 1997). Furthermore, CRH induces Nur77 expression in the PVN in vivo, potentially as a means of autoregulation (Parkes et al., 1993). In our present experiments, expression of Nur77 and Nor1 in the hypothalamus was found to be rapidly induced in response to restraint, and our in situ hybridization data show that Nur77 and Nor1 mRNA indeed overlaps with CRH mRNA in cells of the PVN (Figures 19 and 20). Regulation of Nur77 and Nor1 was significantly blunted, and regulation of CRH completely abolished, in PACAP-deficient compared to wild-type mice. Transcriptional activation of the CRH promoter has been shown for Nurr1 (Murphy and Conneely, 1997), and Nr4a factors are known to antagonize GR-mediated negative feedback via protein-protein interactions and competition for DNA binding (Martens et al., 2005; Philips et al., 1997b). Thus, the PACAP-dependent upregulation of Nur77 and Nor1 we observed could theoretically affect CRH expression directly (activation) and indirectly (inhibition of negative feedback). The latter scenario has previously been proposed for the AP-1 transcription factors Fos and Jun (Umemoto et al., 1997). However, several pieces of evidence suggest that neither ITF nor protein synthesis are required for immediate increases in CRH gene transcription. First, the time course with which ITF and putative target genes are upregulated in the PVN during stress do not appear to match (Imaki et al., 1996; Kovacs and Sawchenko, 1996a; Kovacs and Sawchenko, 1996b). Second, injection of antisense oligonucleotides against Fos or Jun into the PVN (Itoi et al., 1996) or systemic administration of cycloheximide (Kovacs et al., 1998) is ineffective in blocking hypoglycemia- or ether-induced increases in CRH mRNA or hnRNA, respectively. Based on this, it would appear more likely that Nr4a factors control sustained CRH mRNA expression via inhibition of GR-mediated negative feedback, rather than acute and direct transcriptional activation.

Most studies clearly point towards cAMP responsive element binding protein (CREB) as the dominant activator of immediate stress-induced CRH gene transcription [see for example evidence provided by (Itoi et al., 1996; Kovacs et al., 1998)]. In this regard, it is important to note that phosphorylation of CREB in CRH-positive neurons has been observed after i.c.v. injection of PACAP (Agarwal et al., 2005). Thus, it is tempting to speculate that PACAP activates a) CREB to control immediate transcriptional induction of CRH, and b) Nr4a factors to maintain CRH expression in the face of elevated glucocorticoid levels. In fact, given that all three Nr4a factors are known transcriptional targets of CREB, as are the PACAP-dependent transcription factors Egr1 and Fos (Impey et al., 2004), it is possible that PACAPergic signaling in the PVN controls PACAP-dependent expression of ITF via activation of CREB (see Figure 32 for a schematic summary of this proposed mechanism). Supporting this notion, a very recent study showed that the Nr4a factors are induced by CREB and mediate CREB-dependent neuronal survival (Volakakis et al., 2010).

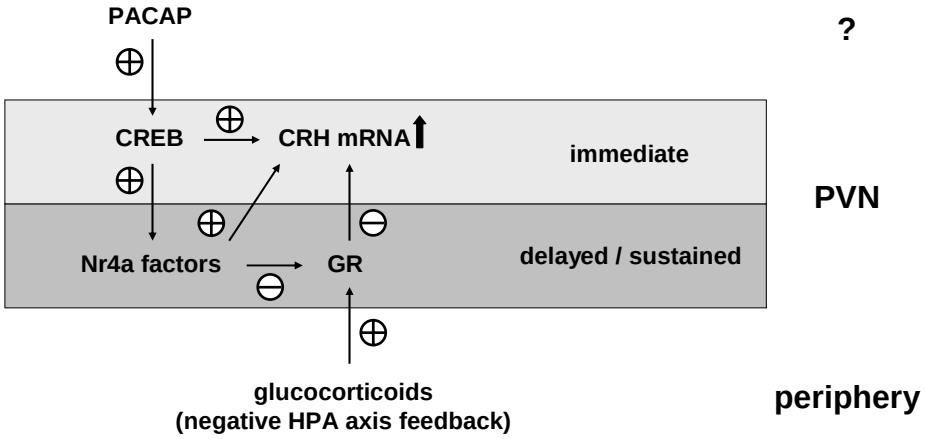

Figure 32. Schematic representation of putative molecular mechanisms by which PACAP controls expression of CRH mRNA in the PVN during stress responses in vivo. Question mark indicates that the source of PACAPergic signals impinging on neurons in the PVN (or hypothalamic areas in the vicinity) is not known with certainty (see section 7.11). Plus signs indicate stimulation, minus signs indicate inhibition. See text for details and abbreviations.

At the least, regardless of the postulated molecular mechanisms, PACAP-dependent induction of Nur77 and Nor1 as reported here indicates PACAP-dependent functional activation of PVN neurons (Chan et al., 1993). The fact that CRH mRNA upregulation is completely abolished in PACAP-deficient mice strongly supports the notion that PACAP controls the HPA axis at this central locus. Our finding of Nurr1 expression being unaffected by stressor exposure is in agreement with previous work (Honkaniemi et al., 1994). Future experiments could address potential colocalization of CRH peptide with Nur77 and Nor1 proteins, using standard immunohistochemical techniques, to see whether they are indeed expressed in the very same hypophysiotropic neurons. Also, it would be very interesting to determine whether Nur77 and Nor1 actually bind to the CRH gene promoter after stressor exposure in vivo, and whether there are other genes in hypophysiotropic neurons regulated by these transcription factors.

Experiments in cell culture could be used to determine whether knock-down of the Nr4a family interferes with target gene expression (such as sustained CRH mRNA elevation), e.g. by application of RNA interference to primary hypothalamic neurons. Unfortunately, the mouse hypothalamic cell lines we intended to use for this purpose did not express CRH, although they had been advertised as such (results not shown).

7.10.2. Potential role in control of pituitary function during stress

Transcripts encoding the three Nr4a factors are upregulated by CRH in pituitary cells and the pituitary-derived cell line AtT-20 (Kovalovsky et al., 2002; Maira et al., 1999; Murphy and Conneely, 1997). The POMC gene promoter is known to be controlled by Nr4a factors (Fernandez et al., 2000; Kovalovsky et al., 2002; Maira et al., 1999; Martens et al., 2005; Murphy and Conneely, 1997), implicating them as mediators of CRH effects. Furthermore, a Nur-responsive element (NurRE) in the POMC promoter is crucial to integration of positive (Nr4a-mediated activation) and negative (GR-mediated glucocorticoid feedback) signals affecting POMC mRNA expression (Martens et al., 2005; Murphy and Conneely, 1997; Philips et al., 1997b). In our current experiments, POMC was found to be upregulated only modestly (1.5-fold at 6h versus untreated mice), which only occurred in wild-type mice but did not reach statistical significance (Figure 21). This suggests that rapid PACAP-dependent upregulation of Nur77 and Nurr1 may contribute to inhibition of negative feedback, perhaps by binding to GR (Martens et al., 2005), rather than directly activating POMC expression, although the latter is also possible. Absence of induction (Moncek et al., 2001) and elevated hnRNA, but unchanged mRNA (Noguchi et al., 2006), have previously been reported for POMC in response to brief acute stress. Other studies indicate that repeated stressor exposure maximally increases POMC mRNA (Marti et al., 1999; Noguchi et al., 2006). PACAP-dependent Nr4a factor induction in the pituitary could therefore support POMC expression during sustained or chronic stress, and the phenotype of PACAP-deficient mice during such paradigms is the subject of future experiments.

Glucocorticoid-dependent negative feedback regulation of ACTH secretion is firmly established (Keller-Wood and Dallman, 1984), and some evidence indicates that it requires new mRNA and protein synthesis (Dayanithi and Antoni, 1989). Notably, overexpression of Nur77 has been shown to antagonize GR-mediated inhibition of ACTH secretion (Okabe et al., 1998), suggesting that PACAP-dependent upregulation of Nr4a factors in vivo could maintain ACTH output of the pituitary via this non-genomic mechanism. See Figure 33 (following page) for a schematic summary of the mechanisms proposed above.

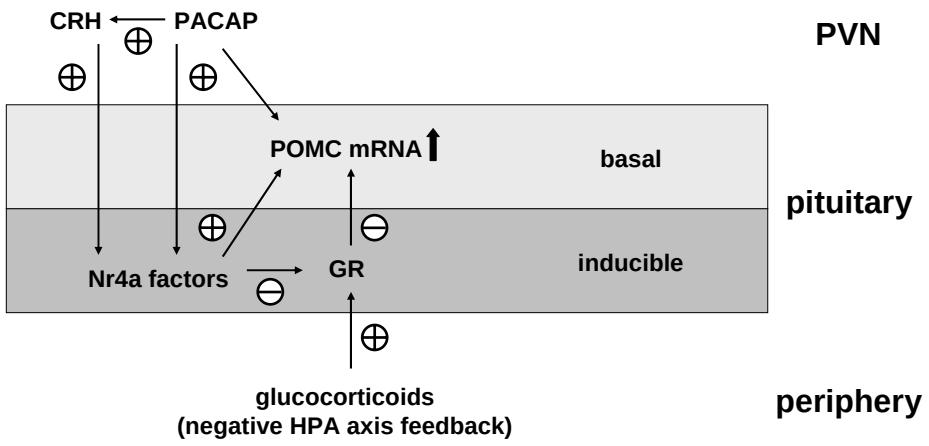

Figure 33. Schematic representation of putative molecular mechanisms by which PACAP controls expression of POMC mRNA in the pituitary gland in vivo. Basal stimulatory effects are deduced from significantly reduced POMC mRNA abundance in pituitary glands from PACAP-deficient mice. Inducible expression (although modest in response to acute stressors) is proposed to proceed via PACAP- and CRH-dependent induction of Nr4a factors (see section 7.10.2). Plus signs indicate stimulation, minus signs indicate inhibition. See text for details and abbreviations.

7.10.3. Potential role in adrenocortical stimulus-transcription coupling

Our experiments show that all three Nr4a family members are PACAP-dependently upregulated in the adrenal cortex during stress. Rapid and pronounced increases in adrenocortical Nur77 and Nurr1 expression are consistent with the literature (Davis and Lau, 1994; Honkaniemi et al., 2000) whereas, to our knowledge, we are the first to describe stressor-induced increases in Nor1 abundance. The zone-specific expression patterns of the three factors were distinct, with Nur77 showing strong upregulation throughout the cortex, while Nurr1 and Nor1 were most prominently induced in the outer layers (Figure 23). The pattern we observed for Nur77 and Nurr1 is in agreement with previous reports and identical with that elicited by ACTH injection (Davis and Lau, 1994), suggesting that PACAP-dependent Nr4a induction in adrenocortical cells is a direct consequence of the PACAP-dependent ACTH secretion shown here.

ACTH controls all of the factors required for adrenocortical steroid biosynthesis, including those that produce corticosterone. Most of these are subject to transcriptional control by SF-1 (Nr5a1) (Sewer and Waterman, 2003), another member of the orphan nuclear receptor superfamily. In the present experiments, SF-1 mRNA was found to be significantly upregulated, with expression levels reaching a peak after 3h of restraint, a response that was significantly attenuated in PACAP-deficient mice (Figure 25).

Most importantly, we found mRNA encoding steroidogenic acute regulatory protein (StAR) to be PACAP-dependently induced in the adrenal glands in response to stress (Figure 25). StAR is the limiting factor for steroidogenesis, mediating the transfer of cholesterol (the precursor for all steroids) to the inner mitochondrial membrane. Production of its mRNA and protein are tightly linked, as well as tightly coupled to steroid biosynthesis (Manna et al., 2009). Transcriptional activators of StAR include SF-1 as well as the Nr4a family (Lavoie and King,

2009; Martin et al., 2008; Martin and Tremblay, 2009). Since Nur77, Nurr1 and Nor1 were all PACAP-dependently induced in the adrenocortical compartment, in addition to SF-1, our data suggest that their upregulation and subsequent increases in StAR provide the link between the PACAP-dependent ACTH release and PACAP-dependent sustained corticosterone secretion demonstrated in the present work.

7.11. Is PACAP released in the PVN? If so, where does it come from, and how does it induce excitatory signaling to mediate stress responses?

Based on the immediate behavioral effects of intracerebroventricular (Agarwal et al., 2005) and intra-PVN infusions (Norrholm et al., 2005), as well as the extensive histochemical and endocrinological evidence cited earlier, including our own, it has convincingly been demonstrated that PACAP's acute role in stressor-responsive pathways is that of an excitatory agent. However, at the central level, it is not known whether this is truly direct, i.e. elicited by PACAP via binding to receptors on hypophysiotropic and preautonomic neurons in the PVN, or via modulation of other transmitter systems. Also, the regional and cellular sources of PACAP-dependent effects are not completely known, such that the underlying neurochemistry and neurocircuitry have yet to be fully elucidated. Figure 34 is a schematic depiction of known PACAPergic pathways impinging on the PVN, as well as subsequent compartments involved in the generation of stress responses. Note that only those compartments are represented in which a direct effect of PACAP has been demonstrated or can reasonably be assumed to occur.

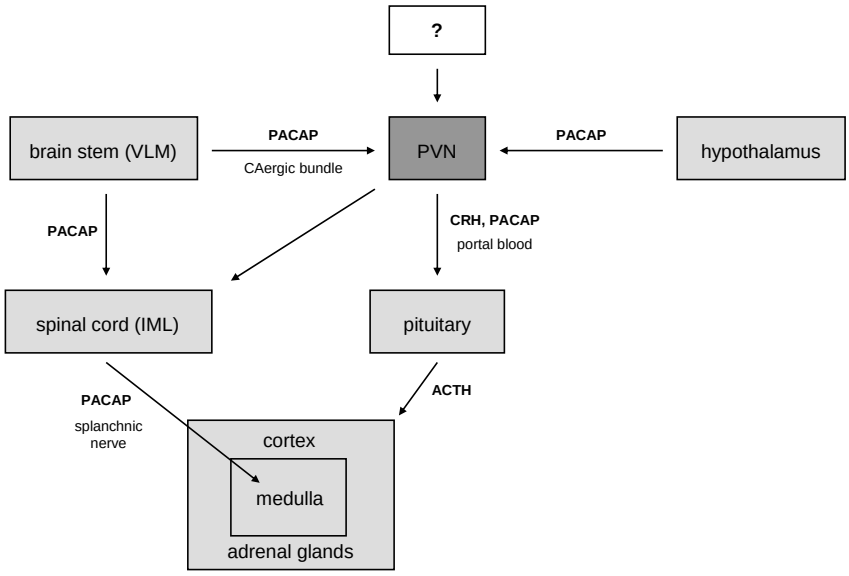

Figure 34. Schematic of PACAPergic stress-responsive pathways. Abbreviations: CAergic bundle, catecholaminergic bundle; IML, intermediolateral column; PVN, paraventricular nucleus of the hypothalamus; VLM, ventrolateral medulla. Note that the most likely sources of PACAP release in the PVN are the brain stem and hypothalamus. Question mark indicates that there could be multiple additional sources, which are unknown. See text for details and references.

PACAP is expressed in several regions of the nervous system that are directly connected with the PVN. Neurons in cell groups A1, A2 and C1-C3 of the ventrolateral medulla oblongata (VLM) send projections to the PVN via the ventral catecholaminergic bundle. This bundle of nerve fibers is activated during stress (Pacak and Palkovits, 2001), and PACAP was recently found to be expressed in a subpopulation of catecholaminergic neurons in the VLM (Das et al., 2007; Farnham et al., 2008). Microdialysis studies have previously shown that PACAP potently causes release of norepinephrine (NE) in the PVN (Huang et al., 1996). Furthermore, it is well documented that NE participates in stimulation of PVN neurons, mainly by driving an excitatory glutamatergic relay system (Herman et al., 2002). Thus, it is possible that PACAP modulates NE-mediated signaling, rather than, or in addition to, stimulating neurons in the PVN directly. Complicating the issue even further, PACAP-immunoreactive cell bodies and nerve fibers are found very abundantly throughout the hypothalamus, including the PVN (Hannibal, 2002), and several PACAP-expressing subregions of the hypothalamus project to the PVN (Das et al., 2007). Given that the microenvironment of the PVN is very complex and involves multi-directional signaling via multiple systems, including classical transmitters, peptides and gaseous substances (Herman et al., 2002), it will be very challenging to dissect the mechanisms through which PACAP exerts its prominent effects. Based on the distribution and known functions of PACAP in the aforementioned circuits, direct and indirect neurotransmitter effects, as well as paracrine/autocrine signaling, are possible sources of PACAP-dependent stimulation of the PVN.

Within the PVN, PACAP has access to the HPA axis and autonomic nervous system via hypophysiotropic and preautonomic neurons, respectively (Das et al., 2007; Yi et al., 2010). Release of PACAP into the hypophyseal portal blood (Dow et al., 1994) may act in parallel with PACAP-dependent CRH to stimulate the anterior pituitary. PACAP-containing neurons of the brain stem that project to the intermediolateral column (IML) of the spinal cord (Das et al., 2007; Farnham et al., 2008) are sources for PACAP-dependent effects mediated via sympathetic nerves (Das et al., 2007; Farnham et al., 2008; Yi et al., 2010). Finally, PACAPergic innervation of the adrenal medulla, originating in the IML, has been shown to control responses to insulin-induced hypoglycemia (Hamelink et al., 2002).

Taken together, PACAP is found in several relay stations within the neuroendocrine circuitry that senses stressor exposure in the periphery, signals to the CNS, and elaborates adequate responses. Disruption of the gene encoding PACAP is therefore likely to affect neural signaling at multiple levels. Nevertheless, we propose that PACAP, originating from neurons either in the brain stem and/or hypothalamus (Das et al., 2007; Farnham et al., 2008; Hannibal, 2002), is released in the PVN to directly affect CRH production and activation of hypophysiotropic (and perhaps preautonomic) cell groups. We further argue that the PACAP-dependent expression of CRH, Nur77 and Nor1 mRNA in response to restraint, described in the present experiments, could serve as an index of this mechanism. This argument is based on the expression pattern of the PACAP-specific PAC1 receptor in the PVN, whose mRNA overlaps largely with mRNA encoding CRH (Nomura et al., 1996), and our finding that Nr4a

factors are rapidly induced by PACAP in a neuroendocrine cell line expressing PAC1 (Eiden et al., 2008).

7.12. PACAP mouse models and mental health – what is the "state of the art"?

Mice with mutations in the genes encoding PACAP or PAC1 have been shown to display abnormalities in prepulse inhibition, social behaviors, learning, fear and locomotion. This has led to the suggestion that they might be useful models for a whole range of psychiatric conditions, including schizophrenia, anxiety, depression, and attention deficit hyperactivity disorder (ADHD) (Girard et al., 2006; Hashimoto et al., 2009; Hashimoto et al., 2001; Ishihama et al., 2010; Nicot et al., 2004; Otto et al., 2001a; Otto et al., 2001b; Shintani et al., 2006; Tanaka et al., 2006). Human association studies of the genes encoding PACAP and PAC1 appeared to strengthen the view that PACAP signaling is involved in neurobiological mechanisms underlying schizophrenia and major depressive disorder (Hashimoto et al., 2007; Hashimoto et al., 2010). However, other studies suggested that genetic susceptibility to schizophrenia is unlikely to be substantially affected by single-nucleotide polymorphisms in the gene encoding PACAP (Ishiguro et al., 2001; Koga et al., 2010). PACAP was also proposed to mediate therapeutic effects of lithium in bipolar disorder (Brandish et al., 2005), but genetic association studies in humans yielded negative results (Ishiguro et al., 2001; Lohoff et al., 2008). Thus, it is clear that there is still a gap between our understanding of the molecular and cellular mechanisms of PACAP signaling, animal models of altered PACAP signaling function, and the human psychiatric disease states in which PACAP is potentially implicated. Despite the limitations in translation of experimental findings from mice to humans, animal models will continue to be critical in dissecting the biology of mental health (Berton and Nestler, 2006; Crawley et al., 1997; Kalueff et al., 2007).

7.13. PACAP, chronic stress, anxiety and depression – problems and perspectives

Glucocorticoids are highly pleiotropic molecules that have important effects on virtually every physiological system in the body. Thus, the consequences of elevated glucocorticoid concentrations during stress are very complex, entailing both positive and negative aspects (Sapolsky et al., 2000). Nevertheless, it is quite clear that chronic stress and chronic hypersecretion of glucocorticoids, acting in concert with genetic predispositions and environmental determinants, are risk factors for many illnesses. These include neurological and psychiatric diseases, such as anxiety disorders and depression [reviewed in (Chrousos, 2009; Cohen et al., 2007; de Kloet et al., 2005; Herman and Seroogy, 2006)].

Since we and others have shown that basal corticosterone concentrations are normal in PACAP-deficient mice, but circadian fluctuations and responses to stressors are blunted [present results, as well as (Hashimoto et al., 2009; Morita et al., 2006; Stroth and Eiden, 2010)], we predict that PACAP-deficient mice will be less susceptible to the effects of chronic

stress, and thus less likely to develop anxiety or depression. In other words, disruption of PACAP signaling is expected to diminish or abolish hypersecretion of corticosterone during chronic stress, while maintaining glucocorticoid concentrations necessary for survival and normal function. Lending preliminary support to this idea, PACAP- and PAC1-deficient mice display strongly reduced anxiety-like behavior compared to wild-types (Girard et al., 2006; Hashimoto et al., 2001; Otto et al., 2001b), and administration of PACAP into the central amygdala has been shown to promote a shift from active to passive coping mechanisms in response to electric shock (Legradi et al., 2007). Furthermore, chronic stress causes upregulation of PACAP and PAC1 in the bed nucleus of the stria terminalis (BNST), and infusion of PACAP into this area elicits a long-lasting anxiogenic response (Hammack et al., 2009). These findings provide evidence for the notion that PACAP is an anxiogenic factor in vivo, and thus potentially represents a target for psychiatric conditions such as anxiety and depression. However, PACAP-deficient mice have also been reported to display increased depression-like behavior compared to wild-types (Hashimoto et al., 2009), an observation that does not fit with the aforementioned decrease in anxiety-like behaviors. One of the challenges in this context is the absence of unequivocal distinctions between anxiety and depression, both in humans and in rodent models (Berton and Nestler, 2006), an issue that is further complicated by numerous problems associated with the use of animal models for stress-triggered psychiatric diseases (Kalueff et al., 2007).

The phenotype of PACAP-deficient mice in chronic stress paradigms has not yet been investigated, and this is an interesting future direction. As a behavioral model for stress-induced anxiety and depression, the usefulness of this approach might be hampered by the fact that mice with a disrupted PACAP-PAC1 signaling system already display strongly reduced anxiety in the absence of challenge, as mentioned above (Girard et al., 2006; Hashimoto et al., 2001; Otto et al., 2001b). In general, it would be preferable to have a strain in which behavioral differences between genetically altered and wild-type mice only manifest after stressor exposure, as this would be required for etiological validity of the model (Berton and Nestler, 2006). For example, mice with a 50% reduction in GR expression levels show depression-like behavior only after stress, thus mimicking the human situation more closely (Chourbaji et al., 2008). Nevertheless, it will be worthwhile to determine whether PACAP-deficient mice display exacerbated or diminished endocrine and neurochemical symptoms of chronic stress, and what the underlying mechanisms are on the cellular and molecular level.

7.14. Concluding remarks and future directions

Our experiments have provided solid evidence for the notion that PACAP is a major player in orchestrating acute stress responses in vivo. As shown by Hamelink and others, PACAP's neurotransmitter role at the sympathoadrenal synapse is a matter of life and death, controlling synthesis and secretion of catecholamines from adrenomedullary chromaffin cells during hypoglycemia-induced stress (Hamelink et al., 2002). As shown by the present results, this is paralleled by PACAP-dependent induction of catecholaminergic enzyme synthesis, as well as release-modulating neuropeptides. Furthermore, we have identified endogenous PACAP as a crucial regulator of CRH-expressing neurons in the hypothalamic PVN, the central integrator of all stress responses (Herman and Cullinan, 1997). Thus, by controlling the HPA axis far upstream, PACAP is required for the acute response to stressors such as restraint, as shown by significantly blunted hormone secretion in PACAP-deficient mice. Our results also suggest that this entails a PACAP-dependent wave of stimulus-transcription coupling throughout the HPA axis, possibly involving Nr4a orphan nuclear receptors at all levels, which is triggered by PACAP-dependent stimulation of the PVN.

Future experiments will determine how PACAP affects responses to chronic stressors on the endocrine and cellular levels. In addition, and perhaps most importantly, they will address the mechanisms underlying PACAP-mediated central control at the level of the hypothalamus. Is PACAP directly affecting neurons in the PVN by binding to PAC1? Or does PACAP modulate signaling via the classical transmitters, such as glutamate, GABA and norepinephrine? Experimental systems such as primary cultures or acute tissue preparations are possible tools to address these questions. By understanding PACAP-induced signaling in more detail, we hope to discover potential molecular targets for therapeutic intervention, such as during chronic stress-induced mental illness. As mentioned earlier, PACAP appears to be a reasonable candidate, based on the fact that its genetic disruption allows basal function of the HPA axis to proceed normally, while most likely dampening excessive glucocorticoid secretion during persistent and chronic stimulation. Thus, there are still many exciting questions regarding the involvement of PACAP in stress responses.

8. References

Adams, B. A., Gray, S. L., Isaac, E. R., Bianco, A. C., Vidal-Puig, A. J., and Sherwood, N. M. (2008). Feeding and metabolism in mice lacking pituitary adenylate cyclase-activating polypeptide. Endocrinology *149*, 1571-1580.

Agarwal, A., Halvorson, L. M., and Legradi, G. (2005). Pituitary adenylate cyclase-activating polypeptide (PACAP) mimics neuroendocrine and behavioral manifestations of stress: Evidence for PKA-mediated expression of the corticotropin-releasing hormone (CRH) gene. Molecular Brain Research *138*, 45-57.

Aguilera, G., Kiss, A., Liu, Y., and Kamitakahara, A. (2007). Negative regulation of corticotropin releasing factor expression and limitation of stress response. Stress *10*, 153-161.

Anouar, Y., and Eiden, L. E. (1995). Rapid and long-lasting increase in galanin mRNA levels in rat adrenal medulla following insulin-induced reflex splanchnic nerve stimulation. Neuroendocrinology *62*, 611-618.

Anouar, Y., Lee, H. W., and Eiden, L. E. (1999). Both inducible and constitutive activator protein-1-like transcription factors are used for transcriptional activation of the galanin gene by different first and second messenger pathways. Mol Pharmacol *56*, 162-169.

Aoki, Y., Iwasaki, Y., Katahira, M., Oiso, Y., and Saito, H. (1997). Regulation of the rat proopiomelanocortin gene expression in AtT-20 cells. II: Effects of the pituitary adenylate cyclase-activating polypeptide and vasoactive intestinal polypeptide. Endocrinology *138*, 1930-1934.

Arimura, A., Somogyvari-Vigh, A., Miyata, A., Mizuno, K., Coy, D. H., and Kitada, C. (1991). Tissue distribution of PACAP as determined by RIA: highly abundant in the rat brain and testes. Endocrinology *129*, 2787-2789.

Armario, A., Escorihuela, R. M., and Nadal, R. (2008). Long-term neuroendocrine and behavioural effects of a single exposure to stress in adult animals. Neurosci Biobehav Rev *32*, 1121-1135.

Armario, A., Valles, A., Dal-Zotto, S., Marquez, C., and Belda, X. (2004). A single exposure to severe stressors causes long-term desensitisation of the physiological response to the homotypic stressor. Stress *7*, 157-172.

Armstrong, W. E., Warach, S., Hatton, G. I., and McNeill, T. H. (1980). Subnuclei in the rat hypothalamic paraventricular nucleus: a cytoarchitectural, horseradish peroxidase and immunocytochemical analysis. Neuroscience *5*, 1931-1958.

Bassett, J. R., and West, S. H. (1997). Vascularization of the adrenal cortex: its possible involvement in the regulation of steroid hormone release. Microsc Res Tech *36*, 546-557.

Bernard, C. (1865). Introduction à l'étude de la médecine expérimentale (Paris: Baillière).

Berton, O., and Nestler, E. J. (2006). New approaches to antidepressant drug discovery: beyond monoamines. Nat Rev Neurosci *7*, 137-151.

Borg, W. P., Sherwin, R. S., During, M. J., Borg, M. A., and Shulman, G. I. (1995). Local ventromedial hypothalamus glucopenia triggers counterregulatory hormone release. Diabetes *44*, 180-184.

Bornstein, S. R., Ehrhart-Bornstein, M., and Scherbaum, W. A. (1997). Morphological and functional studies of the paracrine interaction between cortex and medulla in the adrenal gland. Microsc Res Tech *36*, 520-533.

Bornstein, S. R., Gonzalez-Hernandez, J. A., Ehrhart-Bornstein, M., Adler, G., and Scherbaum, W. A. (1994). Intimate contact of chromaffin and cortical cells within the human adrenal gland forms the cellular basis for important intraadrenal interactions. J Clin Endocrinol Metab *78*, 225-232.

Boutillier, A. L., Monnier, D., Koch, B., and Loeffler, J. P. (1994). Pituitary adenyl cyclase-activating peptide: a hypophysiotropic factor that stimulates proopiomelanocortin gene transcription, and proopiomelanocortin-derived peptide secretion in corticotropic cells. Neuroendocrinology *60*, 493-502.

Braas, K. M., Brandenburg, C. A., and May, V. (1994). Pituitary adenylate cyclase-activating polypeptide regulation of AtT-20/D16v corticotrope cell proopiomelanocortin expression and secretion. Endocrinology *134*, 186-195.

Braas, K. M., Schutz, K. C., Bond, J. P., Vizzard, M. A., Girard, B. M., and May, V. (2007). Microarray analyses of pituitary adenylate cyclase activating polypeptide (PACAP)-regulated gene targets in sympathetic neurons. Peptides *28*, 1856-1870.

Brandish, P. E., Su, M., Holder, D. J., Hodor, P., Szumiloski, J., Kleinhanz, R. R., Forbes, J. E., McWhorter, M. E., Duenwald, S. J., Parrish, M. L., *et al.* (2005). Regulation of gene expression by lithium and depletion of inositol in slices of adult rat cortex. Neuron *45*, 861-872.

Breslow, M. J. (1992). Regulation of adrenal medullary and cortical blood flow. Am J Physiol *262*, H1317-1330.

Buchanan, T. A., Cane, P., Eng, C. C., Sipos, G. F., and Lee, C. (1991). Hypothermia is critical for survival during prolonged insulin-induced hypoglycemia in rats. Metabolism *40*, 330-334.

Buynitsky, T., and Mostofsky, D. I. (2009). Restraint stress in biobehavioral research: Recent developments. Neurosci Biobehav Rev *33*, 1089-1098.

Cannon, W. B. (1927). Bodily changes in pain, hunger, fear and rage (New York: D. Appleton & Co.).

Cannon, W. B. (1929). Organization for Physiological Homeostasis. Physiological Reviews *9*, 399-431.

Cannon, W. B., McIver, M. A., and Bliss, S. W. (1924). A sympathetic and adrenal mechanism for mobilizing sugar in hypoglycemia. Am J Physiol *69*, 46-66.

Cantu, R. C., Correll, J. W., and Manger, W. M. (1968). Reassessment of central neural pathways necessary for adrenal catecholamine output in response to hypoglycemia. Proc Soc Exp Biol Med *129*, 155-161.

Cantu, R. C., Wise, B. L., Goldfien, A., Gullixson, K. S., Fischer, N., and Ganong, W. F. (1963). Neural Pathways Mediating the Increase in Adrenal Medullary Secretion Produced by Hypoglycemia. Proc Soc Exp Biol Med *114*, 10-13.

Cao, X., Mahendran, R., Guy, G. R., and Tan, Y. H. (1992). Protein phosphatase inhibitors induce the sustained expression of the Egr-1 gene and the hyperphosphorylation of its gene product. J Biol Chem *267*, 12991-12997.

Cao, X., Mahendran, R., Guy, G. R., and Tan, Y. H. (1993). Detection and characterization of cellular EGR-1 binding to its recognition site. J Biol Chem *268*, 16949-16957.

Ceresini, G., Sgoifo, A., Freddi, M., Musso, E., Parmigiani, S., Del Rio, G., and Valenti, G. (1998). Effects of galanin and the galanin receptor antagonist galantide on plasma catecholamine levels during a psychosocial stress stimulus in rats. Neuroendocrinology *67*, 67-72.

Chan, R. K., Brown, E. R., Ericsson, A., Kovacs, K. J., and Sawchenko, P. E. (1993). A comparison of two immediate-early genes, c-fos and NGFI-B, as markers for functional activation in stress-related neuroendocrine circuitry. J Neurosci *13*, 5126-5138.

Chen, Y., Samal, B., Hamelink, C. R., Xiang, C. C., Chen, Y., Chen, M., Vaudry, D., Brownstein, M. J., Hallenbeck, J. M., and Eiden, L. E. (2006). Neuroprotection by endogenous and exogenous PACAP following stroke. Regulatory Peptides *137*, 4-19.

Choi, H. J., Park, S. Y., and Hwang, O. (1999). Differential involvement of PKA and PKC in regulation of catecholamine enzyme genes by PACAP. Peptides *20*, 817-822.

Chourbaji, S., Vogt, M. A., and Gass, P. (2008). Mice that under- or overexpress glucocorticoid receptors as models for depression or posttraumatic stress disorder. Prog Brain Res *167*, 65-77.

Chrousos, G. P. (2004). The glucocorticoid receptor gene, longevity, and the complex disorders of Western societies. Am J Med *117*, 204-207.

Chrousos, G. P. (2009). Stress and disorders of the stress system. Nat Rev Endocrinol *5*, 374-381.

Chrousos, G. P., and Gold, P. W. (1992). The concepts of stress and stress system disorders. Overview of physical and behavioral homeostasis. Jama *267*, 1244-1252.

Cohen, S., Janicki-Deverts, D., and Miller, G. E. (2007). Psychological stress and disease. Jama *298*, 1685-1687.

Colwell, C. S., Michel, S., Itri, J., Rodriguez, W., Tam, J., Lelievre, V., Hu, Z., and Waschek, J. A. (2004). Selective deficits in the circadian light response in mice lacking PACAP. Am J Physiol Regul Integr Comp Physiol *287*, R1194-1201.

Conconi, M. T., Spinazzi, R., and Nussdorfer, G. G. (2006). Endogenous ligands of PACAP/VIP receptors in the autocrine-paracrine regulation of the adrenal gland. International Review of Cytology - a Survey of Cell Biology, Vol 249 *249*, 1-51.

Corbitt, J., Hagerty, T., Fernandez, E., Morgan, W. W., and Strong, R. (2002). Transcriptional and post-transcriptional regulation of tyrosine hydroxylase messenger RNA in PC12 cells during persistent stimulation by VIP and PACAP38: differential regulation by protein kinase A and protein kinase C-dependent pathways. Neuropeptides *36*, 34-45.

Coupland, R. E., and Selby, J. E. (1976). The blood supply of the mammalian adrenal medulla: a comparative study. J Anat *122*, 539-551.

Crawley, J. N., Belknap, J. K., Collins, A., Crabbe, J. C., Frankel, W., Henderson, N., Hitzemann, R. J., Maxson, S. C., Miner, L. L., Silva, A. J.*, et al.* (1997). Behavioral phenotypes of inbred mouse strains: implications and recommendations for molecular studies. Psychopharmacology *132*, 107-124.

Cummings, K. J., Gray, S. L., Simmons, C. J., Kozak, C. A., and Sherwood, N. M. (2002). Mouse pituitary adenylate cyclase-activating polypeptide (PACAP): gene, expression and novel splicing. Mol Cell Endocrinol *192*, 133-145.

Das, M., Vihlen, C. S., and Legradi, G. (2007). Hypothalamic and brainstem sources of pituitary adenylate cyclase-activating polypeptide nerve fibers innervating the hypothalamic paraventricular nucleus in the rat. Journal of Comparative Neurology *500*, 761-776.

Davis, I. J., and Lau, L. F. (1994). Endocrine and neurogenic regulation of the orphan nuclear receptors Nur77 and Nurr-1 in the adrenal glands. Mol Cell Biol *14*, 3469-3483.

Dayanithi, G., and Antoni, F. A. (1989). Rapid as well as delayed inhibitory effects of glucocorticoid hormones on pituitary adrenocorticotropic hormone release are mediated by type II glucocorticoid receptors and require newly synthesized messenger ribonucleic acid as well as protein. Endocrinology *125*, 308-313.

de Kloet, E. R., Joels, M., and Holsboer, F. (2005). Stress and the brain: from adaptation to disease. Nat Rev Neurosci *6*, 463-475.

de Vries, M. G., Lawson, M. A., and Beverly, J. L. (2005). Hypoglycemia-induced noradrenergic activation in the VMH is a result of decreased ambient glucose. Am J Physiol Regul Integr Comp Physiol *289*, R977-981.

Denver, R. J. (2009). Structural and functional evolution of vertebrate neuroendocrine stress systems. Ann N Y Acad Sci *1163*, 1-16.

Dogrukol-Ak, D., Kumar, V. B., Ryerse, J. S., Farr, S. A., Verma, S., Nonaka, N., Nakamachi, T., Ohtaki, H., Niehoff, M. L., Edwards, J. C.*, et al.* (2009). Isolation of peptide transport system-6 from brain endothelial cells: therapeutic effects with antisense inhibition in Alzheimer and stroke models. J Cereb Blood Flow Metab *29*, 411-422.

Donnerer, J. (1988). Reflex activation of the adrenal medulla during hypoglycemia and circulatory dysregulations is regulated by capsaicin-sensitive afferents. Naunyn Schmiedebergs Arch Pharmacol *338*, 282-286.

Dow, R. C., Bennie, J., and Fink, G. (1994). Pituitary adenylate cyclase-activating peptide-38 (PACAP)-38 is released into hypophysial portal blood in the normal male and female rat. J Endocrinol *142*, R1-4.

Eells, J. B., Misler, J. A., and Nikodem, V. M. (2006). Reduced tyrosine hydroxylase and GTP cyclohydrolase mRNA expression, tyrosine hydroxylase activity, and associated neurochemical alterations in Nurr1-null heterozygous mice. Brain Research Bulletin *70*, 186-195.

Ehrhart-Bornstein, M., Hinson, J. P., Bornstein, S. R., Scherbaum, W. A., and Vinson, G. P. (1998). Intraadrenal interactions in the regulation of adrenocortical steroidogenesis. Endocrine Reviews *19*, 101-143.

Eiden, L. E., Samal, B., Gerdin, M. J., Mustafa, T., Vaudry, D., and Stroth, N. (2008). Discovery of pituitary adenylate cyclase-activating polypeptide-regulated genes through microarray analyses in cell culture and in vivo. Ann N Y Acad Sci *1144*, 6-20.

Engeland, W. C. (1998). Functional innervation of the adrenal cortex by the splanchnic nerve. Horm Metab Res *30*, 311-314.

Fang, H., Fan, X., Guo, L., Shi, L., Perkins, R., Ge, W., Dragan, Y. P., and Tong, W. (2007). Self-self hybridization as an alternative experiment design to dye swap for two-color microarrays. Omics *11*, 14-24.

Farnham, M. M., Li, Q., Goodchild, A. K., and Pilowsky, P. M. (2008). PACAP is expressed in sympathoexcitatory bulbospinal C1 neurons of the brain stem and increases sympathetic nerve activity in vivo. Am J Physiol Regul Integr Comp Physiol *294*, R1304-1311.

Fernandez, P. M., Brunel, F., Jimenez, M. A., Saez, J. M., Cereghini, S., and Zakin, M. M. (2000). Nuclear receptors Nor1 and NGFI-B/Nur77 play similar, albeit distinct, roles in the hypothalamo-pituitary-adrenal axis. Endocrinology *141*, 2392-2400.

Finotto, S., Krieglstein, K., Schober, A., Deimling, F., Lindner, K., Bruhl, B., Beier, K., Metz, J., Garcia-Arraras, J. E., Roig-Lopez, J. L.*, et al.* (1999). Analysis of mice carrying targeted mutations of the glucocorticoid receptor gene argues against an essential role of glucocorticoid signalling for generating adrenal chromaffin cells. Development *126*, 2935-2944.

Fischer-Colbrie, R., Eskay, R. L., Eiden, L. E., and Maas, D. (1992). Transsynaptic regulation of galanin, neurotensin, and substance P in the adrenal medulla: combinatorial control by second-messenger signaling pathways. J Neurochem *59*, 780-783.

Formigari, A., Irato, P., and Santon, A. (2007). Zinc, antioxidant systems and metallothionein in metal mediated-apoptosis: biochemical and cytochemical aspects. Comp Biochem Physiol C Toxicol Pharmacol *146*, 443-459.

Frodin, M., Hannibal, J., Wulff, B. S., Gammeltoft, S., and Fahrenkrug, J. (1995). Neuronal localization of pituitary adenylate cyclase-activating polypeptide 38 in the adrenal medulla and growth-inhibitory effect on chromaffin cells. Neuroscience *65*, 599-608.

Ghatei, M. A., Takahashi, K., Suzuki, Y., Gardiner, J., Jones, P. M., and Bloom, S. R. (1993). Distribution, molecular characterization of pituitary adenylate cyclase-activating polypeptide and its precursor encoding messenger RNA in human and rat tissues. J Endocrinol *136*, 159-166.

Girard, B. A., Lelievre, V., Braas, K. M., Razinia, T., Vizzard, M. A., Ioffe, Y., El Meskini, R., Ronnett, G. V., Waschek, J. A., and May, V. (2006). Noncompensation in peptide/receptor gene expression and distinct behavioral phenotypes in VIP- and PACAP-deficient mice. J Neurochem *99*, 499-513.

Girotti, M., Pace, T. W., Gaylord, R. I., Rubin, B. A., Herman, J. P., and Spencer, R. L. (2006). Habituation to repeated restraint stress is associated with lack of stress-induced c-fos expression in primary sensory processing areas of the rat brain. Neuroscience *138*, 1067-1081.

Glavin, G. B., Pare, W. P., Sandbak, T., Bakke, H. K., and Murison, R. (1994). Restraint stress in biomedical research: an update. Neurosci Biobehav Rev *18*, 223-249.

Goldstein, D. S., and Kopin, I. J. (2007). Evolution of concepts of stress. Stress *10*, 109-120.

Goldstein, D. S., and Kopin, I. J. (2008). Adrenomedullary, adrenocortical, and sympathoneural responses to stressors: a meta-analysis. Endocr Regul *42*, 111-119.

Gray, S. L., Cummings, K. J., Jirik, F. R., and Sherwood, N. M. (2001). Targeted disruption of the pituitary adenylate cyclase-activating polypeptide gene results in early postnatal death associated with dysfunction of lipid and carbohydrate metabolism. Mol Endocrinol *15*, 1739-1747.

Gray, S. L., Yamaguchi, N., Vencova, P., and Sherwood, N. M. (2002). Temperature-sensitive phenotype in mice lacking pituitary adenylate cyclase-activating polypeptide. Endocrinology *143*, 3946-3954.

Green, M. C., and Witham, B. A. (1991). Handbook on Genetically Standardized JAX Mice 4th edn (Bar Harbor, Maine: The Jackson Laboratory).

Grinevich, V., Fournier, A., and Pelletier, G. (1997). Effects of pituitary adenylate cyclase-activating polypeptide (PACAP) on corticotropin-releasing hormone (CRH) gene expression in the rat hypothalamic paraventricular nucleus. Brain Res *773*, 190-196.

Gruenewald, T. L., Kemeny, M. E., Aziz, N., and Fahey, J. L. (2004). Acute threat to the social self: shame, social self-esteem, and cortisol activity. Psychosom Med *66*, 915-924.

Grumolato, L., Elkahloun, A. G., Ghzili, H., Alexandre, D., Coulouarn, C., Yon, L., Salier, J. P., Eiden, L. E., Fournier, A., Vaudry, H., and Anouar, Y. (2003). Microarray and suppression subtractive hybridization analyses of gene expression in pheochromocytoma cells reveal pleiotropic effects of pituitary adenylate cyclase-activating polypeptide on cell proliferation, survival, and adhesion. Endocrinology *144*, 2368-2379.

Hamel, R., and Ford-Hutchinson, A. W. (1985). Pulmonary and cardiovascular changes in hyperreactive rats from citric acid aerosols. J Appl Physiol *59*, 354-359.

Hamelink, C., Tjurmina, O., Damadzic, R., Young, W. S., Weihe, E., Lee, H. W., and Eiden, L. E. (2002). Pituitary adenylate cyclase-activating polypeptide is a sympathoadrenal neurotransmitter involved in catecholamine regulation and glucohomeostasis. Proc Natl Acad Sci U S A *99*, 461-466.

Hammack, S. E., Cheung, J., Rhodes, K. M., Schutz, K. C., Falls, W. A., Braas, K. M., and May, V. (2009). Chronic stress increases pituitary adenylate cyclase-activating peptide (PACAP) and brain-derived neurotrophic factor (BDNF) mRNA expression in the bed nucleus of the stria terminalis (BNST): roles for PACAP in anxiety-like behavior. Psychoneuroendocrinology *34*, 833-843.

Hannibal, J. (2002). Pituitary adenylate cyclase-activating peptide in the rat central nervous system: an immunohistochemical and in situ hybridization study. J Comp Neurol *453*, 389-417.

Haq, F., Mahoney, M., and Koropatnick, J. (2003). Signaling events for metallothionein induction. Mutat Res *533*, 211-226.

Hashimoto, H., Hashimoto, R., Shintani, N., Tanaka, K., Yamamoto, A., Hatanaka, M., Guo, X., Morita, Y., Tanida, M., Nagai, K.*, et al.* (2009). Depression-like behavior in the forced swimming test in PACAP-deficient mice: amelioration by the atypical antipsychotic risperidone. J Neurochem *110*, 595-602.

Hashimoto, H., Shintani, N., Tanaka, K., Mori, W., Hirose, M., Matsuda, T., Sakaue, M., Miyazaki, J., Niwa, H., Tashiro, F.*, et al.* (2001). Altered psychomotor behaviors in mice lacking pituitary adenylate cyclase-activating polypeptide (PACAP). Proc Natl Acad Sci U S A *98*, 13355-13360.

Hashimoto, R., Hashimoto, H., Shintani, N., Chiba, S., Hattori, S., Okada, T., Nakajima, M., Tanaka, K., Kawagishi, N., Nemoto, K.*, et al.* (2007). Pituitary adenylate cyclase-activating polypeptide is associated with schizophrenia. Mol Psychiatry *12*, 1026-1032.

Hashimoto, R., Hashimoto, H., Shintani, N., Ohi, K., Hori, H., Saitoh, O., Kosuga, A., Tatsumi, M., Iwata, N., Ozaki, N.*, et al.* (2010). Possible association between the pituitary adenylate cyclase-activating polypeptide (PACAP) gene and major depressive disorder. Neurosci Lett *468*, 300-302.

Herman, J. P., and Cullinan, W. E. (1997). Neurocircuitry of stress: central control of the hypothalamo-pituitary-adrenocortical axis. Trends Neurosci *20*, 78-84.

Herman, J. P., Cullinan, W. E., Ziegler, D. R., and Tasker, J. G. (2002). Role of the paraventricular nucleus microenvironment in stress integration. Eur J Neurosci *16*, 381-385.

Herman, J. P., Figueiredo, H., Mueller, N. K., Ulrich-Lai, Y., Ostrander, M. M., Choi, D. C., and Cullinan, W. E. (2003). Central mechanisms of stress integration: hierarchical circuitry controlling hypothalamo-pituitary-adrenocortical responsiveness. Front Neuroendocrinol *24*, 151-180.

Herman, J. P., and Seroogy, K. (2006). Hypothalamic-pituitary-adrenal axis, glucocorticoids, and neurologic disease. Neurol Clin *24*, 461-481, vi.

Hirsch, E., and Reinbach, H. (1913). Die Fesselungshyperglykämie und Fesselungsglykosurie des Kaninchens. Hoppe-Seylers Zeitschrift für physiologische Chemie *87*, 122–141.

Holgert, H., Dagerlind, A., and Hokfelt, T. (1998). Immunohistochemical characterization of the peptidergic innervation of the rat adrenal gland. Horm Metab Res *30*, 315-322.

Holgert, H., Holmberg, K., Hannibal, J., Fahrenkrug, J., Brimijoin, S., Hartman, B. K., and Hokfelt, T. (1996). PACAP in the adrenal gland--relationship with choline acetyltransferase, enkephalin and chromaffin cells and effects of immunological sympathectomy. Neuroreport *8*, 297-301.

Holzbauer, M. (1957). The corticosterone content of rat adrenals under different experimental conditions. J Physiol *139*, 294-305.

Honkaniemi, J., Kononen, J., Kainu, T., Pyykonen, I., and Pelto-Huikko, M. (1994). Induction of multiple immediate early genes in rat hypothalamic paraventricular nucleus after stress. Brain Res Mol Brain Res *25*, 234-241.

Honkaniemi, J., Zhang, J. S., Longo, F. M., and Sharp, F. R. (2000). Stress induces zinc finger immediate early genes in the rat adrenal gland. Brain Res *877*, 203-208.

Hosoya, M., Kimura, C., Ogi, K., Ohkubo, S., Miyamoto, Y., Kugoh, H., Shimizu, M., Onda, H., Oshimura, M., Arimura, A., and et al. (1992). Structure of the human pituitary adenylate cyclase activating polypeptide (PACAP) gene. Biochim Biophys Acta *1129*, 199-206.

Huang, Q., Legradi, G., and Arimura, A. (1996). Perfusion of the paraventricular nucleus with pituitary adenylate cyclase-activating polypeptide and vasoactive intestinal polypeptide stimulates local release of norepinephrine and its metabolite: microdialysis study in freely moving rats. Ann N Y Acad Sci *805*, 737-742.

Imaki, T., Shibasaki, T., Chikada, N., Harada, S., Naruse, M., and Demura, H. (1996). Different expression of immediate-early genes in the rat paraventricular nucleus induced by stress: relation to corticotropin-releasing factor gene transcription. Endocr J *43*, 629-638.

Impey, S., McCorkle, S. R., Cha-Molstad, H., Dwyer, J. M., Yochum, G. S., Boss, J. M., McWeeney, S., Dunn, J. J., Mandel, G., and Goodman, R. H. (2004). Defining the CREB regulon: A genome-wide analysis of transcription factor regulatory regions. Cell *119*, 1041-1054.

Isaac, E. R., and Sherwood, N. M. (2008). Pituitary adenylate cyclase-activating polypeptide (PACAP) is important for embryo implantation in mice. Mol Cell Endocrinol *280*, 13-19.

Ishido, M., and Masuo, Y. (2004). Transcriptome of pituitary adenylate cyclase-activating polypeptide-differentiated PC12 cells. Regul Pept *123*, 15-21.

Ishiguro, H., Ohtsuki, T., Okubo, Y., Kurumaji, A., and Arinami, T. (2001). Association analysis of the pituitary adenyl cyclase activating peptide gene (PACAP) on chromosome 18p11 with schizophrenia and bipolar disorders. J Neural Transm *108*, 849-854.

Ishihama, T., Ago, Y., Shintani, N., Hashimoto, H., Baba, A., Takuma, K., and Matsuda, T. (2010). Environmental factors during early developmental period influence psychobehavioral abnormalities in adult PACAP-deficient mice. Behav Brain Res *209*, 274-280.

Itoi, K., Horiba, N., Tozawa, F., Sakai, Y., Sakai, K., Abe, K., Demura, H., and Suda, T. (1996). Major role of 3',5'-cyclic adenosine monophosphate-dependent protein kinase A pathway in corticotropin-releasing factor gene expression in the rat hypothalamus in vivo. Endocrinology *137*, 2389-2396.

Jordan, D. A., and Miller, E. D., Jr. (1991). Subarachnoid blockade alters homeostasis by modifying compensatory splanchnic responses to hemorrhagic hypotension. Anesthesiology *75*, 654-661.

Kalueff, A. V., Wheaton, M., and Murphy, D. L. (2007). What's wrong with my mouse model? Advances and strategies in animal modeling of anxiety and depression. Behav Brain Res *179*, 1-18.

Kanamatsu, T., Unsworth, C. D., Diliberto, E. J., Jr., Viveros, O. H., and Hong, J. S. (1986). Reflex splanchnic nerve stimulation increases levels of proenkephalin A mRNA and proenkephalin A-related peptides in the rat adrenal medulla. Proc Natl Acad Sci U S A *83*, 9245-9249.

Keegan, C. E., and Hammer, G. D. (2002). Recent insights into organogenesis of the adrenal cortex. Trends Endocrinol Metab *13*, 200-208.

Keller-Wood, M. E., and Dallman, M. F. (1984). Corticosteroid inhibition of ACTH secretion. Endocr Rev *5*, 1-24.

Kikuta, A., and Murakami, T. (1984). Relationship between chromaffin cells and blood vessels in the rat adrenal medulla: a transmission electron microscopic study combined with blood vessel reconstructions. Am J Anat *170*, 73-81.

Kim, K. S., Kim, C. H., Hwang, D. Y., Seo, H., Chung, S., Hong, S. J., Lim, J. K., Anderson, T., and Isacson, O. (2003). Orphan nuclear receptor Nurr1 directly transactivates the promoter activity of the tyrosine hydroxylase gene in a cell-specific manner. J Neurochem *85*, 622-634.

Kiss, J. Z., Martos, J., and Palkovits, M. (1991). Hypothalamic paraventricular nucleus: a quantitative analysis of cytoarchitectonic subdivisions in the rat. J Comp Neurol *313*, 563-573.

Klopotowska, D., Matuszyk, J., Rapak, A., Gidzinska, B., Cebrat, M., Ziolo, E., and Strzadala, L. (2005). Transactivation activity of Nur77 discriminates between Ca2+ and cAMP signals. Neurochem Int *46*, 305-312.

Koch, B., and Lutz-Bucher, B. (1992). Pituitary adenylate cyclase-activating polypeptide (PACAP) stimulates cyclic AMP formation as well as peptide output of cultured pituitary melanotrophs and AtT-20 corticotrophs. Regul Pept *38*, 45-53.

Koga, M., Ishiguro, H., Horiuchi, Y., Inada, T., Ujike, H., Itokawa, M., Otowa, T., Watanabe, Y., Someya, T., and Arinami, T. (2010). Replication study of association between ADCYAP1 gene polymorphisms and schizophrenia. Psychiatr Genet *20*, 123-125.

Kolber, B. J., and Muglia, L. J. (2009). Defining brain region-specific glucocorticoid action during stress by conditional gene disruption in mice. Brain Res *1293*, 85-90.

Kovacs, K. J., Arias, C., and Sawchenko, P. E. (1998). Protein synthesis blockade differentially affects the stress-induced transcriptional activation of neuropeptide genes in parvocellular neurosecretory neurons. Brain Res Mol Brain Res *54*, 85-91.

Kovacs, K. J., and Sawchenko, P. E. (1996a). Regulation of stress-induced transcriptional changes in the hypothalamic neurosecretory neurons. J Mol Neurosci *7*, 125-133.

Kovacs, K. J., and Sawchenko, P. E. (1996b). Sequence of stress-induced alterations in indices of synaptic and transcriptional activation in parvocellular neurosecretory neurons. J Neurosci *16*, 262-273.

Kovalovsky, D., Refojo, D., Liberman, A. C., Hochbaum, D., Pereda, M. P., Coso, O. A., Stalla, G. K., Holsboer, F., and Arzt, E. (2002). Activation and induction of NUR77/NURR1 in corticotrophs by CRH/cAMP: involvement of calcium, protein kinase A, and MAPK pathways. Mol Endocrinol *16*, 1638-1651.

Kudielka, B. M., and Wust, S. (2010). Human models in acute and chronic stress: assessing determinants of individual hypothalamus-pituitary-adrenal axis activity and reactivity. Stress *13*, 1-14.

Kuri, B. A., Chan, S. A., and Smith, C. B. (2009). PACAP regulates immediate catecholamine release from adrenal chromaffin cells in an activity-dependent manner through a protein kinase C-dependent pathway. J Neurochem *110*, 1214-1225.

Kvetnansky, R., Nankova, B., Hiremagalur, B., Viskupic, E., Vietor, I., Rusnak, M., McMahon, A., Kopin, I. J., and Sabban, E. L. (1996). Induction of adrenal tyrosine hydroxylase mRNA by single immobilization stress occurs even after splanchnic transection and in the presence of cholinergic antagonists. J Neurochem *66*, 138-146.

Kvetnansky, R., Pacak, K., Fukuhara, K., Viskupic, E., Hiremagalur, B., Nankova, B., Goldstein, D. S., Sabban, E. L., and Kopin, I. J. (1995). Sympathoadrenal system in stress. Interaction with the hypothalamic-pituitary-adrenocortical system. Ann N Y Acad Sci *771*, 131-158.

Kvetnansky, R., Sabban, E. L., and Palkovits, M. (2009). Catecholaminergic systems in stress: structural and molecular genetic approaches. Physiol Rev *89*, 535-606.

Laburthe, M., Couvineau, A., and Marie, J. C. (2002). VPAC receptors for VIP and PACAP. Receptors Channels *8*, 137-153.

Lavoie, H. A., and King, S. R. (2009). Transcriptional regulation of steroidogenic genes: STARD1, CYP11A1 and HSD3B. Exp Biol Med (Maywood) *234*, 880-907.

Legradi, G., Das, M., Giunta, B., Hirani, K., Mitchell, E. A., and Diamond, D. M. (2007). Microinfusion of pituitary adenylate cyclase-activating polypeptide into the central nucleus of amygdala of the rat produces a shift from an active to passive mode of coping in the shock-probe fear/defensive burying test. Neural Plast *2007*, 79102.

Legradi, G., Hannibal, J., and Lechan, R. M. (1998). Pituitary adenylate cyclase-activating polypeptide-nerve terminals densely innervate corticotropin-releasing hormone-neurons in the hypothalamic paraventricular nucleus of the rat. Neurosci Lett *246*, 145-148.

Lohoff, F. W., Bloch, P. J., Weller, A. E., Ferraro, T. N., and Berrettini, W. H. (2008). Association analysis of the pituitary adenylate cyclase-activating polypeptide (PACAP/ADCYAP1) gene in bipolar disorder. Psychiatr Genet *18*, 53-58.

Luo, Y., Henricksen, L. A., Giuliano, R. E., Prifti, L., Callahan, L. M., and Federoff, H. J. (2007). VIP is a transcriptional target of Nurr1 in dopaminergic cells. Exp Neurol *203*, 221-232.

Machado, H. B., Vician, L. J., and Herschman, H. R. (2008). The MAPK pathway is required for depolarization-induced "promiscuous" immediate-early gene expression but not for depolarization-restricted immediate-early gene expression in neurons. Journal of Neuroscience Research *86*, 593-602.

Maira, M., Martens, C., Philips, A., and Drouin, J. (1999). Heterodimerization between members of the Nur subfamily of orphan nuclear receptors as a novel mechanism for gene activation. Mol Cell Biol *19*, 7549-7557.

Malhotra, R. K., and Wakade, A. R. (1987). Vasoactive intestinal polypeptide stimulates the secretion of catecholamines from the rat adrenal gland. J Physiol *388*, 285-294.

Manna, P. R., Dyson, M. T., and Stocco, D. M. (2009). Regulation of the steroidogenic acute regulatory protein gene expression: present and future perspectives. Mol Hum Reprod *15*, 321-333.

Mannelli, M., Gheri, R. G., Selli, C., Turini, D., Pampanini, A., Giusti, G., and Serio, M. (1982). A study on human adrenal secretion. Measurement of epinephrine, norepinephrine, dopamine and cortisol in peripheral and adrenal venous blood under surgical stress. J Endocrinol Invest *5*, 91-95.

Martens, C., Bilodeau, S., Maira, M., Gauthier, Y., and Drouin, J. (2005). Protein-protein interactions and transcriptional antagonism between the subfamily of NGFI-B/Nur77 orphan nuclear receptors and glucocorticoid receptor. Mol Endocrinol *19*, 885-897.

Marti, O., Harbuz, M. S., Andres, R., Lightman, S. L., and Armario, A. (1999). Activation of the hypothalamic-pituitary axis in adrenalectomised rats: potentiation by chronic stress. Brain Res *821*, 1-7.

Martin, L. J., Boucher, N., Brousseau, C., and Tremblay, J. J. (2008). The orphan nuclear receptor NUR77 regulates hormone-induced StAR transcription in Leydig cells through cooperation with Ca2+/calmodulin-dependent protein kinase I. Mol Endocrinol *22*, 2021-2037.

Martin, L. J., and Tremblay, J. J. (2009). The nuclear receptors NUR77 and SF1 play additive roles with c-JUN through distinct elements on the mouse Star promoter. J Mol Endocrinol *42*, 119-129.

Mazzocchi, G., Malendowicz, L. K., Neri, G., Andreis, P. G., Ziolkowska, A., Gottardo, L., Nowak, K. W., and Nussdorfer, G. G. (2002). Pituitary adenylate cyclase-activating polypeptide and PACAP receptor expression and function in the rat adrenal gland. International Journal of Molecular Medicine *9*, 233-243.

McCulloch, D. A., Lutz, E. M., Johnson, M. S., MacKenzie, C. J., and Mitchell, R. (2000). Differential activation of phospholipase D by VPAC and PAC1 receptors. Ann N Y Acad Sci *921*, 175-185.

McMahon, A., Kvetnansky, R., Fukuhara, K., Weise, V. K., Kopin, I. J., and Sabban, E. L. (1992). Regulation of tyrosine hydroxylase and dopamine beta-hydroxylase mRNA levels in rat adrenals by a single and repeated immobilization stress. J Neurochem *58*, 2124-2130.

Miller, M. M., and McEwen, B. S. (2006). Establishing an agenda for translational research on PTSD. Ann N Y Acad Sci *1071*, 294-312.

Miyata, A., Arimura, A., Dahl, R. R., Minamino, N., Uehara, A., Jiang, L., Culler, M. D., and Coy, D. H. (1989). Isolation of a novel 38 residue-hypothalamic polypeptide which stimulates adenylate cyclase in pituitary cells. Biochem Biophys Res Commun *164*, 567-574.

Miyata, A., Jiang, L., Dahl, R. D., Kitada, C., Kubo, K., Fujino, M., Minamino, N., and Arimura, A. (1990). Isolation of a neuropeptide corresponding to the N-terminal 27 residues of the pituitary adenylate cyclase activating polypeptide with 38 residues (PACAP38). Biochem Biophys Res Commun *170*, 643-648.

Miyata, A., Sano, H., Li, M., Matsuda, Y., Kaiya, H., Sato, K., Matsuo, H., Kangawa, K., and Arimura, A. (2000). Genomic organization and chromosomal localization of the mouse pituitary adenylate cyclase activating polypeptide (PACAP) gene. Vip, Pacap, Glucagon, and Related Peptides *921*, 344-348.

Mohn, C. E., Fernandez-Solari, J., De Laurentiis, A., Prestifilippo, J. P., de la Cal, C., Funk, R., Bornstein, S. R., McCann, S. M., and Rettori, V. (2005). The rapid release of corticosterone from the adrenal induced by ACTH is mediated by nitric oxide acting by prostaglandin E2. Proc Natl Acad Sci U S A *102*, 6213-6218.

Moley, K. H., and Mueckler, M. M. (2000). Glucose transport and apoptosis. Apoptosis *5*, 99-105.

Moller, K., and Sundler, F. (1996). Expression of pituitary adenylate cyclase activating peptide (PACAP) and PACAP type I receptors in the rat adrenal medulla. Regul Pept *63*, 129-139.

Moncek, F., Kvetnansky, R., and Jezova, D. (2001). Differential responses to stress stimuli of Lewis and Fischer rats at the pituitary and adrenocortical level. Endocr Regul *35*, 35-41.

Morita, K., Bell, R. A., Siddall, B. J., and Wong, D. L. (1996). Neural stimulation of Egr-1 messenger RNA expression in rat adrenal gland: possible relation to phenylethanolamine N-methyltransferase gene regulation. J Pharmacol Exp Ther *279*, 379-385.

Morita, Y., Yanagida, D., Shintani, N., Ogita, K., Nishiyama, N., Tsuchida, R., Hashimoto, H., and Baba, A. (2006). Lack of trimethyltin (TMT)-induced elevation of plasma corticosterone in PACAP-deficient mice. Ann N Y Acad Sci *1070*, 450-456.

Muller, M. B., Uhr, M., Holsboer, F., and Keck, M. E. (2004). Hypothalamic-pituitary-adrenocortical system and mood disorders: highlights from mutant mice. Neuroendocrinology *79*, 1-12.

Murakami, T., Oukouchi, H., Uno, Y., Ohtsuka, A., and Taguchi, T. (1989). Blood vascular beds of rat adrenal and accessory adrenal glands, with special reference to the corticomedullary portal system: a further scanning electron microscopic study of corrosion casts and tissue specimens. Arch Histol Cytol *52*, 461-476.

Murphy, E. P., and Conneely, O. M. (1997). Neuroendocrine regulation of the hypothalamic pituitary adrenal axis by the nurr1/nur77 subfamily of nuclear receptors. Molecular Endocrinology *11*, 39-47.

Mustafa, T., Grimaldi, M., and Eiden, L. E. (2007). The hop cassette of the PAC1 receptor confers coupling to Ca2+ elevation required for pituitary adenylate cyclase-activating polypeptide-evoked neurosecretion. J Biol Chem *282*, 8079-8091.

Nankova, B., Kvetnansky, R., McMahon, A., Viskupic, E., Hiremagalur, B., Frankle, G., Fukuhara, K., Kopin, I. J., and Sabban, E. L. (1994). Induction of tyrosine hydroxylase gene expression by a nonneuronal nonpituitary-mediated mechanism in immobilization stress. Proc Natl Acad Sci U S A *91*, 5937-5941.

Nicot, A., Otto, T., Brabet, P., and Dicicco-Bloom, E. M. (2004). Altered social behavior in pituitary adenylate cyclase-activating polypeptide type I receptor-deficient mice. J Neurosci *24*, 8786-8795.

Nogi, H., Hashimoto, H., Fujita, T., Hagihara, N., Matsuda, T., and Baba, A. (1997). Pituitary adenylate cyclase-activating polypeptide (PACAP) receptor mRNA in the rat adrenal gland: localization by in situ hybridization and identification of splice variants. Jpn J Pharmacol *75*, 203-207.

Noguchi, T., Makino, S., Maruyama, H., and Hashimoto, K. (2006). Regulation of proopiomelanocortin gene transcription during single and repeated immobilization stress. Neuroendocrinology *84*, 21-30.

Nomura, M., Ueta, Y., Serino, R., Kabashima, N., Shibuya, I., and Yamashita, H. (1996). PACAP type I receptor gene expression in the paraventricular and supraoptic nuclei of rats. Neuroreport *8*, 67-70.

Norrholm, S. D., Das, M., and Legradi, G. (2005). Behavioral effects of local microinfusion of pituitary adenylate cyclase activating polypeptide (PACAP) into the paraventricular nucleus of the hypothalamus (PVN). Regul Pept *128*, 33-41.

Ohtaki, H., Satoh, A., Nakamachi, T., Yofu, S., Dohi, K., Mori, H., Ohara, K., Miyamoto, K., Hashimoto, H., Shintani, N., *et al.* (2010). Regulation of Oxidative Stress by Pituitary Adenylate Cyclase-Activating Polypeptide (PACAP) Mediated by PACAP Receptor. J Mol Neurosci.

Okabe, T., Takayanagi, R., Adachi, M., Imasaki, K., and Nawata, H. (1998). Nur77, a member of the steroid receptor superfamily, antagonizes negative feedback of ACTH synthesis and secretion by glucocorticoid in pituitary corticotrope cells. J Endocrinol *156*, 169-175.

Otto, C., Kovalchuk, Y., Wolfer, D. P., Gass, P., Martin, M., Zuschratter, W., Grone, H. J., Kellendonk, C., Tronche, F., Maldonado, R., *et al.* (2001a). Impairment of mossy fiber long-term potentiation and associative learning in pituitary adenylate cyclase activating polypeptide type I receptor-deficient mice. J Neurosci *21*, 5520-5527.

Otto, C., Martin, M., Wolfer, D. P., Lipp, H. P., Maldonado, R., and Schutz, G. (2001b). Altered emotional behavior in PACAP-type-I-receptor-deficient mice. Brain Res Mol Brain Res *92*, 78-84.

Pacak, K., and Palkovits, M. (2001). Stressor specificity of central neuroendocrine responses: implications for stress-related disorders. Endocr Rev *22*, 502-548.

Pacak, K., Palkovits, M., Kvetnansky, R., Yadid, G., Kopin, I. J., and Goldstein, D. S. (1995). Effects of various stressors on in vivo norepinephrine release in the hypothalamic paraventricular nucleus and on the pituitary-adrenocortical axis. Ann N Y Acad Sci *771*, 115-130.

Pacak, K., Palkovits, M., Yadid, G., Kvetnansky, R., Kopin, I. J., and Goldstein, D. S. (1998). Heterogeneous neurochemical responses to different stressors: a test of Selye's doctrine of nonspecificity. Am J Physiol *275*, R1247-1255.

Padayatty, S. J., Doppman, J. L., Chang, R., Wang, Y., Gill, J., Papanicolaou, D. A., and Levine, M. (2007). Human adrenal glands secrete vitamin C in response to adrenocorticotrophic hormone. Am J Clin Nutr *86*, 145-149.

Pare, W. P., and Glavin, G. B. (1986). Restraint stress in biomedical research: a review. Neurosci Biobehav Rev *10*, 339-370.

Parkes, D., Rivest, S., Lee, S., Rivier, C., and Vale, W. (1993). Corticotropin-releasing factor activates c-fos, NGFI-B, and corticotropin-releasing factor gene expression within the paraventricular nucleus of the rat hypothalamus. Mol Endocrinol *7*, 1357-1367.

Paxinos, G., and Franklin, K. B. J. (2001). The Mouse Brain in Stereotaxic Coordinates, Second Edition edn: Academic Press).

Philips, A., Lesage, S., Gingras, R., Maira, M. H., Gauthier, Y., Hugo, P., and Drouin, J. (1997a). Novel dimeric Nur77 signaling mechanism in endocrine and lymphoid cells. Mol Cell Biol *17*, 5946-5951.

Philips, A., Maira, M., Mullick, A., Chamberland, M., Lesage, S., Hugo, P., and Drouin, J. (1997b). Antagonism between Nur77 and glucocorticoid receptor for control of transcription. Mol Cell Biol *17*, 5952-5959.

Plotsky, P. M., Bruhn, T. O., and Vale, W. (1985). Evidence for multifactor regulation of the adrenocorticotropin secretory response to hemodynamic stimuli. Endocrinology *116*, 633-639.

Prager, E. M., and Johnson, L. R. (2009). Stress at the synapse: signal transduction mechanisms of adrenal steroids at neuronal membranes. Sci Signal *2*, re5.

Propato-Mussafiri, R., Kanse, S. M., Ghatei, M. A., and Bloom, S. R. (1992). Pituitary adenylate cyclase-activating polypeptide releases 7B2, adrenocorticotrophin, growth hormone and prolactin from the mouse and rat clonal pituitary cell lines AtT-20 and GH3. J Endocrinol *132*, 107-113.

Ravni, A., Eiden, L. E., Vaudry, H., Gonzalez, B. J., and Vaudry, D. (2006). Cycloheximide treatment to identify components of the transitional transcriptome in PACAP-induced PC12 cell differentiation. J Neurochem *98*, 1229-1241.

Rawlings, S. R., and Hezareh, M. (1996). Pituitary adenylate cyclase-activating polypeptide (PACAP) and PACAP/vasoactive intestinal polypeptide receptors: actions on the anterior pituitary gland. Endocr Rev *17*, 4-29.

Rene, F., Monnier, D., Gaiddon, C., Felix, J. M., and Loeffler, J. P. (1996). Pituitary adenylate cyclase-activating polypeptide transduces through cAMP/PKA and PKC pathways and stimulates proopiomelanocortin gene transcription in mouse melanotropes. Neuroendocrinology *64*, 2-13.

Rhee, S. G., Yang, K. S., Kang, S. W., Woo, H. A., and Chang, T. S. (2005). Controlled elimination of intracellular H2O2: Regulation of peroxiredoxin, catalase, and glutathione peroxidase via post-translational modification. Antioxidants & Redox Signaling *7*, 619-626.

Richet, C. R. (1900). Dictionnaire de Physiologie, Vol 4 (Paris: Félix Alcan).

Sabban, E. L., and Kvetnansky, R. (2001). Stress-triggered activation of gene expression in catecholaminergic systems: dynamics of transcriptional events. Trends in Neurosciences *24*, 91-98.

Sabban, E. L., and Serova, L. I. (2007). Influence of prior experience with homotypic or heterotypic stressor on stress reactivity in catecholaminergic systems. Stress *10*, 137-143.

Sacchetti, P., Carpentier, R., Segard, P., Olive-Cren, C., and Lefebvre, P. (2006). Multiple signaling pathways regulate the transcriptional activity of the orphan nuclear receptor NURR1. Nucleic Acids Res *34*, 5515-5527.

Sakurada, K., Ohshima-Sakurada, M., Palmer, T. D., and Gage, F. H. (1999). Nurr1, an orphan nuclear receptor, is a transcriptional activator of endogenous tyrosine hydroxylase in neural progenitor cells derived from the adult brain. Development *126*, 4017-4026.

Samal, B., Gerdin, M. J., Huddleston, D., Hsu, C. M., Elkahloun, A. G., Stroth, N., Hamelink, C., and Eiden, L. E. (2007). Meta-analysis of microarray-derived data from PACAP-deficient adrenal gland in vivo and PACAP-treated chromaffin cells identifies distinct classes of PACAP-regulated genes. Peptides *28*, 1871-1882.

Santajuliana, D., Hornfeldt, B. J., and Osborn, J. W. (1996). Use of ganglionic blockers to assess neurogenic pressor activity in conscious rats. J Pharmacol Toxicol Methods *35*, 45-54.

Sapolsky, R. M., Romero, L. M., and Munck, A. U. (2000). How do glucocorticoids influence stress responses? Integrating permissive, suppressive, stimulatory, and preparative actions. Endocr Rev *21*, 55-89.

Schiltz, J. C., Hoffman, G. E., Stricker, E. M., and Sved, A. F. (1997). Decreases in arterial pressure activate oxytocin neurons in conscious rats. Am J Physiol *273*, R1474-1483.

Selye, H. (1936a). A Syndrome produced by Diverse Nocuous Agents. Nature *138*, 32.

Selye, H. (1936b). Thymus and adrenals in the response of the organism to injuries and intoxications. British Journal of Experimental Pathology *17*, 234-248.

Sewer, M. B., and Waterman, M. R. (2003). ACTH modulation of transcription factors responsible for steroid hydroxylase gene expression in the adrenal cortex. Microsc Res Tech *61*, 300-307.

Shen, L., Guo, J., Santos-Berrios, C., and Wu, M. X. (2006). Distinct domains for anti- and pro-apoptotic activities of IEX-1. J Biol Chem *281*, 15304-15311.

Shintani, N., Hashimoto, H., Tanaka, K., Kawagishi, N., Kawaguchi, C., Hatanaka, M., Ago, Y., Matsuda, T., and Baba, A. (2006). Serotonergic inhibition of intense jumping behavior in mice lacking PACAP (Adcyap1-/-). Ann N Y Acad Sci *1070*, 545-549.

Shintani, N., Mori, W., Hashimoto, H., Imai, M., Tanaka, K., Tomimoto, S., Hirose, M., Kawaguchi, C., and Baba, A. (2002). Defects in reproductive functions in PACAP-deficient female mice. Regul Pept *109*, 45-48.

Shiotani, Y., Kimura, S., Ohshige, Y., Yanaihara, C., and Yanaihara, N. (1995). Immunohistochemical localization of pituitary adenylate cyclase-activating polypeptide (PACAP) in the adrenal medulla of the rat. Peptides *16*, 1045-1050.

Siegmund, A., and Wotjak, C. T. (2006). Toward an animal model of posttraumatic stress disorder. Ann N Y Acad Sci *1071*, 324-334.

Singewald, N., Schneider, C., and Philippu, A. (1993). Effects of blood pressure changes on the catecholamine release in the locus coeruleus of cats anaesthetized with pentobarbital or chloralose. Naunyn Schmiedebergs Arch Pharmacol *348*, 242-248.

Somogyvari-Vigh, A., and Reglodi, D. (2004). Pituitary adenylate cyclase activating polypeptide: a potential neuroprotective peptide. Curr Pharm Des *10*, 2861-2889.

Sparrow, R. A., and Coupland, R. E. (1987). Blood flow to the adrenal gland of the rat: its distribution between the cortex and the medulla before and after haemorrhage. J Anat *155*, 51-61.

Spengler, D., Waeber, C., Pantaloni, C., Holsboer, F., Bockaert, J., Seeburg, P. H., and Journot, L. (1993). Differential signal transduction by five splice variants of the PACAP receptor. Nature *365*, 170-175.

Stowasser, M., Gordon, R. D., Rutherford, J. C., Nikwan, N. Z., Daunt, N., and Slater, G. J. (2001). Diagnosis and management of primary aldosteronism. J Renin Angiotensin Aldosterone Syst *2*, 156-169.

Stroth, N., and Eiden, L. E. (2010). Stress hormone synthesis in mouse hypothalamus and adrenal gland triggered by restraint is dependent on pituitary adenylate cyclase-activating polypeptide signaling. Neuroscience *165*, 1025-1030.

Swanson, L. W., and Kuypers, H. G. (1980). The paraventricular nucleus of the hypothalamus: cytoarchitectonic subdivisions and organization of projections to the pituitary, dorsal vagal complex, and spinal cord as demonstrated by retrograde fluorescence double-labeling methods. J Comp Neurol *194*, 555-570.

Swanson, L. W., Sawchenko, P. E., Lind, R. W., and Rho, J. H. (1987). The CRH motoneuron: differential peptide regulation in neurons with possible synaptic, paracrine, and endocrine outputs. Ann N Y Acad Sci *512*, 12-23.

Swanson, L. W., Sawchenko, P. E., Rivier, J., and Vale, W. W. (1983). Organization of ovine corticotropin-releasing factor immunoreactive cells and fibers in the rat brain: an immunohistochemical study. Neuroendocrinology *36*, 165-186.

Sweat, M. L. (1955). Adrenocorticosteroids in peripheral and adrenal venous blood of man. J Clin Endocrinol Metab *15*, 1043-1056.

Tabarin, A., Chen, D., Hakanson, R., and Sundler, F. (1994). Pituitary adenylate cyclase-activating peptide in the adrenal gland of mammals: distribution, characterization and responses to drugs. Neuroendocrinology *59*, 113-119.

Tai, T. C., Claycomb, R., Siddall, B. J., Bell, R. A., Kvetnansky, R., and Wong, D. L. (2007). Stress-induced changes in epinephrine expression in the adrenal medulla in vivo. J Neurochem *101*, 1108-1118.

Tai, T. C., Morita, K., and Wong, D. L. (2001). Role of Egr-1 in cAMP-dependent protein kinase regulation of the phenylethanolamine N-methyltransferase gene. J Neurochem *76*, 1851-1859.

Tanaka, K., Shintani, N., Hashimoto, H., Kawagishi, N., Ago, Y., Matsuda, T., Hashimoto, R., Kunugi, H., Yamamoto, A., Kawaguchi, C*., et al.* (2006). Psychostimulant-induced attenuation of hyperactivity and prepulse inhibition deficits in Adcyap1-deficient mice. Journal of Neuroscience *26*, 5091-5097.

Tanida, M., Shintani, N., Morita, Y., Tsukiyama, N., Hatanaka, M., Hashimoto, H., Sawai, H., Baba, A., and Nagai, K. (2010). Regulation of autonomic nerve activities by central pituitary adenylate cyclase-activating polypeptide. Regul Pept *161*, 73-80.

Tasker, J. G., Di, S., and Malcher-Lopes, R. (2006). Minireview: rapid glucocorticoid signaling via membrane-associated receptors. Endocrinology *147*, 5549-5556.

Tokunaga, H. (1996). Postnatal development of the blood vasculature in the rat adrenal gland: a scanning electron microscope study of microcorrosion casts. Arch Histol Cytol *59*, 305-315.

Tomimoto, S., Qjika, T., Shintani, N., Hashimoto, H., Hamagami, K., Ikeda, K., Nakata, M., Yada, T., Sakurai, Y., Shimada, T*., et al.* (2008). Markedly reduced white adipose tissue and increased insulin sensitivity in Adcyap1-deficient mice. Journal of Pharmacological Sciences *107*, 41-48.

Tonshoff, C., Hemmick, L., and Evinger, M. J. (1997). Pituitary adenylate cyclase activating polypeptide (PACAP) regulates expression of catecholamine biosynthetic enzyme genes in bovine adrenal chromaffin cells. J Mol Neurosci *9*, 127-140.

Ulrich-Lai, Y. M., and Engeland, W. C. (2002). Adrenal splanchnic innervation modulates adrenal cortical responses to dehydration stress in rats. Neuroendocrinology *76*, 79-92.

Ulrich-Lai, Y. M., and Herman, J. P. (2009). Neural regulation of endocrine and autonomic stress responses. Nat Rev Neurosci *10*, 397-409.

Umemoto, S., Kawai, Y., and Senba, E. (1994). Differential regulation of IEGs in the rat PVH in single and repeated stress models. Neuroreport *6*, 201-204.

Umemoto, S., Kawai, Y., Ueyama, T., and Senba, E. (1997). Chronic glucocorticoid administration as well as repeated stress affects the subsequent acute immobilization stress-induced expression of immediate early genes but not that of NGFI-A. Neuroscience *80*, 763-773.

Ushiyama, M., Ikeda, R., Sugawara, H., Yoshida, M., Mori, K., Kangawa, K., Inoue, K., Yamada, K., and Miyata, A. (2007). Differential intracellular signaling through PAC1 isoforms as a result of alternative splicing in the first extracellular domain and the third intracellular loop. Mol Pharmacol *72*, 103-111.

Vaudry, D., Chen, Y., Ravni, A., Hamelink, C., Elkahloun, A. G., and Eiden, L. E. (2002). Analysis of the PC12 cell transcriptome after differentiation with pituitary adenylate cyclase-activating polypeptide (PACAP). J Neurochem *83*, 1272-1284.

Vaudry, D., Falluel-Morel, A., Bourgault, S., Basille, M., Burel, D., Wurtz, O., Fournier, A., Chow, B. K., Hashimoto, H., Galas, L., and Vaudry, H. (2009). Pituitary adenylate cyclase-activating polypeptide and its receptors: 20 years after the discovery. Pharmacol Rev *61*, 283-357.

Vaudry, D., Gonzalez, B. J., Basille, M., Yon, L., Fournier, A., and Vaudry, H. (2000). Pituitary adenylate cyclase-activating polypeptide and its receptors: from structure to functions. Pharmacol Rev *52*, 269-324.

Verdugo, R. A., and Medrano, J. F. (2006). Comparison of gene coverage of mouse oligonucleotide microarray platforms. BMC Genomics *7*, 58.

Vigh, S., Arimura, A., Gottschall, P. E., Kitada, C., Somogyvari-Vigh, A., and Childs, G. V. (1993). Cytochemical characterization of anterior pituitary target cells for the neuropeptide, pituitary adenylate cyclase activating polypeptide (PACAP), using biotinylated ligands. Peptides *14*, 59-65.

Vinson, G. P., Pudney, J. A., and Whitehouse, B. J. (1985). The mammalian adrenal circulation and the relationship between adrenal blood flow and steroidogenesis. J Endocrinol *105*, 285-294.

Viskupic, E., Kvetnansky, R., Sabban, E. L., Fukuhara, K., Weise, V. K., Kopin, I. J., and Schwartz, J. P. (1994). Increase in rat adrenal phenylethanolamine N-methyltransferase mRNA level caused by immobilization stress depends on intact pituitary-adrenocortical axis. J Neurochem *63*, 808-814.

Vogt, M. (1943). The output of cortical hormone by the mammalian suprarenal. J Physiol *102*, 341-356.

Volakakis, N., Kadkhodaei, B., Joodmardi, E., Wallis, K., Panman, L., Silvaggi, J., Spiegelman, B. M., and Perlmann, T. (2010). NR4A orphan nuclear receptors as mediators of CREB-dependent neuroprotection. Proc Natl Acad Sci U S A *107*, 12317-12322.

Vollmer, R. R., Balcita-Pedicino, J. J., Debnam, A. J., and Edwards, D. J. (2000). Adrenal medullary catecholamine secretion patterns in rats evoked by reflex and direct neural stimulation. Clin Exp Hypertens *22*, 705-715.

Wakade, T. D., Blank, M. A., Malhotra, R. K., Pourcho, R., and Wakade, A. R. (1991). The peptide VIP is a neurotransmitter in rat adrenal medulla: physiological role in controlling catecholamine secretion. J Physiol *444*, 349-362.

Wang, X., and Seed, B. (2003). A PCR primer bank for quantitative gene expression analysis. Nucleic Acids Res *31*, e154.

Waschek, J. A. (2002). Multiple actions of pituitary adenylyl cyclase activating peptide in nervous system development and regeneration. Dev Neurosci *24*, 14-23.

Westberg, J. A., Serlachius, M., Lankila, P., Penkowa, M., Hidalgo, J., and Andersson, L. C. (2007). Hypoxic preconditioning induces neuroprotective stanniocalcin-1 in brain via IL-6 signaling. Stroke *38*, 1025-1030.

Whitnall, M. H. (1993). Regulation of the hypothalamic corticotropin-releasing hormone neurosecretory system. Prog Neurobiol *40*, 573-629.

Whitworth, E. J., Kosti, O., Renshaw, D., and Hinson, J. P. (2003). Adrenal neuropeptides: Regulation and interaction with ACTH and other adrenal regulators. Microscopy Research and Technique *61*, 259-267.

Wingate, A. D., and Arthur, J. S. (2006). Post-translational control of Nur77. Biochem Soc Trans *34*, 1107-1109.

Wong, D. L., Anderson, L. J., and Tai, T. C. (2002). Cholinergic and peptidergic regulation of phenylethanolamine N-methyltransferase gene expression. Ann N Y Acad Sci *971*, 19-26.

Wong, D. L., Lesage, A., Siddall, B., and Funder, J. W. (1992). Glucocorticoid regulation of phenylethanolamine N-methyltransferase in vivo. Faseb J *6*, 3310-3315.

Wong, D. L., Tai, T. C., Wong-Faull, D. C., Claycomb, R., and Kvetnansky, R. (2008). Adrenergic responses to stress: transcriptional and post-transcriptional changes. Ann N Y Acad Sci *1148*, 249-256.

Wu, M. X. (2003). Roles of the stress-induced gene IEX-1 in regulation of cell death and oncogenesis. Apoptosis *8*, 11-18.

Wurtman, R. J. (1966). Control of epinephrine synthesis in the adrenal medulla by the adrenal cortex: hormonal specificity and dose-response characteristics. Endocrinology *79*, 608-614.

Yamamoto, K., Hashimoto, H., Hagihara, N., Nishino, A., Fujita, T., Matsuda, T., and Baba, A. (1998). Cloning and characterization of the mouse pituitary adenylate cyclase-activating polypeptide (PACAP) gene. Gene *211*, 63-69.

Yao, M., and Denver, R. J. (2007). Regulation of vertebrate corticotropin-releasing factor genes. Gen Comp Endocrinol *153*, 200-216.

Yi, C. X., Sun, N., Ackermans, M. T., Alkemade, A., Foppen, E., Shi, J., Serlie, M. J., Buijs, R. M., Fliers, E., and Kalsbeek, A. (2010). Pituitary adenylate cyclase-activating polypeptide stimulates glucose production via the hepatic sympathetic innervation in rats. Diabetes.

Zhang, K., Lindsberg, P. J., Tatlisumak, T., Kaste, M., Olsen, H. S., and Andersson, L. C. (2000). Stanniocalcin: A molecular guard of neurons during cerebral ischemia. Proc Natl Acad Sci U S A *97*, 3637-3642.

9. Abbreviations

ACh	acetylcholine
ACTH	adrenocorticotropic hormone
ADHD	attention deficit hyperactivity disorder
ANOVA	analysis of variance
ANS	autonomic nervous system
ATP	adenosine-5'-triphosphate
BLAST	basic local alignment search tool
bp	base pair
cAMP	cyclic adenosine monophosphate
cDNA	complementary DNA
CREB	cAMP responsive element binding protein
CRH	corticotropin-releasing hormone
CTP	cytidine-5'-triphosphate
DEPC	diethylpyrocarbonate
DNA	deoxyribonucleic acid
DNase	deoxyribonuclease
dNTP	deoxyribonucleoside triphosphate
dpi	dots per inch
dpm	decays per minute
DTT	dithiothreitol
EDTA	ethylene-diamine-tetraacetic acid
EIA	enzyme immunoassay
ELISA	enzyme-linked immunosorbent assay
GPCR	G protein-coupled receptor
GR	glucocorticoid receptor
GTP	guanosine-5'-triphosphate
HCl	hydrochloric acid
hnRNA	heterogenous nuclear RNA
HPA axis	hypothalamic-pituitary-adrenocortical axis
i.c.v.	intracerebroventricular
i.p.	intraperitoneal
IML	intermediolateral column of the spinal cord
IPTG	isopropyl-ß-D-thiogalactopyranoside
ISH	in situ hybridization histochemistry
ITF	inducible transcription factor(s)
IVT	in vitro transcription
kb	kilobases
KO	knock-out
LOWESS	locally weighted scatterplot smoothing
$MgCl_2$	magnesium chloride
mRNA	messenger RNA
NaCl	sodium chloride
NBRE	NGFI-B responsive element
NE	norepinephrine
NGFI-B	nerve growth factor-induced clone B
NHGRI	National Human Genome Research Institute
NIH	National Institutes of Health
NIMH	National Institute of Mental Health
NINDS	National Institute of Neurological Disorders and Stroke
NurRE	Nur response element
O.C.T.	optimal cutting temperature
PACAP	pituitary adenylate cyclase-activating polypeptide
PBS	phosphate-buffered saline
PCR	polymerase chain reaction
PTSD	posttraumatic stress disorder
PVN	paraventricular nucleus of the hypothalamus
qPCR	quantitative PCR
qRT-PCR	quantitative reverse transcription PCR
RIA	radioimmunoassay

RNA	ribonucleic acid
RNase	ribonuclease
rpm	rotations per minute
RT	reverse transcription; reverse transcriptase
RT-PCR	reverse transcription PCR
SDS	sodium dodecyl sulfate
SEM	standard error of the mean
SSC	saline-sodium citrate
TAE	tris-acetate-EDTA
TEA	triethanolamine
tRNA	transfer RNA
U	units
URL	uniform resource locator
UTP	uridine-5'-triphosphate
VLM	ventrolateral medulla oblongata
WT	wild-type
X-Gal	5-bromo-4-chloro-3-indolyl-β-D-galactopyranoside

Common physical abbreviations:

˚C	degree Celsius
Ci	Curie
g	gram(s)
h	hour
l	liter
m	meter
M	mol per liter
%	percent
V	volts
x g	centrifugal force

Common prefixes:

k	kilo (10^{3})
m	milli (10^{-3})
µ	micro (10^{-6})
n	nano (10^{-9})
p	pico (10^{-12})

10. Appendix

10.1. Tabular summary of microarray expression analyses

All microarray analyses were performed with tissue samples from male mice, unless otherwise stated in the headings and legends to the tables. Results from the analyses are listed here.

Table 3a	**Basal adrenal transcriptome -- *PACAP-dependent* transcripts**		
Mean ratio WT/KO	Gene symbol	Description	GeneID
2.13	Akap11	PREDICTED: A kinase (PRKA) anchor protein 11	219181
3.70	Alb	albumin	11657
3.23	Apoa1	apolipoprotein A-I	11806
2.86	Avil	advillin	11567
2.17	Bmi1	Bmi1 polycomb ring finger oncogene	12151
2.27	ENSMUSG00000047334	ENSMUST00000051733	
2.04	Entpd4	ectonucleoside triphosphate diphosphohydrolase 4	67464
3.45	Gap43	growth associated protein 43	14432
2.63	Lep	leptin	16846
2.13	LOC56304	Recombinant antineuraminidase single chain Ig VH and VL domains	56304
2.63	Ly6k	lymphocyte antigen 6 complex, locus K	76486
3.70	Nefl	neurofilament, light polypeptide	18039
2.08	Ngfr	nerve growth factor receptor (TNFR superfamily, member 16)	18053
2.00	Phf20l1	PHD finger protein 20-like 1	239510
2.00	Ppfia2	protein tyrosine phosphatase, receptor type, f polypeptide, interacting protein, alpha 2	327814
3.13	Prph	peripherin	19132

Table 3b	**Basal adrenal transcriptome -- *PACAP-repressed* transcripts**		
Mean ratio WT/KO	Gene symbol	Description	GeneID
0.49	1700041B20Rik	PREDICTED: RIKEN cDNA 1700041B20 gene, transcript variant 1	73338
0.41	2400009B08Rik	RIKEN cDNA 2400009B08 gene	68234
0.36	9530008L14Rik	RIKEN cDNA 9530008L14 gene	109254
0.47	A530050D06Rik	RIKEN cDNA A530050D06 gene	104816
0.46	A530053G22Rik	PREDICTED: RIKEN cDNA A530053G22 gene	208079
0.42	Acaa1b	acetyl-Coenzyme A acyltransferase 1B	235674
0.45	Acot1	acyl-CoA thioesterase 1	26897
0.47	Akr1c20	Aldo-keto reductase family 1, member C20	116852
0.37	Apoc1	apolipoprotein C-I, transcript variant 1	11812
0.50	AU018778	expressed sequence AU018778	234564
0.48	BC054059	cDNA sequence BC054059	246747
0.43	Cd47	CD47 antigen (Rh-related antigen, integrin-associated signal transducer)	16423
0.44	Cox8b	cytochrome c oxidase, subunit VIIIb, nuclear gene encoding mitochondrial protein	12869
0.42	Cpne5	copine V	240058
0.47	Cpt1b	carnitine palmitoyltransferase 1b, muscle	12895

0.49	Egln3	EGL nine homolog 3 (C. elegans)	112407
0.49	Ehhadh	enoyl-Coenzyme A, hydratase/3-hydroxyacyl Coenzyme A dehydrogenase	74147
0.27	Elovl3	elongation of very long chain fatty acids (FEN1/Elo2, SUR4/Elo3, yeast)-like 3	12686
0.34	ENSMUSG00000038882	ENSMUST00000046268	
0.43	Fbp2	fructose bisphosphatase 2	14120
0.44	Gmpr	guanosine monophosphate reductase	66355
0.49	Gyk	glycerol kinase, transcript variant 1	14933
0.47	Gys2	glycogen synthase 2	232493
0.43	Ifi27	interferon, alpha-inducible protein 27	76933
0.50	Impa2	inositol (myo)-1(or 4)-monophosphatase 2	114663
0.49	Irx6	Iroquois related homeobox 6 (Drosophila)	64379
0.48	LOC100044592	PREDICTED: similar to cytochrome c	100044592
0.50	LOC100045837	PREDICTED: similar to cytochrome c	100045837
0.50	LOC100045925	PREDICTED: similar to cytochrome c	100045925
0.45	Otop1	otopetrin 1	21906
0.47	Poln	DNA polymerase N	272158
0.37	Ppara	peroxisome proliferator activated receptor alpha	19013
0.45	Ppargc1a	peroxisome proliferative activated receptor, gamma, coactivator 1 alpha	19017
0.46	Sgsm2	small G protein signaling modulator 2	97761
0.40	Slc14a2	solute carrier family 14 (urea transporter), member 2, transcript variant 1	27411
0.41	Slc27a2	solute carrier family 27 (fatty acid transporter), member 2	26458
0.48	Slc36a2	solute carrier family 36 (proton/amino acid symporter), member 2	246049
0.33	Slc4a4	solute carrier family 4 (anion exchanger), member 4	54403
0.40	Tectb	tectorin beta	21684
0.49	Zfhx3	zinc finger homeobox 3	11906

Table 3. Genes differentially expressed in adrenal glands from untreated wild-type (WT) versus PACAP knock-out (KO) mice. Microarray hybridization was carried out using RNA samples obtained from saline-treated animals (male mice; age range: 4.8-6.4 months). RNA samples from six individual KO mice were hybridized with fractions of a pool generated from six WT samples. Data derived from microarray hybridizations were extracted, normalized (LOWESS correction), quality-filtered (Ratio Quality Measure >= 0.8) and statistically evaluated in mAdb (http://nciarray.nci.nih.gov). False discovery rate was set to ~1%. Data were subsequently exported to Microsoft Excel and only those transcripts with 2-fold or greater difference in abundance between the two genotypes were retained. Furthermore, genes with spurious self-self ratios (greater than 1.5 or smaller than 0.66, respectively) were removed. Multiple oligonucleotide targets representing a single Entrez GeneID were collapsed by calculating the average of the respective mean expression ratios. Table 3a, PACAP-dependent genes (less abundant in KO). Table 3b, PACAP-repressed genes (more abundant in KO).

Table 4	**Basal cerebrocortical transcriptome -- *PACAP-dependent* transcripts**		
Mean ratio WT/KO	Gene symbol	Description	GeneID
2.04	Rtf1	PREDICTED: Rtf1, Paf1/RNA polymerase II complex component, homolog (S. cerevisiae)	76246
2.13	Cdkl3	cyclin-dependent kinase-like 3	213084
2.17	ENSMUSG00000029652	HIGH MOBILITY GROUP PROTEIN 1 (HMG-1) (AMPHOTERIN)	
2.17	Gria3	glutamate receptor, ionotropic, AMPA3 (alpha 3)	53623
2.22	Gabra2	gamma-aminobutyric acid (GABA-A) receptor, subunit alpha 2	14395
2.22	Rasgrp1	RAS guanyl releasing protein 1	19419
2.22	Lancl2	LanC (bacterial lantibiotic synthetase component C)-like 2	71835
2.38	Scn2a1	sodium channel, voltage-gated, type II, alpha 1	110876

Table 4. Genes differentially expressed in cerebral cortex from untreated wild-type (WT) versus PACAP knock-out (KO) mice. Microarray hybridization was carried out using RNA samples obtained from male mice (average age: 3 months). RNA samples from six individual mice were pooled per genotype, and fractions of these two pools were hybridized in triplicate. This "pool versus pool" design was carried out twice, and results were subsequently combined. Data were extracted, normalized (LOWESS correction), quality-filtered (Ratio Quality Measure >= 0.7) and statistically evaluated in mAdb (http://nciarray.nci.nih.gov). False discovery rate was set to ~1%. Data were subsequently exported to Microsoft Excel and only those transcripts with 2-fold or greater difference in abundance between the two genotypes were retained. Furthermore, genes with spurious self-self ratios (greater than 1.5 or smaller than 0.66, respectively) were removed. Multiple oligonucleotide targets representing a single Entrez GeneID were collapsed by calculating the average of the respective mean expression ratios.

Table 5a	**Adrenal transcriptome after hypoglycemia -- *PACAP-dependent* transcripts**		(females)
Mean ratio WT/KO	Gene	Description	GeneID
3.06	1190005F20Rik	RIKEN cDNA 1190005F20 gene	98685
2.41	1810035L17Rik	RIKEN cDNA 1810035L17 gene	380773
2.77	2310040C09Rik	RIKEN cDNA 2310040C09 gene	69640
2.04	2410018M08Rik	RIKEN cDNA 2410018M08 gene	71970
2.15	2810021J22Rik	RIKEN cDNA 2810021J22 gene	69944
2.03	3321401G04Rik	RIKEN cDNA 3321401G04 gene	77574
2.24	5630401D24Rik	RIKEN cDNA 5630401D24 gene	71449
3.64	6720475J19Rik	PREDICTED: RIKEN cDNA 6720475J19 gene	68157
2.09	Acta1	actin, alpha 1, skeletal muscle	11459
2.29	Areg	amphiregulin	11839
2.23	Arntl	aryl hydrocarbon receptor nuclear translocator-like	11865
2.25	AW146020	expressed sequence AW146020	330361
2.13	BC029127	PREDICTED: cDNA sequence BC029127	214368
2.13	Ccnt2	cyclin T2	72949
2.13	Chchd8	coiled-coil-helix-coiled-coil-helix domain containing 8	68185
2.59	D4Wsu53e	DNA segment, Chr 4, Wayne State University 53, expressed	27981
2.05	Dbc1	deleted in bladder cancer 1	56710
2.04	Dtwd1	DTW domain containing 1	69185
3.00	Ecel1	endothelin converting enzyme-like 1	13599
2.06	EG245174	PREDICTED: predicted gene, EG245174	245174
3.91	EG433016	predicted gene, EG433016	433016

2.98	ENSMUSG00000035484	ZINC FINGER PROTEIN BC027407. [Source:RefSeq;Acc:NM_153063]	
2.08	ENSMUSG00000050032	ENSMUST00000051128	
2.18	Fam60a	family with sequence similarity 60, member A	56306
2.29	Fst	follistatin	14313
2.28	Gal	galanin	14419
2.03	Hhip	Hedgehog-interacting protein	15245
2.05	Hlx	H2.0-like homeobox	15284
2.07	Ifi203	interferon activated gene 203, transcript variant 1.	15950
2.18	Klhl8	kelch-like 8	246293
2.47	Lmo1	LIM domain only 1	109594
2.00	LOC100044458	PREDICTED: hypothetical protein LOC100044458	100044458
3.43	LOC545175	PREDICTED: similar to LOC635138 protein	545175
2.44	Madd	MAP-kinase activating death domain	228355
2.29	Metapl1	Methionine aminopeptidase-like 1	66559
2.25	Mitd1	MIT, microtubule interacting and transport, domain containing 1	69028
2.62	Nptx1	neuronal pentraxin 1	18164
4.44	Nr0b2	nuclear receptor subfamily 0, group B, member 2	23957
2.35	Parp16	poly (ADP-ribose) polymerase family, member 16	214424
3.03	Ppcs	phosphopantothenoylcysteine synthetase	106564
2.03	Prdm5	PR domain containing 5	70779
2.59	Prl7b1	prolactin family 7, subfamily b, member 1	75596
2.25	Rab40c	Rab40c, member RAS oncogene family	224624
2.52	Rhebl1	Ras homolog enriched in brain like 1	69159
2.40	Sfrs17b	splicing factor, arginine/serine-rich 17b	338351
2.07	Shpk	sedoheptulokinase	74637
2.02	Smek2	SMEK homolog 2, suppressor of mek1 (Dictyostelium)	104570
2.34	Srd5a2	steroid 5 alpha-reductase 2	94224
2.14	St6galnac1	GalNAc alpha-2,6-sialyltransferase I	20445
4.45	Tac1	tachykinin 1	21333
2.31	Tgds	TDP-glucose 4,6-dehydratase	76355
2.06	Traf2	Tnf receptor-associated factor 2	22030
2.04	Ttc30a1	tetratricopeptide repeat domain 30A1	78802
2.10	Zc3h6	zinc finger CCCH type containing 6	78751
1.98	Zfp273	zinc finger protein 273	212569
2.59	Zfp354a	zinc finger protein 354A	21408
2.78	Zfp455	zinc finger protein 455	218311
2.15	Zfp61	zinc finger protein 61	22719
2.00	Zfp790	zinc finger protein 790	233056
2.36	Zmym1	zinc finger, MYM domain containing 1	68310
2.06		Transcribed locus (UniGene cluster Mm.416451)	
2.27		Transcribed locus (UniGene cluster Mm.444439)	

Table 5b	**Adrenal transcriptome after hypoglycemia -- *PACAP-repressed* transcripts**		(females)
Mean ratio WT/KO	Gene	Description	GeneID
0.46	1700086L19Rik	PREDICTED: RIKEN cDNA 1700086L19 gene	74284
0.49	4931408A02Rik	RIKEN cDNA 4931408A02 gene	70967
0.44	8430408G22Rik	RIKEN cDNA 8430408G22 gene	213393
0.42	9430023L20Rik	RIKEN cDNA 9430023L20 gene	68118
0.46	Abtb2	ankyrin repeat and BTB (POZ) domain containing 2	99382
0.48	Akap2	A kinase (PRKA) anchor protein 2, transcript variant 3	11641
0.37	Ampd1	adenosine monophosphate deaminase 1 (isoform M)	229665
0.34	Arl5b	ADP-ribosylation factor-like 5B	75869
0.48	AU018778	expressed sequence AU018778	234564
0.38	Axud1	AXIN1 up-regulated 1	215418
0.49	Btg2	B-cell translocation gene 2, anti-proliferative	12227
0.29	Cabyr	calcium-binding tyrosine-(Y)-phosphorylation regulated, transcript variant 4	71132
0.43	Cbx4	chromobox homolog 4 (Drosophila Pc class)	12418
0.49	Ccdc57	coiled-coil domain containing 57	71276
0.43	Ccl12	chemokine (C-C motif) ligand 12	20293
0.27	Ccl7	chemokine (C-C motif) ligand 7	20306
0.45	Chka	Choline kinase alpha	12660
0.49	Cyp11b2	cytochrome P450, family 11, subfamily b, polypeptide 2	13072
0.28	Cyr61	cysteine rich protein 61	16007
0.31	D16Ertd472e	DNA segment, Chr 16, ERATO Doi 472, expressed	67102
0.32	Dgat1	Diacylglycerol O-acyltransferase 1	13350
0.46	Dusp1	dual specificity phosphatase 1	19252
0.43	Dusp10	dual specificity phosphatase 10	63953
0.42	Egr1	early growth response 1	13653
0.45	Elf2	E74-like factor 2	69257
0.46	Ell2	elongation factor RNA polymerase II 2	192657
0.37	ENSMUSG00000034313	UNIDENTIFIED READING FRAME. [Source:SPTREMBL;Acc:Q62573]	
0.43	Faim3	Fas apoptotic inhibitory molecule 3	69169
0.48	Fbxo34	F-box protein 34	78938
0.35	Fem1b	feminization 1 homolog b (C. elegans)	14155
0.49	Fem1c	fem-1 homolog c (C.elegans)	240263
0.46	Fosl1	fos-like antigen 1	14283
0.50	Gem	GTP binding protein (gene overexpressed in skeletal muscle)	14579
0.31	Gm889	gene model 889, (NCBI)	380755
0.50	Hist1h3b	histone cluster 1, H3b	319150
0.48	Hist2h3b	histone cluster 2, H3b	319154
0.50	Homer1	Homer homolog 1 (Drosophila)	26556
0.28	Ibrdc1	PREDICTED: IBR domain containing 1	268291
0.47	Ier3	immediate early response 3	15937
0.43	Kcnk2	potassium channel, subfamily K, member 2	16526
0.23	Klf4	Kruppel-like factor 4 (gut)	16600
0.47	Lgr5	leucine rich repeat containing G protein coupled receptor 5	14160
0.39	Ltf	lactotransferrin	17002
0.49	Mafk	v-maf musculoaponeurotic fibrosarcoma oncogene family, protein K (avian)	17135

0.25	Metrnl	meteorin, glial cell differentiation regulator-like	210029
0.38	Mt1	Metallothionein 1	17748
0.32	Nr1d1	nuclear receptor subfamily 1, group D, member 1	217166
0.30	Nr4a1	nuclear receptor subfamily 4, group A, member 1	15370
0.14	Nr4a2	nuclear receptor subfamily 4, group A, member 2	18227
0.50	Nr4a3	nuclear receptor subfamily 4, group A, member 3	18124
0.32	Orm1	orosomucoid 1	18405
0.45	Phlda1	pleckstrin homology-like domain, family A, member 1	21664
0.46	Pim3	proviral integration site 3	223775
0.42	Rassf8	Ras association (RalGDS/AF-6) domain family (N-terminal) member 8	71323
0.27	Rchy1	Ring finger and CHY zinc finger domain containing 1	68098
0.47	Rdx	radixin, transcript variant 3	19684
0.33	S100a8	S100 calcium binding protein A8 (calgranulin A)	20201
0.32	S100a9	S100 calcium binding protein A9 (calgranulin B)	20202
0.34	Slc25a25	solute carrier family 25 (mitochondrial carrier, phosphate carrier), member 25	227731
0.20	Snf1lk	SNF1-like kinase	17691
0.45	Taok2	TAO kinase 2	381921
0.43	Tiparp	TCDD-inducible poly(ADP-ribose) polymerase	99929
0.46	Usp2	ubiquitin specific peptidase 2, transcript variant 2	53376
0.42	Usp53	Ubiquitin specific peptidase 53	99526
0.44	Zbtb24	zinc finger and BTB domain containing 24	268294
0.49		Transcribed locus, similar to cAMP responsive element binding protein 5 isoform beta	

Table 5. Genes differentially expressed in wild-type (WT) versus PACAP knock-out (KO) adrenal glands 3h after insulin-induced hypoglycemia. Microarray hybridization was carried out using RNA samples obtained from animals treated with 2 U/kg insulin (female mice; age range: 12-17 months). Samples from six insulin-treated WT mice were pooled, and fractions of this pool were hybridized with samples from six individual insulin-treated KO mice. Duplicates of these six hybridizations were carried out as a “dye-swap” control (labeling of WT/KO with Cy3/Cy5 reversed), such that a total of 12 microarray slides were used, each slide representing $KO_{insulin}/WT_{insulin}$. Data were extracted, normalized (LOWESS correction), quality-filtered (Ratio Quality Measure >= 0.8) and statistically evaluated in mAdb (http://nciarray.nci.nih.gov). False discovery rate was set to ~1%. Data were subsequently exported to Microsoft Excel and only those transcripts with 2-fold or greater difference in abundance between the two genotypes were retained. Multiple oligonucleotide targets representing a single Entrez GeneID were collapsed by calculating the average of the respective mean expression ratios. Table 5a, PACAP-dependent genes (less abundant in KO after hypoglycemia). Table 5b, PACAP-repressed genes (more abundant in KO after hypoglycemia).

Table 6a	**Adrenal glands after hypoglycemia – transcripts upregulated in PACAP-/- mice** **("fold increase" values in parentheses reflect changes in adrenal glands from PACAP+/+ mice)**		
fold increase	Gene symbol	Description	GeneID
3.04	2010002N04Rik	RIKEN cDNA 2010002N04 gene	106878
2.42 (2.11)	2010003K11Rik	RIKEN cDNA 2010003K11 gene	69861
5.38	2010109I03Rik	RIKEN cDNA 2010109I03 gene	67038
2.18	2900027M19Rik	RIKEN cDNA 2900027M19 gene	
3.90 (2.54)	4930430E16Rik	RIKEN cDNA 4930430E16 gene	73873
2.69	4931408A02Rik	RIKEN cDNA 4931408A02 gene	70967
3.27	4933407C03Rik	PREDICTED: RIKEN cDNA 4933407C03 gene, transcript variant 6	74440
2.04	6530403A03Rik	RIKEN cDNA 6530403A03 gene	67797
4.75	9430023L20Rik	RIKEN cDNA 9430023L20 gene	68118
2.37	9430076C15Rik	RIKEN cDNA 9430076C15 gene	320189
3.56	9830163H01Rik	RIKEN cDNA 9830163H01 gene	414109
2.13	Acvr1	activin A receptor, type 1, transcript variant 2	11477
3.95	Adarb1	adenosine deaminase, RNA-specific, B1, transcript variant 1	110532
2.72	Agrp	agouti related protein	11604
3.55	Akap2	A kinase (PRKA) anchor protein 2, transcript variant 3	11641
2.02	Ankhd1	Ankyrin repeat and KH domain containing 1	108857
2.40 (2.41)	Areg	amphiregulin	11839
2.34	Atp13a2	ATPase type 13A2	74772
2.16	Atp7a	ATPase, Cu++ transporting, alpha polypeptide, transcript variant 2	11977
2.81	Axud1	AXIN1 up-regulated 1	215418
2.08	Bag3	Bcl2-associated athanogene 3	29810
2.15	BC011487	cDNA sequence BC011487	232748
3.22	BC023892	PREDICTED: cDNA sequence BC023892, transcript variant 1	212943
3.92	BC056923	cDNA sequence BC056923	227358
2.30	Bdkrb1	bradykinin receptor, beta 1	12061
2.10	Bean	PREDICTED: brain expressed, associated with Nedd4, transcript variant 3	65115
2.05	Bhlhb2	basic helix-loop-helix domain containing, class B2	20893
2.13	Bin1	bridging integrator 1, transcript variant 2	30948
2.54	Btg2	B-cell translocation gene 2, anti-proliferative	12227
2.03	Bzw1	basic leucine zipper and W2 domains 1	66882
2.39 (2.06)	C630004H02Rik	RIKEN cDNA C630004H02 gene	217310
2.23	C79267	expressed sequence C79267	212632
5.20	Cabyr	calcium-binding tyrosine-(Y)-phosphorylation regulated, transcript variant 4	71132
2.47	Cacna2d1	calcium channel, voltage-dependent, alpha2/delta subunit 1, transcript variant e	12293
2.17	Cald1	Caldesmon 1	109624
2.15	Camk2d	calcium/calmodulin-dependent protein kinase II, delta, transcript variant 3	108058
2.23	Camk2n2	Calcium/calmodulin-dependent protein kinase II inhibitor 2	73047
2.37 (2.06)	Cbr4	carbonyl reductase 4	234309
2.04	Cbx4	chromobox homolog 4 (Drosophila Pc class)	12418
3.06	Ccdc64	Coiled-coil domain containing 64	75665
3.01	Ccl2	chemokine (C-C motif) ligand 2	20296
4.53	Ccl7	chemokine (C-C motif) ligand 7	20306
2.30	Ccne1	cyclin E1	12447
2.02	Ccnl1	cyclin L1	56706

2.31	Cdkn1a	cyclin-dependent kinase inhibitor 1A (P21), transcript variant 1	12575
2.59	Chd7	chromodomain helicase DNA binding protein 7	320790
2.25	Chka	Choline kinase alpha	12660
2.28	Chst11	carbohydrate sulfotransferase 11	58250
2.08	Chst8	carbohydrate (N-acetylgalactosamine 4-0) sulfotransferase 8	68947
2.17	Clasp2	CLIP associating protein 2, transcript variant 1	76499
2.26	Coq10b	coenzyme Q10 homolog B (S. cerevisiae), transcript variant 1	67876
5.95 (2.56)	Crem	CAMP-RESPONSIVE ELEMENT MODULATOR. [Source:SWISSPROT;Acc:P27699]	12916
2.19	Cryba4	crystallin, beta A4	12959
2.04	Csnk1d	casein kinase 1, delta, transcript variant 2	104318
2.03	Csnk2a1	Casein kinase 2, alpha 1 polypeptide	12995
2.17	Cxcl1	chemokine (C-X-C motif) ligand 1	14825
2.84	Cyp2t4	cytochrome P450, family 2, subfamily t, polypeptide 4	384724
2.68 (2.10)	Cyp4v3	cytochrome P450, family 4, subfamily v, polypeptide 3	102294
2.01	Dbc1	deleted in bladder cancer 1 (human)	56710
2.14	Ddit4	DNA-damage-inducible transcript 4	74747
2.28	Ddx3x	DEAD/H (Asp-Glu-Ala-Asp/His) box polypeptide 3, X-linked	13205
2.42	Ddx5	DEAD (Asp-Glu-Ala-Asp) box polypeptide 5	13207
3.65	Dnajc5b	DnaJ (Hsp40) homolog, subfamily C, member 5 beta	66326
2.83	Dos	downstream of Stk11	216164
2.08	Dpysl3	dihydropyrimidinase-like 3	22240
2.37	Dusp1	dual specificity phosphatase 1	19252
2.22	Dusp10	dual specificity phosphatase 10	63953
2.41	Dusp14	dual specificity phosphatase 14	56405
3.46	Dusp5	dual specificity phosphatase 5	240672
3.25	EG639787	PREDICTED: predicted gene, EG639787	639787
3.65	Egr1	early growth response 1	13653
2.32	Eid2	EP300 interacting inhibitor of differentiation 2	386655
2.19	Eif1a	eukaryotic translation initiation factor 1A	13664
2.53	Eif5	eukaryotic translation initiation factor 5, transcript variant 2	217869
2.17	Ell2	elongation factor RNA polymerase II 2	192657
2.16	Emd	emerin	13726
2.04	Eml5	Echinoderm microtubule associated protein like 5	319670
3.45	ENSMUSG00000020666	ENSMUST00000020995	
2.14	ENSMUSG00000021314	SIMILAR TO AMPHIPHYSIN (FRAGMENT). [Source:SPTREMBL;Acc:Q8R1C4]	
3.78	ENSMUSG00000031759	ENSMUST00000034209	
2.74	ENSMUSG00000033588	ENSMUST00000039706	
2.55	ENSMUSG00000034735	ENSMUST00000058019	
2.11	ENSMUSG00000036248	ENSMUST00000042684	
2.21	ENSMUSG00000042088	ENSMUST00000040304	
2.05	ENSMUSG00000042865	ENSMUST00000052242	
2.36	ENSMUSG00000043566	ENSMUST00000049510	
2.36	ENSMUSG00000045357	ENSMUST00000062053	
3.42	ENSMUSG00000047796	ENSMUST00000055149	
2.09	ENSMUSG00000049727	ENSMUST00000054572	
2.46	ENSMUSG00000051075	ENSMUST00000057179	

4.66 (2.47)	Eprs	glutamyl-prolyl-tRNA synthetase	107508
2.79	Errfi1	ERBB receptor feedback inhibitor 1	74155
2.17	Fbxl10	F-box and leucine-rich repeat protein 10, transcript variant 3	30841
4.35	Fem1b	feminization 1 homolog b (C. elegans)	14155
2.28	Fgfr2	fibroblast growth factor receptor 2, transcript variant 2	14183
2.02	Fndc3b	Fibronectin type III domain containing 3B	72007
2.17	Fndc4	fibronectin type III domain containing 4	64339
2.70	Fos	FBJ osteosarcoma oncogene	14281
7.84 (2.12)	Fosl1	fos-like antigen 1	14283
2.20	Frmd6	FERM domain containing 6	319710
2.13	Fst	follistatin	14313
2.53	Gadd45b	growth arrest and DNA-damage-inducible 45 beta	17873
2.84 (2.31)	Gclc	glutamate-cysteine ligase, catalytic subunit	14629
2.57	Gdf9	growth differentiation factor 9	14566
5.77	Gem	GTP binding protein (gene overexpressed in skeletal muscle)	14579
2.74	Gpr98	G protein-coupled receptor 98	110789
2.85	Gramd1b	GRAM domain containing 1B	235283
3.00	Hdc	histidine decarboxylase	15186
2.47	Herc4	hect domain and RLD 4	67345
2.35	Hist1h3b	histone cluster 1, H3b	319150
2.36	Hist2h3b	histone cluster 2, H3b	319154
2.60	Hmgcr	3-hydroxy-3-methylglutaryl-Coenzyme A reductase	15357
2.00	Hnrpdl	heterogeneous nuclear ribonucleoprotein D-like	50926
2.02	Hsd17b7	hydroxysteroid (17-beta) dehydrogenase 7	15490
2.00	Hspb8	heat shock protein 8	80888
2.26	Ibrdc1	PREDICTED: IBR domain containing 1	268291
2.21	Id1	inhibitor of DNA binding 1	15901
3.89	Ier3	immediate early response 3	15937
2.19	Ifrd1	interferon-related developmental regulator 1	15982
2.73	Il6	interleukin 6	16193
2.40	Impdh2	inosine 5'-phosphate dehydrogenase 2	23918
2.23	Irf2bp2	PREDICTED: interferon regulatory factor 2 binding protein 2, transcript variant 1	270110
2.41	Isy1	ISY1 splicing factor homolog (S. cerevisiae)	57905
2.95 (2.13)	Kiss1	KiSS-1 metastasis-suppressor	280287
2.27	Klf13	Kruppel-like factor 13	50794
3.86	Klf4	Kruppel-like factor 4	16600
2.52 (2.51)	Ldlr	low density lipoprotein receptor	16835
2.33	LOC100047762	PREDICTED: similar to Aspartate aminotransferase, cytoplasmic (Transaminase A)	100047762
2.88	LOC100047937	PREDICTED: similar to Aldehyde dehydrogenase 1 family, member L1	100047937
2.32 (2.07)	LOC218501	PREDICTED: similar to calponin 3, acidic	218501
2.54 (2.04)	LOC432554	PREDICTED: similar to Ddx5 protein	432554
2.07	LOC623115	PREDICTED: similar to heterogeneous nuclear ribonucleoprotein D-like	623115
2.56 (2.04)	LOC667737	PREDICTED: similar to basic leucine zipper and W2 domains 1	667737
2.02	Luc7l	Luc7 homolog (S. cerevisiae)-like	66978
4.12 (2.19)	Maff	v-maf musculoaponeurotic fibrosarcoma oncogene family, protein F (avian)	17133
2.79	Map3k6	mitogen-activated protein kinase kinase kinase 6	53608

2.03	March7	membrane-associated ring finger (C3HC4) 7	57438
3.63	Mat2a	methionine adenosyltransferase II, alpha	232087
2.44	Mbnl2	muscleblind-like 2, transcript variant 2	105559
2.62	Mcl1	myeloid cell leukemia sequence 1	17210
5.13	Mcm10	minichromosome maintenance deficient 10 (S. cerevisiae)	70024
2.39	Mef2d	myocyte enhancer factor 2D	17261
2.23	Metrnl	meteorin, glial cell differentiation regulator-like	210029
4.11 (2.37)	Mrap	melanocortin 2 receptor accessory protein	77037
8.15 (2.29)	Mt1	Metallothionein 1	17748
2.69	Mt2	metallothionein 2	17750
2.67	Mycn	v-myc myelocytomatosis viral related oncogene, neuroblastoma derived (avian)	18109
2.98	Myd116	myeloid differentiation primary response gene 116	17872
4.53	Nek1	NIMA (never in mitosis gene a)-related expressed kinase 1	18004
2.13	Nfkbia	nuclear factor of kappa light chain gene enhancer in B-cells inhibitor, alpha	18035
2.35	Nfkbiz	nuclear factor of kappa light polypeptide gene enhancer in B-cells inhibitor, zeta	80859
2.74	Nol5	nucleolar protein 5	55989
2.80 (2.21)	Npal1	NIPA-like domain containing 1	70701
2.24	Nr1d1	nuclear receptor subfamily 1, group D, member 1	217166
2.75	Nr4a1	nuclear receptor subfamily 4, group A, member 1	15370
3.73	Nr4a2	nuclear receptor subfamily 4, group A, member 2	18227
2.07	Nucks1	nuclear casein kinase and cyclin-dependent kinase substrate 1	98415
2.87 (2.08)	Odc1	ornithine decarboxylase, structural 1	18263
2.72	Olfr1403	olfactory receptor 1403	258645
2.66	Olfr1510	olfactory receptor 1510	258423
2.54	Olfr854	olfactory receptor 854	258515
2.39	Osbpl7	oxysterol binding protein-like 7	71240
3.20	Pag1	phosphoprotein associated with glycosphingolipid microdomains 1	94212
2.47	Pde4b	phosphodiesterase 4B, cAMP specific	18578
2.00	Pim1	proviral integration site 1	18712
2.31	Pip5k1a	phosphatidylinositol-4-phosphate 5-kinase, type 1 alpha	18720
2.06	Plat	plasminogen activator, tissue	18791
2.27	Plcb4	phospholipase C, beta 4	18798
2.00	Ppap2b	phosphatidic acid phosphatase type 2B	67916
2.10	Prl8a2	prolactin family 8, subfamily a, member 2	13529
2.26	Prnd	prion protein dublet	26434
4.61 (2.16)	Procr	Protein C receptor, endothelial	19124
2.13	Pthlh	Parathyroid hormone-like peptide	19227
2.16	Pvr	poliovirus receptor	52118
2.02	Rab6	RAB6, member RAS oncogene family	19346
2.19	Rbm25	RNA binding motif protein 25	67039
4.21	Rchy1	Ring finger and CHY zinc finger domain containing 1	68098
2.69	Rdx	radixin, transcript variant 1	19684
2.07	Reg3d	regenerating islet-derived 3 delta	30053
3.08	Rgs1	regulator of G-protein signaling 1	50778
3.07	Rgs4	regulator of G-protein signaling 4	19736
2.06	Rnf125	ring finger protein 125	67664

2.07	Scarb1	scavenger receptor class B, member 1	20778
11.08 (4.32)	Serpine1	Serine (or cysteine) peptidase inhibitor, clade E, member 1	18787
3.18	Sfrs10	Splicing factor, arginine/serine-rich 10 (transformer 2 homolog, Drosophila)	20462
2.58 (2.16)	Sfrs5	splicing factor, arginine/serine-rich 5 (SRp40, HRS), transcript variant 3	20384
2.17	Sfrs7	splicing factor, arginine/serine-rich 7	225027
2.11	Sgk1	serum/glucocorticoid regulated kinase 1	20393
2.02	Sgtb	small glutamine-rich tetratricopeptide repeat (TPR)-containing, beta	218544
4.42 (2.77)	Sh3rf1	SH3 domain containing ring finger 1	59009
2.59 (2.19)	Slc10a6	solute carrier family 10 (sodium/bile acid cotransporter family), member 6	75750
2.40	Slc23a2	solute carrier family 23 (nucleobase transporters), member 2	54338
4.26 (2.14)	Slc25a25	solute carrier family 25 (mitochondrial carrier, phosphate carrier), member 25	227731
2.16	Slc41a3	solute carrier family 41, member 3, transcript variant 2	71699
3.66	Slc6a5	solute carrier family 6 (neurotransmitter transporter, glycine), member 5	104245
4.34	Snf1lk	SNF1-like kinase	17691
5.51 (3.44)	Srxn1	sulfiredoxin 1 homolog (S. cerevisiae)	76650
3.81	Stat3	signal transducer and activator of transcription 3, transcript variant 3	20848
2.42	Syt4	synaptotagmin IV	20983
2.47	Taar4	trace amine-associated receptor 4	209513
2.69 (2.58)	Tac1	tachykinin 1	21333
2.47	Taok2	TAO kinase 2	381921
2.43	Tiparp	TCDD-inducible poly(ADP-ribose) polymerase	99929
3.73 (2.12)	Tm4sf4	transmembrane 4 superfamily member 4	229302
2.00	Tmem144	transmembrane protein 144	70652
2.99	Tnfrsf12a	tumor necrosis factor receptor superfamily, member 12a	27279
4.22 (2.23)	Trp53inp1	transformation related protein 53 inducible nuclear protein 1	60599
2.22	Tubb2a	tubulin, beta 2a	22151
2.88	Tubb6	tubulin, beta 6	67951
2.07	Txndc11	thioredoxin domain containing 11, transcript variant 2	106200
2.04	Ubr2	ubiquitin protein ligase E3 component n-recognin 2	224826
2.26	Usp53	Ubiquitin specific peptidase 53	99526
2.43	Vdr	vitamin D receptor	22337
2.30	Wdr43	PREDICTED: WD repeat domain 43, transcript variant 9	72515
2.23	Zan	zonadhesin	22635
2.27	Zbtb24	zinc finger and BTB domain containing 24	268294
2.24	Zfand5	zinc finger, AN1-type domain 5	22682
3.13	Zfhx3	zinc finger homeobox 3	11906
2.87	Zfp113	zinc finger protein 113	56314
2.29	Zfp192	zinc finger protein 192	93681
2.74	Zfp36	zinc finger protein 36	22695
3.27 (3.17)	Zswim6	PREDICTED: zinc finger, SWIM domain containing 6	67263

Table 6b	**Adrenal glands after hypoglycemia – transcripts upregulated only in PACAP+/+ mice (PACAP-dependent transcripts)**		
fold increase	Gene symbol	Description	GeneID
2.31	Cyp51	Cytochrome P450, family 51	13121
2.59	ENSMUSG00000020666		
2.18	ENSMUSG00000033588		
2.08	ENSMUSG00000046206		
2.42	ENSMUSG00000047796		
2.06	ENSMUSG00000050648		
2.17	Hhip	Hedgehog-interacting protein	15245
2.17	Lep	Leptin	16846
2.16	Optn	Optineurin	71648

Table 6. Transcripts upregulated in adrenal glands 3h after hypoglycemia-induced stress. Microarray hybridization was carried out using RNA samples obtained from animals treated with 2 U/kg insulin or saline (male mice; age range 4.8-6.4 months). Samples from six saline-treated mice were pooled, and fractions of this pool were hybridized with samples from six individual insulin-treated mice. Expression levels (fold increase) as measured by microarray thus represent $WT_{insulin}/WT_{saline}$ and $KO_{insulin}/KO_{saline}$. No dye-swap was performed. Data were extracted, normalized (LOWESS correction), quality-filtered (Ratio Quality Measure >= 0.8) and statistically evaluated in mAdb (http://nciarray.nci.nih.gov). False discovery rate was set to <1%. Data were subsequently exported to Microsoft Excel and only those transcripts showing 2-fold or greater induction were retained. Genes with spurious self-self ratios (greater than 1.5 or smaller than 0.66, respectively) were removed. Multiple oligonucleotide targets representing a single Entrez GeneID were collapsed by calculating the average of the respective mean expression ratios. Table 6a, transcripts induced in KO mice. Transcripts also induced in WT are noted in parentheses. Table 6b, PACAP-dependently upregulated transcripts (induced only in WT). Note that most transcripts upregulated in WT are also upregulated in KO, with only nine transcripts being PACAP-dependent according to our microarray results.

Overlap of PACAP-repressed transcripts from microarray Experiments 1 and 2				Table 7
Experiment 1	Experiment 2			
KO ins/WT ins	KO ins/KO sal	Gene	Description	GeneID
2.05	2.37	9430076C15Rik	RIKEN cDNA 9430076C15 gene	320189
2.03	2.69	4931408A02Rik	RIKEN cDNA 4931408A02 gene	70967
2.38	4.75	9430023L20Rik	RIKEN cDNA 9430023L20 gene	68118
2.09	3.55	Akap2	A kinase (PRKA) anchor protein 2, transcript variant 3	11641
2.62	2.81	Axud1	AXIN1 up-regulated 1, mRNA.	215418
2.06	2.54	Btg2	B-cell translocation gene 2, anti-proliferative, mRNA.	12227
3.49	5.20	Cabyr	calcium-binding tyrosine-(Y)-phosphorylation regulated (fibrousheathin 2)	71132
2.30	2.04	Cbx4	chromobox homolog 4 (Drosophila Pc class), mRNA.	12418
3.74	4.53	Ccl7	chemokine (C-C motif) ligand 7, mRNA.	20306
2.21	2.25	Chka	Choline kinase alpha	12660
2.15	2.84	Cyp2t4	cytochrome P450, family 2, subfamily t, polypeptide 4, mRNA.	384724
2.15	2.37	Dusp1	dual specificity phosphatase 1, mRNA.	19252
2.31	2.22	Dusp10	dual specificity phosphatase 10, mRNA.	63953
2.36	3.65	Egr1	early growth response 1, mRNA.	13653
2.18	2.17	Ell2	elongation factor RNA polymerase II 2, mRNA.	192657
2.85	4.35	Fem1b	feminization 1 homolog b (C. elegans), mRNA.	14155
2.17	7.84	Fosl1	fos-like antigen 1	14283
2.00	5.77	Gem	GTP binding protein (gene overexpressed in skeletal muscle), mRNA.	14579
2.00	2.35	Hist1h3b	histone cluster 1, H3b, mRNA.	319150
2.08	2.36	Hist2h3b	histone cluster 2, H3b, mRNA.	319154
3.81	2.26	Ibrdc1	PREDICTED: IBR domain containing 1, mRNA.	268291
2.11	3.89	Ier3	immediate early response 3, mRNA.	15937
4.39	3.86	Klf4	Kruppel-like factor 4 (gut)	16600
4.04	2.23	Metrnl	meteorin, glial cell differentiation regulator-like, mRNA.	210029
2.65	8.15	Mt1	Metallothionein 1	17748
3.14	2.24	Nr1d1	nuclear receptor subfamily 1, group D, member 1, mRNA.	217166
3.35	2.75	Nr4a1	nuclear receptor subfamily 4, group A, member 1, mRNA.	15370
6.96	3.73	Nr4a2	nuclear receptor subfamily 4, group A, member 2, mRNA.	18227
3.66	4.21	Rchy1	Ring finger and CHY zinc finger domain containing 1	68098
2.13	3.56	Rdx	RIKEN cDNA 9830163H01 gene	414109
2.91	4.26	Slc25a25	solute carrier family 25 (mitochondrial carrier, phosphate carrier), member 25	227731
4.96	4.34	Snf1lk	SNF1-like kinase	17691
2.21	2.47	Taok2	TAO kinase 2	381921
2.31	2.43	Tiparp	TCDD-inducible poly(ADP-ribose) polymerase	99929
2.41	2.26	Usp53	Ubiquitin specific peptidase 53	99526
2.30	2.27	Zbtb24	zinc finger and BTB domain containing 24	268294

Table 7. Overlap of PACAP-repressed transcripts from Experiments 1 and 2, i.e. transcripts more abundant in KO adrenals compared to WT adrenals 3h after insulin (Experiment 1), and upregulated only or more strongly in KO adrenals 3h after insulin (Experiment 2). See legends to tables 5 and 6 for details.

Information on website URLs is current as of 8/13/09.

10.2. List of academic teachers

The following professors were my teachers at Philipps-University Marburg:
Aumüller, Berndt, Besedovsky, Czubayko, Daut, del Rey, Eilers, Elsässer, Feuser, Garten, Gromes, Gudermann, Hasilik, Heimbrodt, Jacob, Jungclas, Koolman, Kunz, Lang, Lill, Löffler, Müller, Petz, Renkawitz-Pohl, Renz, Röhm, Röper, Schäfer, Seitz, Steiniger, Suske, Voigt, Weihe.

10.3. Acknowledgments

Life inside and outside the lab has been most memorable since I arrived in the United States approximately 2370240 minutes ago, thanks to a myriad of people. There are too many to name, but I shall endeavor to do justice to those individuals who have rendered their support, and indelibly impressed me (in one way or another), by acknowledging their names as follows:

Prof. Dr. Eberhard Weihe – my mentor since the early days at Philipps-Universität Marburg, and German doctoral thesis supervisor. Thank you very much for being a role model with respect to scientific rigor and integrity, and for your continued support.

Lee E. Eiden, Ph.D. – my chief at the Section on Molecular Neuroscience, and supervisor at the American business end of this thesis project. Thank you very much for providing me with the great opportunity of working at the National Institutes of Health, and for allowing me to freely pursue my ideas and experiments in the context of your laboratory.

Dr. Martin K.-H. Schäfer – friend and former advisor from the Philipps-Universität Marburg. Your technical expertise, scientific wit and cordial ways are greatly appreciated. Thank you for teaching a significant part of the skills that allowed me to tackle my thesis projects.

Yvonne Holighaus – comrade, colleague and good friend for the past ten years. For all the things we have been through together in this first decade of the current millennium, thank you very much. My best wishes and good luck for your future endeavors.

Babru Samal, Chang-Mei Hsu, Charisse "Winston" Winston, David Huddleston, Djida Ait-Ali, Matt Gerdin, Tomris Mustafa, Xiuhuai "Dr. Liu" Liu – my colleagues from the Section on Molecular Neuroscience. Thank you for the years of collaborative effort, fun and interesting conversations, as well as exposure to multicultural foods.

Abdel Elkahloun – for microarray hybridizations and fruitful discussions.

Maribeth Eiden, Scott Young, Jon Marsh and their entire labs – for being such good neighbors on the 5th floor of Building 49.

Medinat, Dilia, Ana, Manit, Sherry – my friends from the NIH cafeteria and Federal Credit Union, whose smiles made having lunch and paying the rent so much more enjoyable.

Shelley, Maria, Ruth, Paul, Isaac, Samir, Edouard, Angela – your help greatly facilitated running our mouse colony throughout the years, and your friendly ways were much appreciated.

All members of the Laboratory of Cellular and Molecular Regulation – I really enjoyed our seminars and everybody's friendly attitude.

Florian, Elise, Davide, Kalle, Mattias, Susannah, Cecile, Gian Marco – my dear friends, without whom this whole story would not have been half as rewarding. I look forward to seeing you all again in Europe!

Claudio, Fiscia, Michele, Andrea, Filippo, Francesca S., Isabella, Maria-Isabel, Pablo, Sofia, Eugenio – The Italian-Chilean-Paraguayan Connection, whose warm and sociable character was a true pleasure.

My family – you mean everything to me. Thank you for your unconditional love and support.

. . .o.0.O.0.o. . .

In zweifelhaften Fällen entscheide man sich für das Richtige.

-- Karl Kraus